The silica and inorganic carbon system in tidal marshes of the Elbe estuary, Germany: Fluxes and spatio-temporal patterns

Dissertation

zur Erlangung des Doktorgrades

der Naturwissenschaften im Fachbereich

Geowissenschaften

der Universität Hamburg

vorgelegt von

Andreas Weiss

aus

Buenos Aires

Hamburg

2013

Als Dissertation angenommen vom Fachbereich Geowissenschaften der Universität Hamburg auf Grund der Gutachten von Prof. Dr. Jens Hartmann und Prof. Dr. Kai Jensen.

Hamburg, den 27.06.2013
(Datum der vorläufigen Bescheinigung)

_____

Prof. Dr. Jürgen Oßenbrügge

(Leiter des Fachbereichs Geowissenschaften)

Eidesstattliche Versicherung

Hiermit erkläre ich an Eides statt, dass ich die vorliegende Dissertationsschrift selbst verfasst und keine anderen als die angegebenen Quellen und Hilfsmittel benutzt habe.

Hamburg, den

_____

Andreas Weiss

Content

Abstract

Tidal marshes are interfaces between terrestrial and aquatic ecosystems. They are known for their transformation capacities regarding inorganic and organic nutrients and can influence lateral nutrient fluxes in estuarine and coastal systems. In this study the tidal marshes of the Elbe estuary, Germany, were studied with respect to the silica cycle and the inorganic carbon system. Therefore, three sampling sites along the estuarine salinity gradient were sampled over a two year period to represent the whole land ocean transition zone.

Results confirmed the tidal patterns of dissolved silica (DSi) concentrations observed in other tidal marsh environments. Seepage concentrations were several fold higher then concentrations during the bulk phase. Along the salinity gradient DSi concentrations increased from the freshwater to the brackish marsh as expected from the influence of salinity on biogenic silica (BSi) dissolution rates. Seasonally, DSi concentrations increased from spring to autumn at the brackish and salt marsh site. The impact on benthic DSi uptake on seepage concentrations could be studied in March 2011. There, DSi concentrations were reduced by 18.6% between sunrise and noon, corroborating the importance of benthic diatoms for the regulation of nutrient fluxes in these ecosystems. DSi fluxes from the tidal marshes were significant contributors to the estuarine DSi budget in July, accounting for 52-70% of the total DSi load of the Elbe River.

The second part of the thesis explored the importance of DSi fluxes for the total North Sea DSi budget to answer the question whether these fluxes can be significant on larger than estuarine scales. Geographic information system (GIS) data of salt marsh areas was combined with published DSi fluxes from salt marshes in Europe and the USA to derive the total DSi flux into the North Sea. It could be shown that the annual average contribution of salt marshes to the DSi budget of the North Sea amounted to only 0.7% of the annual riverine input. During summer this contribution was larger (2.4%) but still insignificant compared to the riverine inputs. It was concluded that salt marshes do not play an important role in the DSi budget of the North Sea. However, in coastal regions with low riverine DSi input and large salt marsh areas, like the English Channel, the

contribution could become significant in summer. Therefore, studies of smaller coastal segments should consider tidal marshes when assessing land ocean Si fluxes.

In the third part of the thesis the distribution of stable silicon isotopes (d30Si) was studied. For the first time δ^{30}Si were measured in water of tidal marsh ecosystems. It was shown that the tidal pattern of δ^{30}Si was different at each sampling station. At the freshwater site flooding previous to the sampling caused the seepage and bulk signal to be virtually equal. At the brackish site seepage water had higher δ^{30}Si values than the bulk water, indicating fractionation processes in the soil-plant system. These values were also amongst the highest reported for soil solutions, reaching 3.26‰. Surprisingly, the isotopic signal of the seepage water at the saline site was significantly lower than at the brackish site, probably due to less intense fractionation processes in the soil-plant system. The data from the estuarine transects revealed that the freshwater zone is a location of intense modification of the δ^{30}Si signal. Uptake of DSi by diatoms caused increasing δ^{30}Si values and a decrease of DSi concentrations along the estuary in October. In December, when biological activity was minimal, the estuary was a source for DSi, probably due to the input of DSi by tributaries. The isotopic signal was heavily altered in the region of the Hamburg harbour. Unfortunately, the lack of complementary data did not allow an identification of the main processes responsible for the alteration. In conclusion, this study showed for the first time, that the δ^{30}Si signal is altered during estuarine transition even in month where biological DSi uptake is low.

The last part of the thesis shed light on the spatio-temporal variability of the inorganic carbonate system in tidal marsh systems. It could be shown that carbonate dissolution in the tidal marshes of the Elbe estuary is the main process that turns these areas into sources of dissolved inorganic carbon and alkalinity for the estuary. On average the DIC export from the marsh areas could account for about 17% of the excess DIC in the estuary. This process was not accounted for in previous studies conducted in US tidal marshes. It was hypothesised that the different TA sources in US marshes and the study areas are related to the morphology and hydrology of the coastal zone, i.e. the presence of a shallow shelf sea combined with higher tidal forces. Due to the absence $CaCO_3$ dissolution, soil pH is possibly lower in the US marshes which would decrease the BSi dissolution rates of BSi and affects the overall long term storage capacity of those

marshes, which implies a coupling between the inorganic carbon cycle and the silica cycle in tidal marshes.

In summary, it could be shown that the tidal marsh areas in the Elbe estuary are important parts of the estuarine silica and carbon cycle, with respect to lateral export fluxes. For the silica cycle however, the spatial significance of tidal marsh system seems to be small at scales larger than an estuarine system, as was shown for the North Sea. Regarding the inorganic carbon system of tidal marshes, it could be shown that calcium carbonate dissolution was the main TA generating process and not sulphate reduction as in tidal marshes of the USA. This finding lead to the hypothesis that the absence of the carbonate buffer might lead to an increased BSi long term storage, due to lower BSi dissolution rates – a link between the inorganic carbon cycle and silica cycle which had not been addressed.

Zusammenfassung

Tidemarschen sind Schnittstellen zwischen terrestrischen und aquatischen Ökosystemen. Sie sind für ihre Transformationskapazitäten in Bezug auf anorganische und organische Nährstoffe bekannt und können laterale Nährstoffflüsse in der Küstenzone beeinflussen. In dieser Studie wurden die Tidemarschen des Elbe Ästuars, Deutschland, in Bezug auf den Silizium- und den anorganischen Kohlenstoffkreislauf hin untersucht. Dafür wurden drei Messstationen entlang des ästuarinen Salzgehaltsgradienten über einen Zeitraum von zwei Jahren beprobt, um die ganze Land Ozean Übergangszone einzubeziehen.

Die Ergebnisse bestätigten die tidalen Muster gelöster Siliziumkonzentrationen (DSi), welche auch in anderen Tidemarschen beobachtet worden waren. Sickerwasser-konzentrationen waren um ein Mehrfaches höher als Konzentrationen während des Hochwassers. Entlang des Salzgehaltsgradienten erhöhten sich DSi Sickerwasser-konzentrationen von der Süßwassermarsch bis zur Brackwassermarsch, wie aufgrund des Einflusses von Salzgehalt auf die Lösungsraten von biogenem Silizium (BSi) erwartet. Im Jahresverlauf stiegen die DSi Konzentrationen in der Brackwasser- und Salzmarsch von Frühling bis Herbst an. Die Auswirkungen der benthischen DSi Aufnahme auf die Sickerwasserkonzentrationen konnte im März untersucht werden. Die DSi Konzentrationen wurden zwischen Sonnenaufgang und Mittag um 18,6% reduziert, was die Bedeutung von benthischen Diatomeen für die Regulation von Nährstoffflüssen in diesem Ökosystemen untermauert. Im Juli trugen die DSi Flüsse von den Tidemarschen signifikant zum DSi Budget des Elbe Ästuars bei und machten zwischen 52-70% der DSi Gesamtfracht der Elbe aus.

Der zweite Teil der Arbeit untersuchte die Bedeutung der DSi Flüsse für das DSi Budget der Nordsee, um die Frage zu beantworten, ob diese Flüsse auf Skalen, die ästuarine Systeme überschreiten, signifikant sein können. Geographische-Informations-System (GIS) Daten von Salzwiesen wurde mit publizierten Salzmarsch DSi Flüssen aus Europa und der USA kombiniert, um den totalen Salzmarsch DSi Fluss in die Nordsee zu berechnen. Es konnte gezeigt werden, dass der mittlere jährliche Beitrag der Salzmarschen zum DSi Budget der Nordsee nur 0.7% des fluvialen Eintrags ausmachte. Im Sommer war dieser Beitrag höher (2.4%), aber immer noch unbedeutend im Vergleich zum fluvialen Eintrag.

Daraus wurde gefolgert, dass Salzmarschen keine wichtige Rolle im DSi Budget der Nordsee einnehmen. In Küstenregionen jedoch, in denen der fluviale DSi Eintrage niedrig und die Salzmarschflächen hoch sind, z.B. in Bereichen wie dem Ärmelkanal, kann der Beitrag im Sommer bedeutsam werden. Deshalb sollten Studien kleiner Küstenabschnitte, die den Land-Ozean Fluss von Silizium untersuchen, Salzmarschen berücksichtigen.

Im dritten Teil der Arbeit wurde die Verteilung der stabilen Silizium Isotope (δ^{30}Si) in den Tidemarschen und im Elbe Ästuar selbst untersucht. Es wurde gezeigt, dass die tidalen Muster des δ^{30}Si an jeder Messstation verschieden waren. In der Süßwassermarsch verursachten Überflutungen eine Angleichung der δ^{30}Si Werte aus Sickerwasser und Überschwemmungswasser an nahezu identische Werte. In der Brackwassermarsch hatte das Sickerwasser höhere δ^{30}Si Werte als das Hochwasser, was auf Fraktionierungsprozesse im Boden-Pflanzen System hinweist. Diese Werte waren unter den höchsten, die für Bodenlösungen publiziert worden sind und erreichten Werte von 3,26‰. Überraschenderweise was das Isotopensignal in der Salzmarsch signifikant niedriger als in der Brackwassermarsch, was möglicherweise auf weniger intensive Fraktionierungsprozesse zurückzuführen war. Die Daten des ästuarinen Längsprofils zeigten, dass die Süßwasserzone des Ästuars ein Ort starker Modifikationen des δ^{30}Si Signals ist. Im Oktober verursachten die Aufnahme von DSi durch Diatomeen steigende δ^{30}Si Werte und sinkende DSi Konzentrationen entlang des Längstprofils. Im Dezember war das Ästuar eine Quelle für DSi, was möglicherweise auf den DSi Eintrag über Nebenflüsse zurückzuführen war. Das Isotopensignal wurde in der Region des Hamburger Hafens stark verändert. Bedauerlicherweise erlaubte der Mangel an komplementären Daten keine Identifizierung der Hauptprozesse, die für die Veränderung des δ^{30}Si Signals verantwortlich waren. Zusammenfassend zeigte diese Studie zum ersten Mal, dass das δ^{30}Si Signal während des ästuarinen Übergangs auch in Monaten, in denen die biologische Aktivität niedrig ist, stark verändert werden kann.

Der letzte Teil der Arbeit untersuchte die räumlich-zeitliche Variabilität des anorganischen Karbonatsystems in Tidemarschen der Elbe. Es konnte gezeigt werden, dass die Tidemarschen der Elbe Quellen für gelösten anorganischen Kohlenstoff (DIC) und Alkalinität (TA) waren. Im Durchschnitt war der DIC Export von den Marschflächen für 17% des überschüssigen DIC des Ästuares verantwortlich. Zusätzlich wurde gezeigt, dass

die wichtigste Quelle für TA Kalziumcarbonat Lösung war. Dieser Prozess wurde in vorhergehenden Studien in den USA nicht berücksichtigt. Es wurde vermutet, dass die Verschiedenen TA Quellen in US Marschen und den Elbmarschen auf die unterschiedliche Morpho- und Hydrologie der Küstenzonen zurückgeht, d.h. die Präsenz einer Flachwasserküste in Kombination mit höheren Tidekräften. Aufgrund des Fehlens der $CaCO_3$ Lösung in US Marschen ist der Boden pH möglicherweise niedriger, was eine Erniedrigung der BSi Lösungsraten zur Folgen haben könnte. Dies würde die Langzeitspeicherung von BSi in diesen Marschböden erhöhen.

Zusammenfassend konnte gezeigt werden, dass die Tidemarschen der Elbe, in Bezug auf laterale Stoffflüsse, wichtige Teile des ästuarinen Silizium- und Kohlenstoffkreislaufs sind. Für den Siliziumkreislauf jedoch, sind die DSi Flüsse von Salzmarschen in der Küstenzone auf Skalen, die die ästuarine Dimension überschreiten, von geringer Bedeutung, wie am Beispiel der Nordsee gezeigt worden ist. Bezüglich des anorganischen Kohlenstoffsystems der Tidemarschen konnte gezeigt werden, dass Kalziumkarbonat Lösung der wichtigstes TA erzeugende Prozess war und nicht Sulfatreduktion, wie es in US amerikanischen Tidemarschen der Fall ist. Dieser Befund führte zur Hypothese, dass das Fehlen des Karbonatpuffers in den Böden der Tidemarschen zu einer erhöhten Langzeitlagerung von BSi aufgrund niedriger BSi Lösungsraten kommen könnte. Dies würde eine neue Verbindung zwischen dem anorganischen Kohlenstoffkreislauf und dem Silizium Kreislauf darstellen, die bisher noch nicht Untersuchungsgegenstand biogeochemischer Studien gewesen ist.

List of publications

See Appendix 8 for a description of the contribution to each work

Published or submitted

Weiss, A., Amann, T., Hartmann, J. (2013) Silica Dynamics of Tidal Marshes in the Inner Elbe Estuary, Germany. Silicon 5:75-89. DOI: 10.1007/s12633-012-9131-1

This publication is part of the thesis (chapter 3)

Amann, T., **Weiss, A.**, Hartmann, J. (2012) Carbon dynamics in the freshwater part of the Elbe estuary, Germany: Implications of improving water quality. Estuarine, Coastal and Shelf Science 107:112-121. DOI: 10.1016/j.ecss.2012.05.012.

Parts of this publication are part of the thesis (chapter 2, section 2.1)

Müller, F., Struyf, E., Hartmann, J., **Weiss, A**., Jensen, K. (in press) Impact of grazing management on silica export dynamics of Wadden Sea saltmarshes. Estuarine, Coastal and Shelf Science. DOI: 10.1016/j.ecss.2013.03.010.

Moosdorf, N., **Weiss, A**., Müller, F., Lauerwald, R., Worrall, F., Hartmann, J. (submitted) The role of salt marshes in the silica budget of the North Sea.

This publication is part of the thesis (chapter 4)

In preparation

Weiss, A., Böttcher, M. Amann, T., Jensen, K., Hartmann, J. (in prep.) Sources and export of DIC and TA from tidal creeks along a salinity gradient in the Elbe estuary, Germany

This publication is part of the thesis (chapter 6)

Weiss, A., De La Rocha, C., Amann, T., Hartmann, J. (in prep.) Silicon isotopes in the Elbe estuary, Germany.

This publication is part of the thesis (chapter 5)

Amann, T., **Weiss, A**., Hartmann, J. (in prep.) Inorganic carbon cycling and CO_2 fluxes in the inner Elbe estuary, Germany.

Amann, T., **Weiss, A**., Hartmann, J. (in prep.) A silica budget of the inner Elbe estuary, Germany

1 General introduction

The direct interface between the land and the ocean are estuaries. There, the mixing of freshwater with seawater and the presence of tidal forces create a unique environment for biogeochemical transformations to take place. Recently, the fate of carbon (C) and silicon (Si) during the estuarine transition came in focus of biogeoscientists around the world due to the importance of these two elements for the global climate.

Silicon is the second most abundant element of earth (Garrels & Mackenzie 1971). Its cycle is tightly linked with the carbon cycle via chemical weathering and the subsequent use of Si by diatoms, a group of silica-secreting algae. During the chemical weathering process water and carbon dioxide (CO_2) react with the silicate minerals, breaking up the mineral bonds and bringing Si into solution. Over geological timescales this process controls the atmospheric CO_2 concentration (Kempe 1979, Zeebe & Caldeira 2008). Once in solution it forms silicic acid (H_4SiO_4, dissolved silica (DSi)), which is an essential nutrient for diatom growth (Paasche 1980). Diatoms use DSi to form a silicified cell wall composed of amorphous silica also referred to as biogenic silica (BSi). As diatomaceous primary production (PP) accounts for ~40% of the marine PP (i.e. ~¼ of global PP) and for ~50% of the organic carbon exported to the oceans interior (Nelson et al. 1995) the availability of DSi in the ocean partly controls our climate on glacial-interglacial timescales (Falkowski et al. 1998). Hence, the availability of DSi in the oceans is of global importance for earth's climate.

Anthropogenic influence has disturbed the silica cycle, especially the delivery to the ocean (Ittekkot et al. 2000, Laruelle et al. 2010). As about 62% of the total Si input into the ocean is delivered by river discharge (Tréguer & De La Rocha 2013), it is important to understand the effect of the land ocean interfaces on to silica fluxes to the ocean, because of the direct effect on the coastal and marine carbon cycle (see above).

Tidal marshes are such interfaces between terrestrial and aquatic ecosystems. They are found worldwide along coastal or estuarine shores (Mitsch & Gosselink 1993). Their biogeochemistry is influenced by physical and chemical variables such as tidal flooding frequency and duration, soil salinity, and nutrient limitation, especially nitrogen (Mitsch &

Gosselink 1993). These ecosystems are dominated by wetland grasses which are adapted to these conditions. Their primary productivity is amongst the highest in the world with values of up to 8000 g m^{-2} yr^{-1} (Mitsch & Gosselink 1993). Additionally, benthic diatoms inhabit these ecosystems, which also can sustain high rates of primary production (Macintyre et al. 1996).

The pulsing of the tides drives the exchange of matter with the adjacent water body, e.g. the estuary or the coastal seas. This natural phenomenon was conceptualised in the "outwelling hypothesis" (c.f. Odum 2000), which linked the productivity in tidal marshes to the one of the estuary. Many studies, inspired by the "outwelling hypothesis", focused on the nitrogen, phosphorus and the carbon cycle in marsh-estuary systems because of the apparent anthropogenic influence on these cycles (e.g. Valiela & Teal 1979; Jordan et al. 1983; Bowden 1986; Loomis & Craft 2010; Sousa et al. 2010). The carbon cycle, however, was only assessed with regard to the organic fraction, because of its importance for marsh and estuarine food webs (Sherr 1982, Borey et al. 1983, Chalmers et al. 1985). Its inorganic component was only included episodically in studies (Winter et al. 1996). Likewise, the silicon cycle gained not much attention except for episodically reports on DSi concentrations (Imberger et al. 1983, Dankers et al. 1984).

For the silicon cycle, this changed with the publication of the paper "Silicon is the link between tidal marshes and estuarine fisheries: A new paradigm" by Hackney et al. (2000). In this work the authors suggested that estuarine foodwebs are fuelled by the export of DSi from tidal marsh areas. This hypothesis was put to test only recently by scientist (Struyf et al. 2005a, Struyf et al. 2005b, Struyf et al. 2006a, Struyf et al. 2007, Jacobs et al. 2008, Vieillard et al. 2011, Müller et al. in press). These studies revealed that tidal marshes are indeed hot spots for the cycling of silica. The growth of silica accumulating plant species, i.e. grasses and diatoms, leads to an enrichments of BSi in the soil, which is partly recycled partly stored. The recycled part leaves the system as DSi. The export fluxes of only a few tidal exchanges can equal the monthly DSi flux of the estuarine or river systems to the coastal zone which was shown in the Scheldt estuary, Belgium (Struyf et al. 2006a) and a saltmarsh system in Massachusetts, USA (Vieillard et al. 2011). Understanding the silica cycle of the tidal marshes is thus an important prerequisite for the understanding of the land – ocean delivery of Si, especially in times where

2

anthropogenic influence has severely disturbed the natural fluxes of nutrients to the coastal zone.

The interest in the coastal carbon cycle, including the one of tidal marshes, grew because studies showed that inner estuaries play a disproportionately important role in the marine carbon cycle despite its small areal fraction (Gattuso et al. 1998, Borges 2005).

Estuaries are net heterotrophic systems where organic carbon is transformed to inorganic carbon (Cadée & Laane 1983, Eisma et al. 1985, Abril et al. 2002, Middelburg & Herman 2007) turning inner estuaries into sources of CO_2. These systems emit about 22.5 ± 19.2 Tmol C yr^{-1} (1 Tmol = 10^{12} mol) which is close to the amount that is absorbed on the continental shelf (Laruelle et al. 2010). The net heterotrophy in inner estuaries is partly fuelled by the lateral input from tidal marshes (Winter et al. 1996, Raymond & Ab 1997, Cai et al. 1999). In tidal marshes soil respiration creates CO_2 which dissolves in the soil porewater, resulting in high DIC concentrations. Advective transport of soil porewater and diffusive exchange during flooding are the processes that lead to enrichment of estuarine water with dissolved inorganic carbon (DIC) (Cai et al. 1999, Cai et al. 2000, Wang & Cai 2004). If marsh areas are large enough this can lead to significant contribution to the estuarine net heterotrophy (Neubauer & Anderson 2003). This DIC export was termed "marsh CO_2 pump" (Wang & Cai 2004) and is an important process at the marsh dominated estuaries and continental margin of the Southern Bight, USA (Cai et al. 2003a). Because estuaries are an important component in the coastal carbon cycle the knowledge about the influence of tidal marshes on the net heterotrophy is important to understand the carbon cycle in the land ocean transition zone.

1.1 Identifying research gaps

Existing studies about the silica cycle in tidal marshes only focussed either on freshwater or on salt marshes (e.g. Struyf et al. 2006a, Vieillard et al. 2011). This does not allow a complete description of the estuarine silica cycle, because the representation of the brackish zone is missing. This zone is characterized by huge salinity variations. Salinity is an important variable with major influence on BSi dissolution rates. Salinity affects the BSi dissolution rates directly due to the presence of cations which have a catalytic effect on the hydrolysis of siloxane bonds at the silica surface (Loucaides et al. 2008). Additionally, salinity fluctuations can have an indirect influence on BSi dissolution via its simulating

effect on microbiological respiration rates (Capone & Kiene 1988, Cunha et al. 2000). Bacteria decompose the organic coatings of phytoliths or diatom frustules which make them more prone to dissolution (Bartoli & Wilding 1980, Bidle 1999, Rickert et al. 2002). The BSi dissolution rate plays a key role in the tidal marsh silica cycle, because it determines the accumulation rate of BSi and the amount of DSi which is available for export. Therefore, the investigation of freshwater, brackish and saltmarshes along an estuarine salinity gradient could deliver valuable information about the pattern of DSi export and BSi accumulation in marsh soils which is still missing for the complete description of the estuarine silica cycle.

Also unaccounted for is the relative importance of tidal marsh DSi export on regional or global scale. The existing studies showed that the DSi export from tidal marsh areas can be of local importance in estuarine (Struyf et al. 2006a) and coastal systems (Vieillard et al. 2011). Regional and global land ocean flux studies (Beusen et al. 2009, Laruelle et al. 2009, Dürr et al. 2011, Tréguer & De La Rocha 2013) or continental to global scale studies on terrestrial DSi mobilisation (Hartmann et al. 2010, Jansen et al. 2010, Moosdorf et al. 2011) currently do not include tidal marsh areas in their models. To answer the question whether or not the tidal marsh DSi fluxes are also significant on regional or global scale, studies should analyse the importance of tidal marsh DSi export on these scales with respect to riverine DSi fluxes.

Another topic that only started to gain attention is the isotopic silica cycling in estuaries and tidal marshes. The average isotopic composition (δ^{30}Si) of seawater reflects the balance between river and hydrothermal inputs of DSi into the ocean. The average δ^{30}Si value of the oceans is about 1 ‰. This values reflects the much greater input of riverine DSi (δ^{30}Si = 0.5-3.4 ‰) (Opfergelt & Delmelle 2012) to the ocean than of hydrothermal DSi from ridge flanks (δ^{30}Si = -0.4 ‰) (Basile-Doelsch 2006). Additionally, there removal of DSi in estuaries is only poorly constrained (Tréguer et al. 1995, Tréguer & De La Rocha 2013). Better understanding the effect of estuaries on the riverine inputs and δ^{30}Si values would help to improve the global budget for the Si cycle as well as to constrain the isotopic input of the ridge flank hydrothermal flux of Si and Si isotopes into the ocean.

Regarding the carbon cycle the majority of studies were conducted in the tidal marsh systems of the south-east USA, (Cai & Wang 1998, Cai et al. 1998, Cai et al. 1999, Cai et

al. 2000). These marshes differ from the tidal marshes in the southern North Sea with regard to their, soil properties, tidal regimes and coastal zone topology (compare Mitsch & Gosselink 1993, Allen 2000). Their soils are mostly organic soils with high carbon concentrations (> 10%) and low soil densities (< 0.6 g cm^{-3}) (Mitsch & Gosselink 1993), while the European marsh soils are mineral soils (Allen 2000), with low organic carbon contents and higher soil densities. The tidal amplitude at the southeaster coast of the USA is lower (0.9 – 2.1 m Flick et al. (1999)) than in the southern North Sea (2 – 3 m BSH (2010). The topological difference is related to the presence of the "Wadden Sea" along the eastern shore of the North Sea. It is the largest unbroken system of intertidal sand and mud flats in the world (UNESCO 2013) and a source for carbonate rich sediments. It is hypothesised that these differences affect the inorganic carbon cycling in tidal marshes, which would question the applicability of the results obtained in the US marshes to tidal marsh systems in Europe. So far, only a few studies have investigated the inorganic carbon chemistry of tidal marshes and the adjacent estuary outside of North America (Winter et al. 1996, Hellings et al. 2000, Forja et al. 2003, La Paz et al. 2008). These studies indicate that calcium dissolution could be the source of alkalinity (TA) in European marshes soils, a process which is absent in the US systems (Wang & Cai 2004 p. 352). The applicability of the results regarding the inorganic carbon cycle, which were obtained in the US tidal marshes, to European systems must therefore be doubted and should be investigated.

1.2 Contribution of this thesis

This thesis tries to close the research gaps, which were presented in the previous section to advance the understanding of the silicon and carbon cycling in tidal marsh systems and the influence of the intertidal ecosystems on the biogeochemistry of the estuary itself.

In the first part the seasonal and spatial variation of DSi and BSi as well as the export of DSi in tidal marshes in the inner Elbe estuary is investigated. It is hypothesised that the stimulating effect of salinity on the dissolution of BSi will be reflected in the concentration pattern along the estuarine salinity gradient. Factors, steering the seasonality of DSi export and differences between the sites like temperature, hydrology, salinity and plant uptake of DSi are discussed.

The second part tries to answer the question if DSi export from tidal salt marsh areas is significant for regional land ocean DSi fluxes using the example of the North Sea. Additionally, the influence of seasonality on the relative contribution of salt marsh DSi export in the North Sea DSi budget is explored using data from the GLORICH river chemistry database.

The third part takes a look into the isotopic signature (δ^{30}Si) of dissolved silica in the Elbe estuary, including tidal marsh areas. Because it is the first study that has measured δ^{30}Si values in tidal marshes the main research questions are: What is the range of δ^{30}Si values in tidal marsh surface waters? Do differences in δ^{30}Si exist between the marsh areas along the salinity gradient? What is the seasonal influence on δ^{30}Si values at the brackish marsh? The discussion focusses on the controlling factors which influence δ^{30}Si signatures of DSi. Regarding the δ^{30}Si values in the estuarine water, the questions concern the spatial patterns of δ^{30}Si values: How are δ^{30}Si values altered during estuarine transition and what are the main processes responsible for those alterations?

The fourth part of the thesis deals with the carbonate system in tidal marsh creeks. Furthermore the DIC export from the tidal marsh areas in the Elbe estuary is assessed to analyse its influence on the estuarine carbonate system and its importance for land ocean DIC fluxes. The contribution of different biogeochemical processes, such as carbonate dissolution and sulphate reduction, is analysed using cation measurements in combination with stoichiometric relationships of these processes. The results are compared to studies conducted in the US, to answer the question if the results obtained in these systems are applicable to north European tidal marsh system.

2 Study area

2.1 The Elbe estuary

The river Elbe forms - with a length of 1094 km and a catchment area of 148,268 km^2 - the fourth largest river basin in central Europe. The catchment supports more than 24.5 million people (as of the year 2003) with densities varying from 40 to more than 3000 inhabitants per km^2 (IKSE, 2005). The Elbe can be divided into the non-tidal middle and

upper Elbe and the tidal stretch (the latter one is 142 km in length), which is located in Northern Germany and feeds into the German Bight, North Sea (Figure 2.1, all data from IKSE (2005)).

The Elbe runoff features high discharges in winter and spring with a long-term maximum occurring in April (Kempe 1992). The mean annual long-term discharge of the Elbe river at the last non-tidal gauge of Neu Darchau (Elbe-km 536) is 704 $m^3 s^{-1}$ (std. dev. 442 $m^3 s^{-1}$; years 1900-2011). This gauge has a catchment area of 131,950 km^2 which represents 89% of the total catchment (IKSE 2005).

The tidal Elbe is a turbid, well-mixed, macrotidal estuary (Middelburg & Herman 2007) with a pronounced maximum turbidity zone (MTZ), on average located around Elbe-km 695 (Brunsbüttel). The range of the semi diurnal tide at the Hamburg harbour is 3.6 m. High tidal current velocities (up to 1.8 $m s^{-1}$) (Bergemann & Gaumert 2010) cause a steep horizontal salinity gradient. The freshwater section reaches from the weir downstream to about Elbe-km 670 (Glückstadt). The water residence time in the tidal stretch ranges from 2 to 12 weeks depending on discharge (Table 2.1).

Table 2.1: Typical residence time in the four zones of the Elbe estuary as a function of low, mean and high discharge (Q) (Bergemann et al. 1996). Typical summer discharge ranges between 300 and 550 $m^3 s^{-1}$.

zone	name	Elbe-km	residence time (days)		
			Q=250 $m^3 s^{-1}$	Q=700 $m^3 s^{-1}$	Q=1200 $m^3 s^{-1}$
I	pre-OMZ	585-620	3	1	<1
II	OMZ	620-650	11	4	2
III	MTZ	650-705	35	14	10
IV	post-MTZ	705-730	30	11	6

The Elbe estuary can be divided into four distinct zones (Table 2.1, Figure 2.1 C) with different dominating biogeochemical processes:

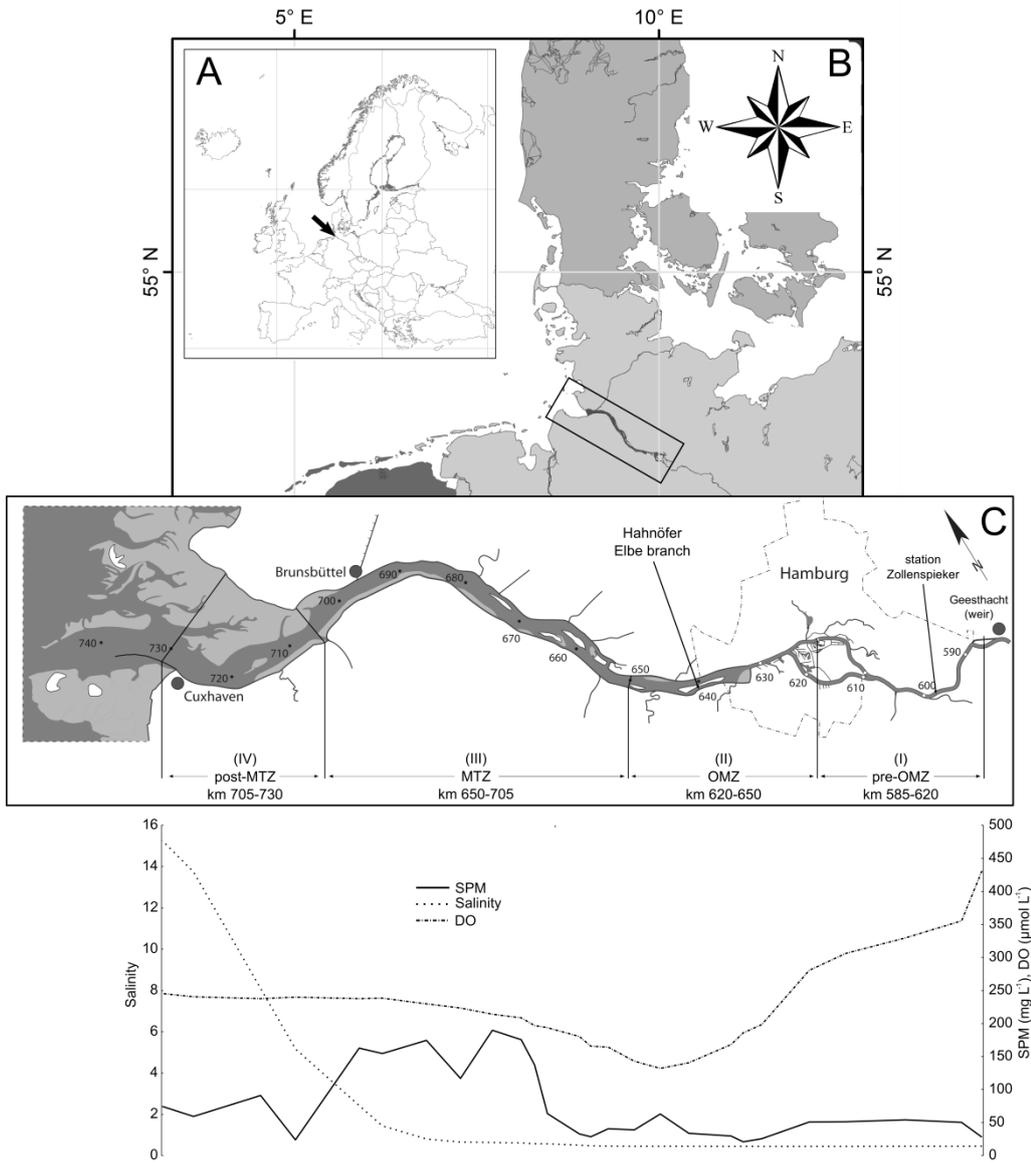Figure 2.1: (A) Overview of Europe, (B) Elbe estuary (marked with black box) located in Northern Germany, (C) detailed view on the estuary, numbers are river kilometres (count starts at the German border). The bottom graph shows an exemplary distribution (2007 summer means) of the zone characteristic parameters suspended matter (SPM), dissolved oxygen (DO) and salinity (graphic courtesy of ARGE Elbe, modified).

1. The pre-OMZ, zone characterised by high values of dissolved oxygen (DO) due to upstream primary production (salinity <1);
2. The oxygen minimum zone (OMZ), including the harbour of the city of Hamburg, shows the abrupt decrease of oxygen. Its formation occurs mainly during the summer months (salinity <1);
3. The maximum turbidity zone (MTZ) with high concentrations of suspended matter (SPM) due to a long residence time (salinity range between <1 and 5);
4. The transition to the full marine system (post-MTZ) of the German Bight shows increasing salinity and stabilised DO and SPM values (salinity range between 1 and 20).

2.2 Tidal marshes of the Elbe estuary

Between Hamburg and Cuxhaven (km 637-721) an area of about 79 km^2 can be regarded as dyke foreland (Figure 2.2). That is the area between the dyke foot and the estuarine channel (Figure 2.3). Not included in this definition are the pioneer zone, mudflats and buildings. The dyke foreland in the Elbe estuary is a mixture of natural and artificial areas covered by different vegetation communities. The artificial areas are covered mainly with grassland. These areas are normally grazed by sheep in the summer and can be found along the whole salinity gradient. Adjacent to this artificial dyke foreland, bordering the estuarine channel, natural vegetation communities can be found.

Along the longitudinal axis of the Elbe estuary the salinity as well as the dominant vegetation cover of the dyke foreland changes (Table 2.2). The natural vegetation covers about 40% of the total dyke foreland of the Elbe estuary. The remaining 60% are meadows which were or are used for cattle or sheep grazing. Salinity increases from freshwater values of <0.5 units to mesohaline values of up to 30 units in the mixing zone of Elbe river water and water from the North Sea.

The whole dyke foreland is drained via a network of ditches and creeks with a characteristic design (Figure 2.3). Small drainage ditches are connected perpendicular to the main creek and together are forming a channel network. Each main creek is separated from the neighbouring one via a dam, so that one creek is separated from the others. The sampling point was located near the outlet of the main drainage creek, to

include as much area of the creek's drainage network as possible. All three sampling locations in this study do not receive terrestrial runoff via rivers or channels.

2.2.1 Sampling sites

To represent the three salinity classes of the inner Elbe estuary (Table 2.2) three sampling sites were chosen. The freshwater site (HDM), the brackish site (NF), and the saline site (DSK).
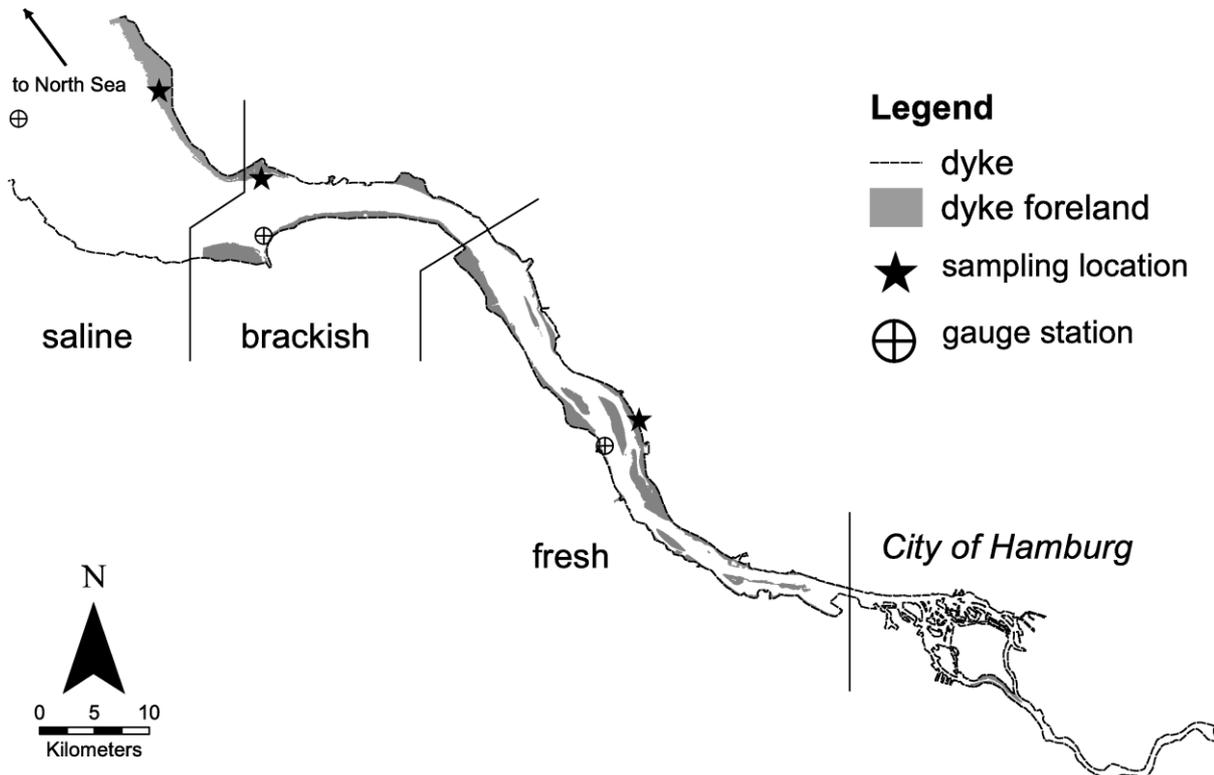
Figure 2.2: Overview of the Elbe estuary. The dyke line (---) and the dyke foreland areas (grey shade) are shown, together with the sampling sites (★) and the position of the gauge stations (⊕)

Freshwater (HDM)

The freshwater site (Figure 2.3 A; 9°33.125''E, 53°39.116''N; km 657) is located in a side branch of the Elbe estuary and is part of a nature protection area. Its total area is 0.171 km². Today the area is intermittently grazed by cows. *Phalaris arudinaceae / Glyceria maxima* reed covers 23% of the total sampling area. The northern border of the site is a dam which connects to a small woodland. Adjacent to the dam, an artificial pond is located, which is covered with *Typha* sp. This pond is connected to the Elbe estuary by a tidal creek. At the outlet of the creek and behind the pond a dense population of *Phragmites australis* can be found. Together these two species cover 25% of the total

area. The tidal range in this area is 3.1 m with a mean high tide of +1.8 m above sea-level (m.a.s.l. according to German height reference system, Potsdam level; (BSH 2010)). The grassland area lies about +2.1 m.a.s.l. Therefore the total marsh surface is inundated only during very high spring tides and storm surges. The elevation of the artificial pond is +1.6 m.a.s.l. and gets inundated every tide, except during very strong neap tides.

Brackish (NF)

The brackish marsh is located at the beginning of the estuarine mouth (Figure 2.3 B; 9°1'47.209"E 53°54'8.073"N, km 703). The main creek, where sampling took place, drains an area of 0.167 km^2. Three vegetation types cover 95% of its area. *Phragmites australis* covers 45%, *Elymus athericus* 15% of the area. The rest is grassland (37%). The main creek itself is fed by smaller ditches which are perpendicular to the main channel. The tidal range is 2.9 m with a mean high water of +1.5 m.a.s.l. (BSH 2010). The upper marsh only gets flooded during spring tides with water levels of +2.0 m.a.s.l.

Saline (DSK)

This site is located at the mouth of the estuary (Figure 2.3 C; 8°52'55.674"E 53°58'26.242"N, km 713.5) and part of the Schleswig-Holstein Wadden Sea National Park. The sampling site has an area of 0.568 km^2. Water samples were taken from a creek which divides an experimental area. Pasture land on the northern side of the creek is grazed by sheep whereas the southern side was abandoned in 1990 and is no longer grazed. Vegetation on the northern site is dominated by *Festuca rubra* meadow, the southern side by *Elymus athericus* meadow. The watershed of the creek had a mean elevation of 2.1 m. The tidal range of the area is 2.9 m with a mean high tide at +1.6 m.a.s.l. (BSH 2010). Even at spring tide, most of the area is not inundated.

2.2.2 Hydrology of sampling sites

According to UVU (1997) the sampling sites differ in their hydrology. The groundwater table is deepest at the freshwater site with >80 cm below the soil surface. At the brackish and saline site the groundwater table lies 40-80 cm below the soil surface.

Furthermore, the saturated water conductivity of the soils associated with the sampling sites changes along the salinity gradient. The freshwater site has the highest saturated

water conductivity with 10-40 cm d^{-1} whereas the soils at the brackish and saline site have lower values with 1-10 cm d^{-1} (UVU 1997).

Table 2.2: Summary of the characteristics of the three salinity classes in which the sampling sites were located. For each salinity class possible salinity range is given as well as the dominant vegetation type of each zone. The area is the total area of the salinity class in the Elbe estuary (see Figure 2.2). Note that the species resolution of the saline sampling site is higher, because different vegetation maps were used

sampling site	salinity class	Elbe km	salinity[a]	area (km^2)	dominant vegetation[b]	areal proportion (%)
fresh (HDM)	limnic	638-680	< 0.5	40.58	Phragmites australis	37
					trees/scrubs	30
					grassland	27
brackish (NF)	mixo-mesohaline	680-705	5-18	20.68	grassland	41
					Phragmites australis	17
					salt meadow	15
saline (DSK)	mixo-mesohaline / euhaline	705-721	5-30	17.90	Festuca rubra	22
					Elymus athericus	20
					Puccinella maritima	14
					Spartina anglica	13
	total			79.16		

[a] salinity characterization was taken from (UVU 1997), chapter 4, table 4.2
(http://www.portal-tideelbe.de/Projekte/FRA1999/Antragsunterlagen/UVU/Kartenband/index.html)

[b] Data for the zones between Elbe km 638-705 were taken from the vegetation map "Biotopenkartierung 2006", Zentrales Datenmanagement der WSD Nord, www.portaltideelbe.de, May 2011. Data for the saline site were taken from the vegetation map "Salzwiesenkartierung 2006/2007", LKN-Schleswig-Holstein/Nationalparkverwaltung
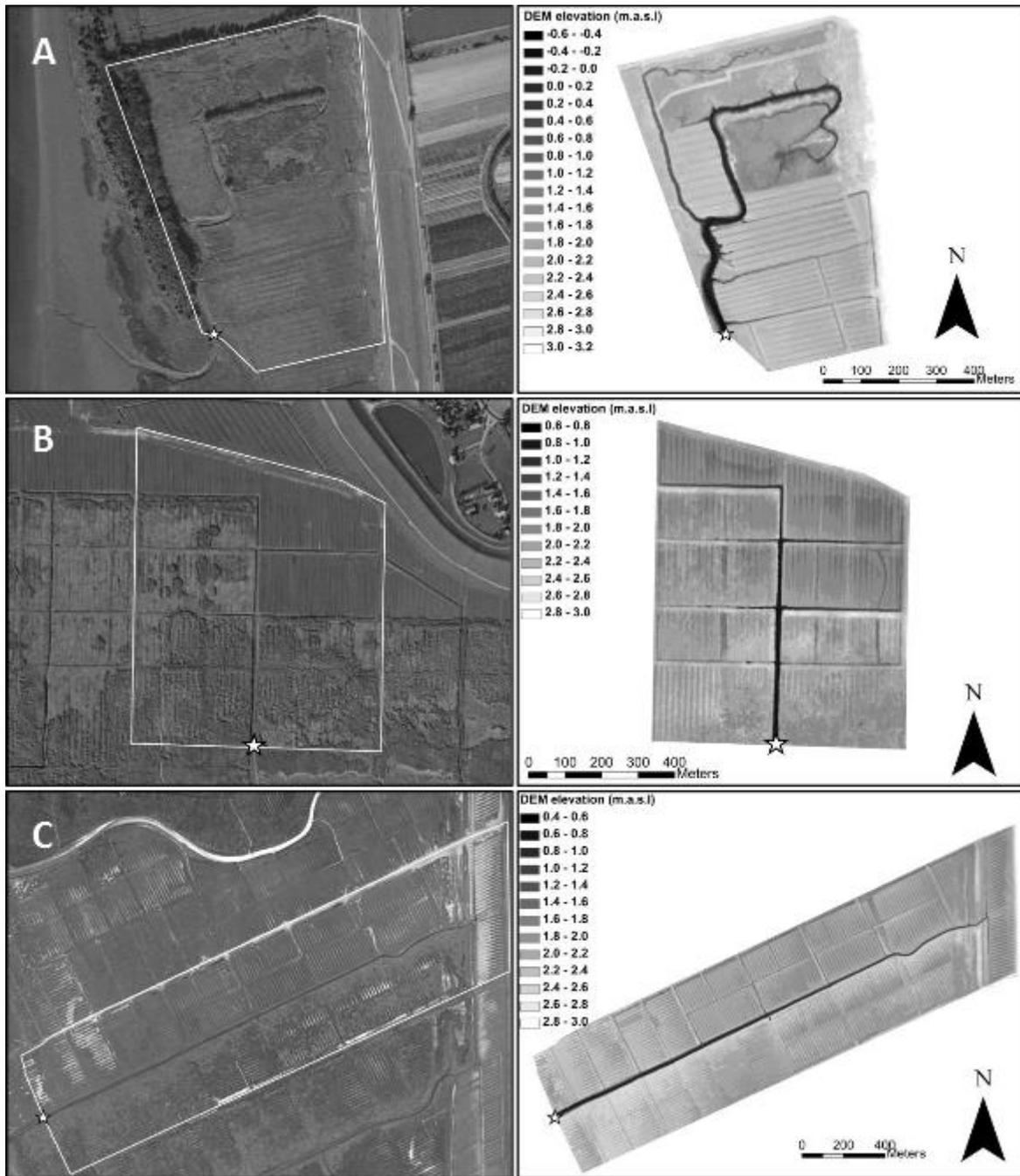
Figure 2.3: Aerial photographs (left) and DEM representation of the sampling sites (right). A) Freshwater site (HDM), B) brackish site (NF) and C) saline site (DSK). The white border encloses the area of the creek's drainage network. The DEM shows the terrain which is enclosed in the white border seen on the aerial photographs. The white star indicates the sampling location for the creek water. The elevation scale is given in metres above sea level (m.a.s.l, according to German height reference system, Potsdam level; (BSH 2010))

3 Silica dynamics of tidal marshes in the inner Elbe estuary, Germany

3.1 Abstract

In this study the seasonal and spatial variation of dissolved silica (DSi) and biogenic silica (BSi) in tidal marshes in the inner Elbe estuary was investigated. Seasonal sampling was conducted at three sites in the dyke foreland - the stretch of land between dyke and estuary - of the Elbe estuary, Germany. To assess the potential DSi export from the dyke foreland geographic information systems were used to calculate the DSi flux. Mean annual seepage DSi concentrations increased along the salinity gradient from 270 µmol L-1 to 380 µmol L^{-1}. BSi concentration of the soil showed the opposite trend decreasing from 15.8 to 4.8 mg g^{-1}. Temporal variations of DSi concentrations were lowest at the freshwater site. At the brackish and saline site DSi concentrations increased about 2-fold from March to November from 200 to 500 and from 300 to 550 µmol L^{-1}, respectively. In March a diurnal signal of DSi uptake by diatoms could be observed at the saline sampling site, DSi concentrations were reduced by 18.6 % between sunrise and noon, highlighting the role of sampling time and irradiance for the DSi-flux estimate. The DSi export from the dyke foreland is significant and equals the riverine DSi input into the estuary during times of low DSi concentrations. Furthermore the marsh DSi fluxes surpass DSi fluxes from highly active weathering regions, as reported in the literature, which corroborates the importance of tidal marsh areas for the coastal silica cycle. Factors steering the seasonality of DSi export and differences between the sites (temperature, hydrology, salinity and plant uptake of DSi) are discussed.

3.2 Introduction

Tidal marshes are important ecosystems for silica (Si) cycling in the land-ocean-transition zone (Struyf & Conley 2009). In these ecosystems the dissolved silica (DSi) which originates from weathering of silicate minerals (Garrels & Mackenzie 1971) is cycled through the vegetation (Norris & Hackney 1999). In tidal marshes diatoms and wetland grasses are the dominant plant taxa involved in the silica cycle (Struyf & Conley 2009).

Diatoms have an essential need for Si for their growth (Paasche 1980). During growth silicic acid is used to build up the cell wall called a frustule. Wetland grasses are also known to accumulate Si. These species take DSi up faster than expected from non-selective uptake of DSi with water (Raven 2003). The DSi is deposited in the plant as amorphous silica structures known as phytoliths (Kaufman et al. 1981). Therefore these Si accumulator species can have silica contents between 1-70 mg Si g^{-1} dry weight (Struyf and Conley (2009), supplemental information). Both, the diatom frustules and the plant phytoliths are referred to as biogenic silica (BSi) due to their origin.

The plant derived BSi will eventually be buried in the marsh soil. The burial however is not complete because of the high solubility of the plant derived BSi. At soil pH between 4-8 this material is 100-10,000 times more reactive than clay minerals, primary mafic silicates and feldspars (Fraysse et al. 2009). Dissolution processes in the marsh soil transform a part of the BSi back to DSi, which results in the enrichment of DSi in the pore water of marsh soils and can lead to concentrations of 100-600 µmol L^{-1} (Norris & Hackney 1999, Struyf et al. 2005b), which is below the saturation concentration of amorphous silica (Loucaides et al. 2008, Fraysse et al. 2009). Gravitational drainage of soil pore water into the tidal creeks creates a slow stream of seepage water highly enriched in DSi. During flood tide this seepage water mixes with inflowing water and increases its concentrations. During ebb tide the enriched flooding water leaves the marsh. Additionally, DSi is exported during the seepage phase. The latter period of the tidal cycle can be responsible for up to 90% of the total DSi export from tidal marshes (Struyf et al. 2006a).

In estuarine and coastal ecosystems diatoms build the base of the food web (Peterson & Howarth 1987, Sullivan & Monceriff 1990, Fry & Wainright 1991). The availability of DSi, which is an essential nutrient for diatoms, is thus a precondition for their growth. In eutrophic ecosystems DSi can become a limiting nutrient for diatom growth, decreasing their abundance in the ecosystem (Brush & Davis 1984). One possible consequence is a species shift towards non siliceous algae (Officer & Ryther 1980, Hecky & Kilham 1988), which may have negative effects on the ecosystem (Anderson et al. 2002). During times of DSi limitation marsh areas could mitigate growth limitation of diatoms in the adjacent

estuary due to the extra DSi input and thus play an important role for estuarine food webs (Norris & Hackney 1999, Hackney et al. 2000)

This hypothesis was recently supported by the work of Struyf and colleagues (2006a) who showed that in the Scheldt estuary only six tidal cycles were necessary to resupply the total monthly estuarine DSi load of 280 Mmol (Mmol = 10^6 mol). Vieillard et al. (2011) showed that the "summerly" DSi export of the Rowley salt marsh in Massachusetts, USA to the coastal zone equalled the DSi input of the Ipswich River. Despite the possible importance of tidal marsh systems for the DSi delivery to the coastal zone these areas have been not well recognized in recent estimates of DSi fluxes in coastal zones (Beusen et al. 2009, Dürr et al. 2011).

Until now, no study has investigated the silica distribution along an estuarine transect, but focused only either on freshwater or salt marshes from different geographical locations. This study evaluates for the first time the variability of Si in tidal areas along the inner Elbe estuary to better understand the role these areas play in the estuarine system and coastal Si cycle. This study compares DSi and BSi concentrations in one freshwater and two mesohaline tidal creek systems in the dyke foreland area of the Elbe estuary, northern Germany and applies geographic information systems (GIS) to estimate the DSi export from this areas.

3.3 Material and Methods

3.3.1 Sampling and analysis

Water sampling

From April 2010 to November 2011 an intensive sampling campaign took place at all three marsh sites (see Table 3.1 for sampling dates). At each sampling day, water samples were taken approximately every hour in the main creek of each sampling site to cover the seepage and the flood phase. All samples were surface samples, taken in the centre of the creek. The samples were filtered in the field using 0.45 μm nylon filters (Minisart®) and were stored in a cool box. In the laboratory they were stored at 4°C until analysis. Dissolved silica concentrations were obtained by using standard colorimetric techniques (Hansen & Koroleff 1983). It was assured that all chemicals and samples had no contact with glassware during handling and analysis and never froze.

Salinity, temperature and pH of the samples were measured in the field with handheld sensors (ConOX, WTW; Primatrode 6.0228.020, Methrom).

Samples from the estuary were taken aboard of the R/V "Prandtl" with a Niskin bottle from approximately one metre depth. Samples were filtered immediately through membrane filters ($\varnothing$ 47mm, 0.45μm; Sartorius) and were stored at 4°C until analysis in the laboratory (see above).

Soil sampling

Soil profiles were taken on 2010-07-25 and 2010-06-30 at the fresh and brackish site, respectively. At the salt marsh samples were taken on 2010-06-19 and on 2010-09-08 on the grazed and ungrazed side respectively. For sampling, a pit was opened from the soil surface to 40-135 cm depth. From each soil horizon one mixed sample over the depth of one horizon was taken and stored in a plastic bag. In the laboratory, the samples were homogenized manually.

For BSi analysis a subsample of the homogenized samples of each horizon were taken, sieved through a 400 μm mesh and freeze-dried. After drying, samples were pound carefully with a mortar and pestle to break down small soil pellets. No brute force was applied during this procedure to avoid pulverization of the sample.

For the analysis of BSi a variation of the DeMaster (1981) method was used. Approximately 30 mg of sediment per sample were leached in 40 ml 1% sodium carbonate (Na_2CO_3) in a shaking bath at 85°C. Aliquots were withdrawn at 3, 4, and 5 hours, neutralized in 0.021 M HCl and analysed for DSi (see above).

The amount of BSi was estimated from the intercept of the linear regression line through the time course aliquots. If no variation of DSi concentration during the time course was detected, the mean of all three time point was taken as the final BSi concentration in the sample. We are aware that the wet-alkaline extraction is prone to additional release of DSi from amorphous mineral silicates present in the soil. The term BSi for soil samples is therefore not exact, but for reasons of readability we use this term to refer to plant and soil derived BSi in following sections.

Samples for soil density were taken after the method described in (Eckelmann et al. 2006) using a handheld corer with a total volume of 100 cm^3. Soil density was measured at the Institute of Soil Science, University of Hamburg.

3.3.2 Digital elevation model and monitoring database

To quantify the potential DSi export from the sampling sites and to place our data in a larger ecological context, we assessed the DSi export using GIS. Therefore a digital elevation model (DEM), water level data from gauge stations along the estuary, and DSi concentrations measured during two cruises along the Elbe estuary in July 2010 and 2011 were used together with the DSi concentration data from the marsh sites.

The DEM was provided by the State Office for Agriculture, Environment and Rural Areas, Schleswig-Holstein, Germany (Amtliche Geobasisdaten Schleswig-Holstein, © VermKatV-SH). It was obtained by LIDAR technique in 2007 and included corrections for different vegetation cover, leading to an overall vertical accuracy of +/- 20 cm. The resolution of a raster cell was 1x1 metre (see Figure 2.3, right panels).

To assess the watershed area of the sampling creeks in the DEM we firstly marked the creeks at its outlet. To assure that the creek visible in the DEM was the sampling creek, we compared them with the Microsoft Virtual Earth (© 2009 Microsoft Corporation) Map, which is linked into the ArcGIS software (ESRI® Version 10.0).

In the next step the watershed of each creek point was calculated by applying the "flow direction", "flow accumulation", "fill" and finally the "calculate watershed" function in ArcGIS for the creek points. The obtained watershed was in good agreement with the drainage network design described in section 2.2, which confirmed that the DEM could reproduce the main features of the drainage network (see Figure 2.3). The watersheds were then corrected manually to fit the watershed of the main drainage creek. This was done using the Microsoft Virtual Earth© Map.

For each sampling station the nearest gauge station was chosen to obtain the water level of every sampling time point (Figure 2.2). The accuracy of these data was +/- 2 cm. Because the gauge stations were located in the channel of the Elbe differences in water height between the marsh areas and the river were possible. We checked for these

differences with data from water level sensors which were placed in the same or in an adjacent creek. Because these water level sensors were removed prior to the end of our study, we used the water level data from the gauge station in the Elbe. Good agreement between the two measurements was found (water level$_{river}$ = 1,0367 * water level$_{marsh}$-0.0533, R^2 = 0.9658). Because of the higher uncertainty of the DEM elevation, we assumed that the use of the gauge data in the main stream was sufficiently accurate for our approach.

Export calculations

For the export calculation we applied the equation published in Neubauer and Anderson (2003). Firstly, for each set of adjacent time point during ebb tide *t(i)* and *t(i+1)* the average DSi enrichment (DSi$_{enrichment}$, mmol m^{-3}) was calculated (Eq.)

$$DSi_{enrichment} = DSi_{marsh} - DSi_{river}$$
<div align="right">Eq. 3.1</div>

where DSi$_{marsh}$ is the DSi concentration measured in the tidal creek at high tide and DSi$_{river}$ is the DSi concentration in the estuary obtained during the the two Elbe cruises in July.

To calculate the DSi export per ebb tide (DSi$_{export}$, mmol tide^{-1}) the DSi$_{enrichment}$ was multiplied by the change in volume (*V*, in m^3, Eq) between two sampling time points. The volumes at each sampling time point were calculated for each sampling site with the DEM and the water level from the nearest gauge using the build in function "Surface Volume" of the ArcGIS software (ESRI® Version 10.0). This calculation was done with the original DEM elevation and an elevation which was 20 cm lower to account for the uncertainty of the DEM due to vegetation cover.

$$DSi_{export} = \frac{(DSi_{enrichment,t(i)} + DSi_{enrichment,t(i+1)})}{2} * (V_{t(i)} - V_{t(i+1)})$$
<div align="right">Eq. 3.2</div>

To obtain the DSi flux from the sampling sites the mean DSi$_{export}$ was calculated from the original and the -20 cm DEM and was then divided by the area of the sampling site. For the extrapolation to the whole Elbe estuary the fluxes from the fresh, brackish and saline sampling site were multiplied with the total dyke foreland area of the respective salinity

class in the Elbe estuary (Table 2.2). The total DSi flux from the dyke foreland of the Elbe estuary was calculated by summing up the individual fluxes of the three salinity classes.

It is important to note that the calculated DSi export only represents the bulk phase of the ebb flow. The contribution of the seepage phase is not included in Eq. 3.2. Furthermore evapotranspiration is not included in the DSi export calculation.

3.3.3 Statistics

To test for differences of DSi and BSi concentrations between the three sampling sites (fresh, brackish, saline) the nonparametric Mann-Whitney U-Test was used, because samples were not normally distributed. All statistical analyses were carried out in STATISTICA 8.0 (StatSoft Inc.).

3.4 Results

3.4.1 Physical characteristics of the sampling sites

A clear salinity gradient between the sites was detected (Table 3.1). Salinity increased about 4 units between the fresh and the brackish site and about 11 units between the brackish and the saline site, respectively. There was no clear seasonal pattern of salinity at all sites.

Temperature showed a seasonal signal with lowest temperatures in March and November and highest in July. The freshwater site had on average the lowest temperatures throughout the year never exceeding 20°C. At the brackish and the salt marsh maximum temperature reached 27.9 and 32.9°C, respectively.

The pH showed high variability at all three sites and did not show a seasonal signal.

3.4.2 Silica concentrations of the fresh, brackish and saline sampling site

Temporal development of seepage DSi concentrations
DSi concentrations throughout the year differed between sampling sites and tidal phases. Average DSi concentrations were lower during the bulk tidal phase (Figure 3.1 A) than during the seepage phase (Figure 3.1 B).

Bulk DSi concentrations at the fresh and brackish site showed a seasonal pattern with lower concentrations in spring and summer and higher concentrations in autumn. At the saline site no such trend was detected and DSi concentrations stayed at the same level the whole year. The similar bulk and seepage concentrations at the saline site in 2011-07 were caused by an afflux of seepage water at the sampling location. Also at the saline site, there was no bulk inflow of estuarine water during the sampling in 2011-03; due to a very low high tide, therefore this data point is missing in Figure 3.1 A.

At the freshwater site seepage DSi concentrations did not follow a seasonal pattern (Figure 3.1 B). Maximum concentrations of 299 µmol L^{-1} were reached in July while the September concentrations were the lowest during the year, with 235 µmol L^{-1}. The seepage water DSi concentration at the brackish site showed a clear seasonal pattern with minimum concentrations in March and maximum concentrations of in November. In 2010 concentrations nearly doubled from March to November from 270 to 535 µmol L^{-1}. In 2011 concentrations also doubled between March and November, but on a lower level.
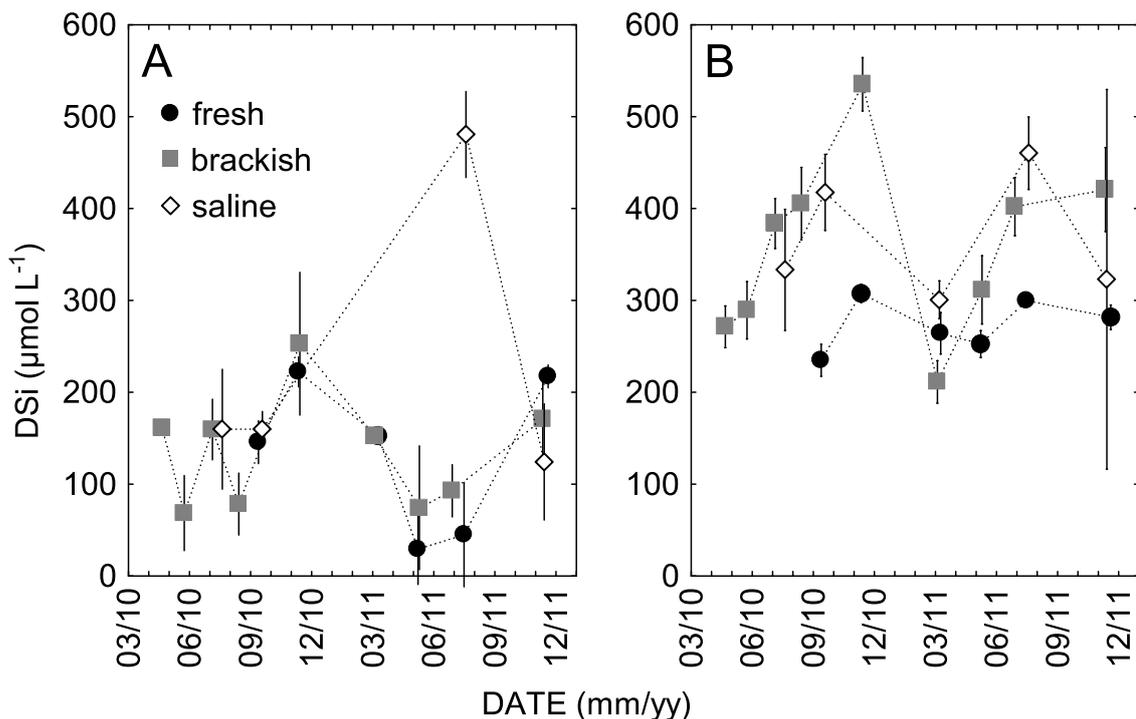
Figure 3.1 Temporal development of the mean ± standard deviation DSi concentrations of the bulk (A) and seepage phase (B) of all three salinity types. No data of bulk DSi concentrations was available in 2011-03 (see text for explanation). The number of measurement for each data point ranged between 1-11 for both bulk and seepage phase. Note that the dotted lines also connect non adjacent data points for visual guidance and readability.

21

At the saline site DSi concentrations also increased during the course of the year. Due to the low temporal resolution the pattern is less clear than at the brackish site.

On 2011-03-14 (Figure 3.2) the water level in the Elbe estuary was low and did not enter the creek of the saline sampling site, which made it possible to observe the development of the DSi concentrations in the seepage water over a period of twelve hours.
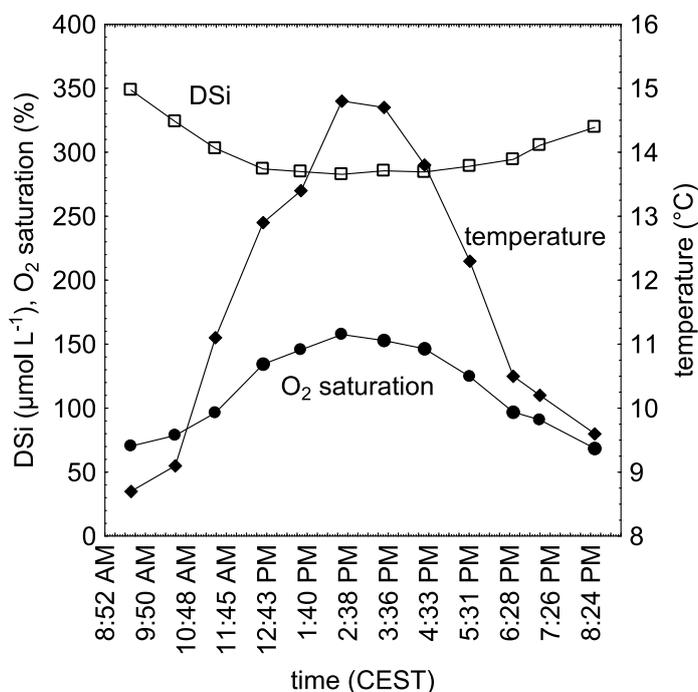
Figure 3.2 Diurnal pattern of DSi, O_2 concentrations and temperature of seepage water at the saline site on 2011-03-14. The sampling time is given in Central European Summer Time (CEST). During this sampling the creek was not flooded and only out-flowing seepage water was sampled.

During the first four hours of sampling DSi concentrations dropped with a rate of 20 $\mu mol\ L^{-1}\ h^{-1}$ from 348.6 $\mu mol\ L^{-1}$ at 8:52 a.m. to 282.7 $\mu mol\ L^{-1}$ at 12:43 p.m. DSi concentrations stayed at the same level until 5:31 p.m. when they started to raise again. The drop in DSi concentrations was accompanied by an increase of dissolved oxygen saturation from 70% to 150% in the seepage water until 2:38 pm. Afterwards oxygen saturation decreased to the initial level.

Spatial distribution of DSi and soil BSi concentrations

The comparison of the mean seepage DSi concentration and soil BSi concentrations of the three sampling sites showed that the concentrations follow opposed trends along the salinity gradient (Figure 3.3).

The average seepage DSi concentrations were significantly lower at the freshwater site (p< 0.01) and increased, yet non-significantly, towards the saline site.

Table 3.1 Summary of physico-chemical parameters of all samplings. N is the number of samples taken at the sampling day. Normally, samples were taken every hour with the exception of 2010-05-25 at the brackish site, where samples were taken every 30 minutes during the flooding. For salinity, temperature and DSi concentrations minimum values where normally measured during flooding and maximum values during seepage phase. For pH no such relationship could be observed.

| site	date	N	pH (NBS)			temperature (°C)			salinity			DSI (μmol L^{-1})		
			mean	min	max	mean	min	max	mean	min	max	mean	min	max
fresh	2010-9-15	8	7.89	7.66	8.31	16.0	15.1	16.9	0.3	0.3	0.3	168.0	121.6	247.2
(HDM)	2010-11-15	12	7.84	7.73	7.99	8.3	7.3	10.0	0.3	0.3	0.3	243.5	201.5	316.4
	2011-3-16	12	8.56	7.94	8.83	4.2	1.8	5.5	0.4	0.2	0.4	217.7	150.8	291.4
	2011-5-16	12	7.76	7.52	7.96	14.0	12.6	14.7	0.4	0.4	0.5	85.2	7.6	262.6
	2011-7-25	7	7.74	7.57	7.92	17.8	17.5	18.7	0.5	0.5	0.5	81.4	10.4	299.5
	2011-11-30	7	7.94	7.78	8.05	6.2	5.7	6.5	0.5	0.5	0.5	235.7	209.1	291.1
brackish	2010-4-22	12	8.23	7.77	8.51	12.1	7.3	15.2	2.9	2.3	3.3	262.1	161.3	283.7
(NF)	2010-5-25	15	8.28	7.94	8.58	15.6	11.4	18.4	2.9	2.0	3.9	127.4	21.4	319.8
	2010-7-7	11	8.27	7.99	8.45	25.5	18.7	30.2	4.7	3.8	5.5	322.6	122.4	412.4
	2010-8-16	10	8.10	7.83	8.37	21.9	20.3	24.1	4.5	3.0	5.4	307.3	58.5	440.5
	2010-11-17	8	8.02	7.75	8.31	6.3	5.7	6.8	2.7	1.4	3.4	429.4	195.0	566.3
	2011-3-11	12	8.11	7.77	8.57	6.8	3.3	9.8	2.3	2.1	2.7	186.8	147.4	240.0
	2011-5-18	12	8.20	7.66	8.93	20.1	15.7	23.6	5.1	4.9	5.4	232.4	31.3	361.0
	2011-7-7	12	7.99	7.72	8.35	27.5	22.1	32.9	6.3	5.8	6.8	273.2	66.0	445.2
	2011-11-22	7	8.24	8.21	8.30	4.6	3.7	5.6	5.6	5.3	5.9	277.8	138.4	458.6
saline	2010-9-21	12	7.90	7.65	8.08	16.0	12.8	18.5	13.2	12.5	14.4	374.6	146.2	459.5
(DSK)	2011-3-14	12	7.97	7.80	8.13	11.7	8.7	14.6	12.0	11.5	12.8	300.7	282.7	348.6
	2011-7-28	8	7.97	7.80	8.35	24.4	19.9	27.9	18.7	17.9	19.5	467.8	399.5	525.6
	2011-11-11	8	7.98	7.72	8.07	7.0	6.2	7.6	19.1	15.8	20.5	198.7	69.2	561.2
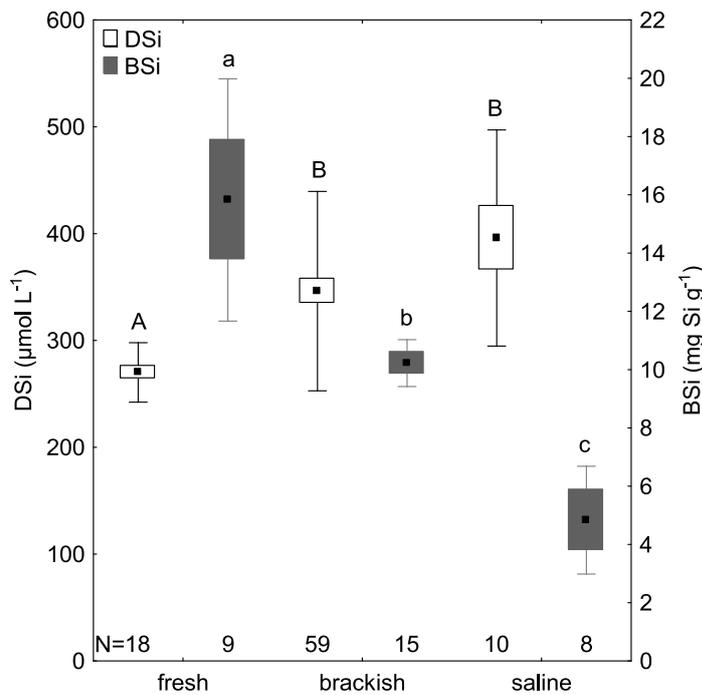
Figure 3.3: Averages of all seepage DSi concentration measurements (white) and depth integrated BSi concentrations (grey) of the three sampling sites along the salinity gradient. Depth was integrated over 40 cm. Whiskers indicate the standard deviation of the mean, boxes are the standard error. In each group (DSi or BSi) different letters indicate a statistically significant difference between the concentrations. The differences in DSi concentrations were significant with $p < 0.01$. For the BSi concentrations the significant differences were significant with $p<0.05$. N indicates the number of total measurements.

The soil BSi contents opposed the increasing trend of the seepage DSi concentrations along the salinity gradient. A statistically significant decrease of about 50% between each salinity class was observed (Figure 3.3).

DSi export in July

The DSi export from the sampling sites were calculated for July using DSi concentration data obtained during two cruises in 2010 and 2011. The distribution of DSi concentrations along the Elbe estuary is shown in Figure 3.5.

The results of the DSi export calculations of the individual samplings in July are shown in Figure 3.4. The DSi export from the fresh site is 2.0 ± 0.4 mmol m^{-2} tide^{-1}. At the brackish site the DSi export in 2010 was lower than in 2011 and in the range of the freshwater site. At the saline site the export is 2 to 3.5 times higher than at the other two sampling sites and reaches 4.6 ± 1.1 and 7.3 ± 1.7 mmol m^{-2} tide^{-1} in 2010 and 2011, respectively.

Extrapolation of the average DSi exports shown in Figure 3.4 to the area of the whole dyke foreland of the respective salinity is summarised in Table 3.2. The DSi export from the saline dyke foreland is highest followed by the freshwater class. Export from the brackish areas is about 40% smaller. In total 14.0 ± 2.8 Mmol DSi per month is exported from the dyke foreland areas of the Elbe estuary. Compared to the monthly DSi load of the Elbe estuary in July, the DSi export from the dyke foreland amounts to 52-70%.

24

3.5 Discussion

3.5.1 Temporal development of DSi concentrations along the salinity gradient

The seasonality observed in the bulk water of the fresh and brackish site clearly reflects the seasonality of the DSi concentrations in the Elbe estuary. From November till February the estuary receives water with high DSi concentration of 180-200 µmol L^{-1}. In March, April, and September and October intermediate concentrations of 60-100 µmol L^{-1} are common. From May to August concentrations stay below 20 µmol L^{-1} or can even reach the detection limit (all data taken from (ARGE 2000)). At the saline site DSi concentrations are similar in 2010-07 and 2010-09 which could be attributed to the morphology of the sampling site. Water that enters the tidal creek has travelled over extensive tidal flats and through a 1.8 km long tidal creek in the lower marsh. When it reaches the sampling location, it has mixed with outflowing seepage water and pore water from the tidal flat and no longer represents the DSi concentration in the estuary.

Seepage DSi concentrations at the brackish and saline sites increased during the course of the year. This observation was also made in a mesohaline marsh in North Carolina, USA where DSi pore water concentrations at three different depths nearly doubled between January and September (Norris & Hackney 1999). In a salt marsh in the Ems-Dollard estuary, The Netherlands, concentrations of 120-180 µmol L^{-1} were measured between August and November. During the rest of the year they were considerably lower with concentrations between 60-100 µmol L^{-1} (Dankers et al. 1984). A similar temporal pattern was also described in freshwater marshes of the Scheldt estuary, Belgium between January and July (Struyf
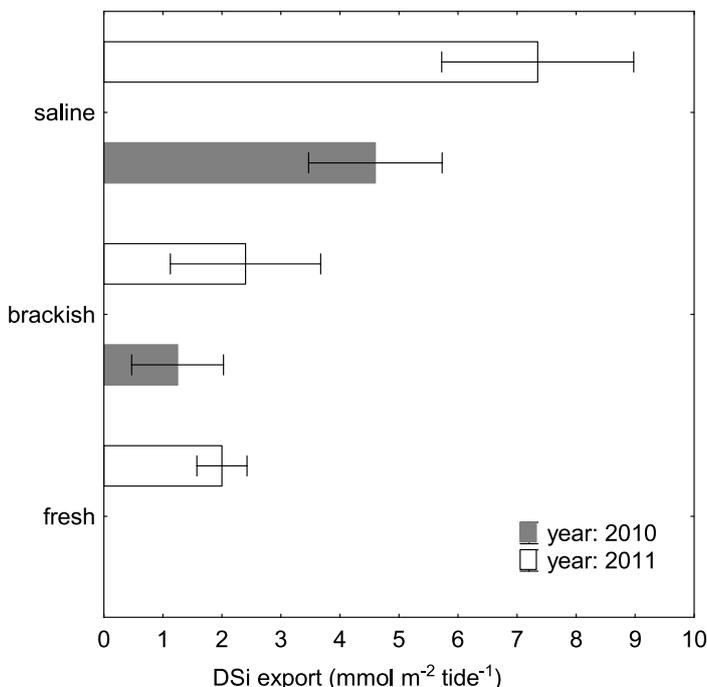

Figure 3.4: Areal DSi export from the three sampling location from 2010-07 and 2011-07. At the freshwater site no sampling took place in 2010-07.
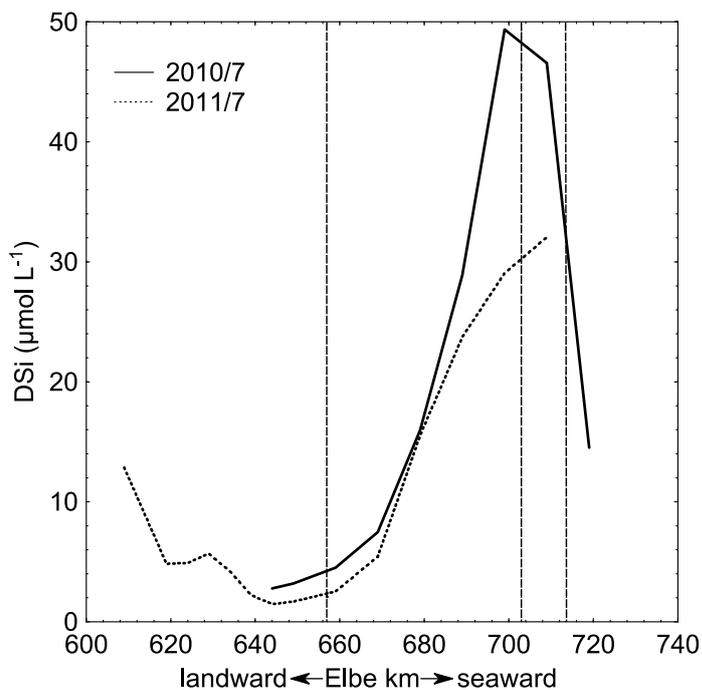
Figure 3.5: DSi concentrations in the Elbe estuary in 2010/7 and 2011/7 along the longitudinal axis of the estuary. The vertical dotted lines indicate the position of the sampling sites in the dyke foreland

et al. 2005b).

The increase of DSi concentrations towards July is most likely the result of higher temperatures (Table 3.1). BSi dissolution rates are doubled by a temperature increase of 10°C (Kamatani 1982). Thus more BSi is transformed into DSi during summer which leads to an accumulation of DSi in the soil pore water. At higher temperatures evapotranspiration is also increased, which lead to an up-concentration of dissolved matter in the soil solution further increasing the DSi concentrations.

Additionally BSi dissolution rates could be enhanced by biological activity, which is also stimulated under higher temperatures. Bacteria release exoenzymes which could break up organic matter coatings around BSi particles creating fresh weathering spots on the particle surface which enhances their dissolution (Bidle 1999, Bidle & Azam 2001, Roubeix et al. 2008a). Vascular wetland plants are known to release organic acids into the rhizosphere which enhance the dissolution of Aluminium oxy-hydroxides and can form organometallic complexes (Jones & Kochian 1996). Mucha and colleges (Mucha et al. 2010) could show for the salt marsh plant *Scirpus maritimus* and *Juncus maritimus* that the release of such substances is highest in summer and autumn. The organic acids could thus increase the solubility of BSi particles in two different ways. On the one hand organic acids could remove the Aluminium oxy-hydroxide coatings which form on BSi particles during aging. The removal of these coatings is known to increase the solubility of the aged particles (Michalopoulos & Aller 2004). On the other hand the organic acids could adsorb dissolved Aluminium from the soil pore water making it unavailable for the

26

formation process of Aluminium oxy-hydroxide coatings which would prevent aging of the BSi particles making them more susceptible to dissolution.

Table 3.2: DSi export from the total dyke foreland area of the Elbe estuary and its contribution to the total DSi load of the estuary (%-Elbe load) for the month of July. To calculate the monthly DSi load of the Elbe estuary a dataset from the monitoring station "Wehr Geesthacht", which is located at the beginning of the estuary, was used. The database covered the years 1996-2004 and included bi-monthly measurements of DSi concentration and monthly mean discharge from July.

salinity class	area (km^{-2})	dyke foreland DSi export ($Mmol\ month^{-1}$)		Elbe DSi load ($Mmol\ month^{-1}$)	% Elbe load
		mean	stdev		
fresh	40.6	5.1	1.1	22.9	18-27
brackish	20.7	2.3	1.4	22.9	4-16
saline	17.9	6.6	2.2	22.9	20-38
total	79.2	14.0	2.8	22.9	52-70

The fact that the influence of DSi uptake by plants is not visible in our data suggests that the above mentioned factors exert a stronger control on the DSi concentrations than the DSi uptake by plants itself. Struyf et al. (2005b) argued that the influence of plant uptake may not be visible if the DSi stock in the soil solution is high enough that the amount of DSi removed by plants is low in comparison to the total DSi amount in the soil solution.

DSi concentrations kept rising after July, which is the warmest month during the year (Table 3.1). This is surprising because declining temperatures decrease the above mentioned influence of temperature on the BSi dissolution. A possible explanation could be the extra BSi input from the plants which is added to the soil after the vegetation period. At this age they contain high amounts of easily dissolvable BSi (Norris & Hackney 1999, Struyf et al. 2005b, Querné et al. 2011). Additionally the cessation of DSi uptake by plants and benthic diatoms would allow the DSi concentrations to increase. Together, these two factors seem to outweigh the negative effect of low temperatures on the dissolution of BSi, further increasing the DSi concentrations in the seepage water.

The difference between the November and March DSi concentrations could be a result of the combined effect of low BSi dissolution rates at low temperatures and the constant dilution of soil pore water due to storm surge flooding, which allows a larger amount of water to infiltrate the marsh surface than flooding under non storm surge conditions

(Duve 1999) and precipitation. The low BSi dissolution rates cannot resupply the DSi which is washed out after the storm surges or rainfall events, which is reflected in the lower seepage DSi concentrations.

At the freshwater site the seasonal fluctuation of seepage DSi concentrations was less pronounced and the concentrations significantly lower than at the mesohaline sites. Two factors might explain these observations; the difference in soil-hydrology of the freshwater site and its lower salinity. At the freshwater site the saturated water conductivity of the soil is higher than at the brackish and saline site (see section 2.2.2). Therefore, the soil pore water residence time at the freshwater site may be lower as well. As a consequence the reaction time between the soil BSi and the pore water is shorter and result in lower DSi equilibrium concentrations, as shown by Gerard et al. (2002) for an acidic brow soil. Additionally, low salinity further impedes BSi dissolution. Loucaides and colleagues (2008) showed that the dissolution rates of fresh diatom frustules increased 2.7 or 4-fold if the salinity increases from 0 to 3.5 or 8.75, respectively. The corresponding salinity increase from the fresh to the brackish or saline site was 4 and 15 units, respectively. The observed decrease of soil BSi concentrations from the freshwater to the saline site, from about 16 mg g^{-1} to 5 mg g^{-1} therefore might be the result of overall higher BSi dissolution rate at the brackish and the saline site.

However, salinity might not be the only variable that controls the BSi concentration in the soils. It could be possible that the BSi input is just highest at the freshwater site. Therefore the factors that control the BSi input should also be considered. These factors are vegetation cover and net sedimentation.

Wetland grasses contain high amounts of BSi. With their ability to accumulate silica they can alter the BSi content of the soils because not all of the incorporated silica is dissolved after the vegetation period and is stored in the soil matrix. Struyf et al. (2005b) showed, that the sediment under *P. australis* stands in a tidal freshwater marsh in the Scheldt estuary contained more BSi than under stands of other plant species. The BSi content of *P. australis* was one to two orders of magnitude higher than in the other plant species, indicating that the difference in plant BSi concentrations could have caused the different soil BSi contents. However, to quantify the influence of different plant species on the soil BSi concentrations plant production data is necessary. Unfortunately, no such data exists

for the sampling sites, that only a qualitative discussion about this factor can be made. We did not measure plant BSi contents in our study but can infer typical plant BSi contents from the literature (Table 3.3). The dominant vegetation cover of the freshwater sampling site was meadow / scrubs and *Glyceria maxima / Phalaris arudinaceae* which contain less BSi than *P. australis.* At the brackish site *P. australis* was dominant with 43% coverage. Following the assumption that the soil BSi concentration reflects the plant BSi concentration the brackish site should have the highest soil BSi concentrations, which was not the case. At the saline site the BSi content of the dominant plant species also did not match with the soil BSi content.

Sedimentation may import considerable amounts of BSi to the marsh surface, as was shown for tidal freshwater marshes in the Scheldt estuary (Struyf et al. 2005a, Jacobs et al. 2008). The BSi delivery to the marsh surface due to sedimentation depends on the quality of the suspended matter and its quantity. Sedimentation of small amounts of diatom and phytoliths rich sediment can lead to higher BSi delivery as sedimentation of huge amounts of BSi depleted sediments. Mean annual sedimentation rates in the dyke foreland of the Elbe estuary which were measured from 2010-03 to 2011-03 at the fresh, brackish and saline site showed values of 2445 ± 1607 g m-2 yr-1, 3079 ± 1875 g m-2 yr-1 and 1050 ± 609 g m-2 yr-1, respectively (data from Butzeck et al., in prep.). Most of the sediment is deposited on the marsh surface in winter when storm surges frequently occur (Duve 1999, Müller et al. in press). It can be assumed that the BSi in winter consists mostly from phytoliths, which were brought into the river by soil erosion (Cary et al. 2005). In summer a substantial amount of the total BSi can consist of diatoms (Carbonnel et al. 2009). In the Elbe estuary diatom concentrations are highest in the freshwater part and decline towards the brackish part due to unfavourable growth conditions and subsequent die-off (Wolfstein & Kies 1995, Kerner 1997). In the brackish part suspended matter accumulates due to higher residence times than in the upstream parts (Herman & Heip 1999), which includes the remaining diatom frustules from the freshwater zone. The brackish part of the estuary should thus have the highest BSi concentrations and BSi components of similar quality (fresh diatom frustules) than the freshwater part.

Table 3.3: Compilation of the dominant vegetation types at the sampling sites. The BSi concentrations of the plant species were taken from the literature to complement the soil BSi data which were measured in this study.

Salinity class	Vegetation type[a]	ASi content (mg g^{-1})	Source
fresh	meadow / scrubs	n.d.	
	Glyceria maxima / Phalaris arudinaceae	~13 / ~12	(Schoelynck et al. 2010)
	Typha angustifolia[+]	3.7	(Lanning & Eleuterius 1983)
	Phragmites australis	15 - 60	(Lanning & Eleuterius 1983) (Struyf et al. 2005b, Schoelynck et al. 2010)
	woodland	n.d.	
brackish	*Phragmites australis*	15 - 60	(Lanning & Eleuterius 1983) (Struyf et al. 2005b, Schoelynck et al. 2010)
	Elymus athericus	13.8, 16	(de Bakker et al. 1999, Bauer 2010)
	meadow	n.d.	
saline	*Festuca rubra*	11.5, 12	(Bauer 2010)
	Elymus athericus	13.8, 16	(Lanning & Eleuterius 1983, Bauer 2010)
	Puccinellia maritima	5.5	(Bauer 2010)

[a] only vetetation types with a cover of ≥ 10% were listed, exception Puccinellia maritime

n.d.: no data

Together with the high sedimentation rates, the brackish sampling site should receive the highest amounts of BSi. The fact that the soil BSi concentrations at the brackish site is lower than at the freshwater site suggests that the excess BSi deposit at the brackish site compared to the freshwater site is lost. One possibility could be the erosion of BSi from the site, but erosion data is missing to proof this hypothesis.

The effect of salinity on dissolution rates of BSi could explain the observed pattern reasonable well and would explain the overall higher seepage DSi concentrations at the mesohaline sites as well as the decreasing soil BSi concentrations along the salinity gradient.

Diurnal patterns of seepage DSi concentrations

DSi uptake by vegetation and benthic diatoms during the course of the day was studied for the saline site (Figure 3.2). In March 2011 the high water did not reach the sampling location and as a result only seepage water was sampled over a 12 h period during the day. A decrease of DSi concentrations by 18.9% in the first four hours of sampling was

measured. The decrease was accompanied by raising temperatures and increasing oxygen saturation of the seepage water. Latter observation suggests that the DSi concentration decrease is due to uptake by benthic diatoms, supported by the observations of biofilms in the creek bed (A. Weiss, field obs.). Despite the fact, that DSi uptake in diatoms is not directly coupled to their primary production (Brzezinski 1992, Claquin et al. 2002), light availability seems to enhance it (Bartoli et al. 2003, Leynaert et al. 2011), which would explain the diurnal pattern of the DSi concentration.

This observation has important implications for the DSi export from the dyke foreland area of the Elbe estuary and possibly of other tidal marsh systems as well. Because of the biological uptake of DSi, the DSi export from those sites during daylight will be significantly lower than during the night. Higher irradiance and longer light periods in April to September in comparison to March may decrease DSi concentrations even more. Future studies should therefore include nightly sampling to assess difference in DSi export during day and night time.

3.5.2 DSi export

The DSi export was calculated for the month of July for all three sampling sites in order to assess the influence of the dyke foreland areas on the estuarine DSi concentration. The individual samplings showed the highest export rates at the saline site and similar export at the brackish and freshwater site. The differences between the fresh, brackish and saline systems in the Elbe estuary are likely a result of the morphology of the saline site and not a result of the different DSi concentrations at the sampling sites. At the saline site the flooding water flows over extensive tidal flats and through a 1.8 km long channel before entering the sampling creek. It mixes with seepage water which is enriched in DSi and therefore already has high DSi concentrations when it reaches the sampling creek, which can be seen in the tidal patter of DSi concentrations (see Appendix 1).

The spatial separation of estuarine water and sampling site by tidal flats and tidal creeks causes an overestimation into the DSi export calculation. The assumption that all DSi enrichment happens in the sampling creek is no longer valid when the above mentioned morphological features are present. Thus the here applied method for the DSi export calculation most likely overestimates the DSi export of the saline site.

At the brackish and the freshwater site the tidal flats are less extensive and there are no long tidal creeks through which the flooding water has to pass. The DSi concentration of the inflowing water at the fresh and brackish site is therefore closer to the estuarine value (see Appendix 1) and the error associated with Eq. 3.1 lower.

The values from the freshwater site lie in the range of those measured by Struyf and colleagues in a tidal freshwater marsh in the Scheldt estuary, Belgium (Struyf et al. 2006a) There, DSi export ranged from 0.2 mmol m^{-2} tide^{-1} to 7.7 mmol m^{-2} tide^{-1} around the year. Another study from the same tidal marsh reported a DSi export of 15.5 mmol m^{-2} tide^{-1} for the month of July (Struyf et al. 2005a).

Because the DSi export calculation of the study at hand does not include the seepage phase, which can be the most significant contributor to the total DSi export (Struyf et al. 2005a, Struyf et al. 2006a) export rates are likely to be underestimated. The magnitude of seepage flow was not assessed, but data from a study published in 1999 (Duve 1999) showed that the seepage flow from a mesohaline tidal creek in the dyke foreland of the Elbe estuary in July, was 0.005 m^3 m^{-2} tide^{-1}. If we use this value and the mean seepage DSi concentration at the brackish site from 2011-07 (445 µmol L-1) to calculate the seepage DSi export, we derive a seepage DSi export of 2.2 mmol m^{-2} tide^{-1}. The mean DSi export during bulk phase was 1.8 mmol m^{-2} tide^{-1}. Thus the DSi export during the seepage phase would account for 54% of the total export and should be taken into account in future studies.

The extrapolation of the DSi export to the whole dyke foreland area in the Elbe estuary showed that the tidal exchange could be an important contributor of DSi to the estuary. The fresh and the brackish areas contribute equally to the DSi load of the estuarine system in July. The saline site seems to be most important in terms of DSi input into the estuary but the results have to be interpreted with caution because of the above mentioned uncertainties of the DSi export calculations.

As already mentioned by Struyf and colleagues (Struyf et al. 2005a, Struyf et al. 2006a) the DSi export from marshes in the freshwater part of estuaries might sustain diatom growth in times of DSi limitation. The DSi input in the brackish part of the estuary however does not directly promote diatom growth in the estuarine channel because of

the light limiting condition in this part of the system (Wolfstein & Kies 1995). The DSi input from the brackish part can accumulate in the estuarine water because of the higher residence time of the brackish part of the estuary in comparison to the upstream freshwater part. The accumulation of DSi forms a leaky reservoir towards the North Sea, from which DSi is mixed into the coastal water (see Figure 3.5). The DSi from the dyke foreland areas in the brackish zone might therefore not be reducing the DSi limitation in the estuary itself but providing additional DSi to the coastal waters where it may also prolong diatom growth.

The DSi export numbers from the dyke foreland areas seem to be the same order of magnitude as DSi export rates from pyroclastic flows and fresh volcanic rocks in humid areas. DSi fluxes in such areas can reach of up to 1.4 Mmol Si km^{-2} a^{-1} (Beusen et al. 2009, Hartmann et al. 2010). If the monthly DSi export rates from the fresh and brackish zone of the Elbe estuary are converted into annual export rates, the DSi export of each zone is of similar magnitude as the export from pyroclastic flows and fresh volcanic rocks (1.5 and 1.3 Mmol Si km^{-2} a^{-1}). In the Scheldt estuary, Struyf and colleagues (Struyf et al. 2006a) have shown that the marsh areas can replenish the total DSi load of the estuary. In their study only six tidal cycles were necessary to deliver the total amount of Si transported by the estuary in summer. Another study conducted in a salt marsh system in Massachusetts, USA (Vieillard et al. 2011) could also show that the DSi delivery by the salt marsh could equal the DSi input of a small river, stressing the importance of tidal marsh areas in the coastal silica cycle.

The extrapolated DSi exports however have to be seen as a first estimate and more precise data is needed to reduce the uncertainty of the flux calculations. The lack of DSi flux measurements during the seepage phase of one tidal cycle, as discussed above, could introduce an error of at least 50% or more into the DSi export calculations. In other tidal marsh exchange studies the contribution of the DSi export during the seepage phase can be as high as 90% due to the very high DSi concentrations in the seepage water (Struyf et al. 2006a). The combination of low water volumes and high DSi concentrations (up to 556 µmol L^{-1}, Table 3.1) outweigh the high volumetric exchange combined with low DSi concentrations during the bulk tide (Struyf et al. 2006a).

Another problem is associated with the use of the DEM for the DSi export calculations. To derive the correct water volume from the DEM the model has to represent the creeks and drainage ditches at the sampling watersheds. The comparison with aerial photos confirmed that the large creeks and ditches were reproduced correctly by the DEM (Figure 2.3). However the extend of smaller drainage ditches were not reproduced correctly. The reason for this underestimation of the creek length is the interference of vegetation in the LIDAR technique. If the vegetation covers the channel the incoming laser impulses cannot penetrate to the channel bottom, which leads to a false elevation in the DEM. The elevation bias on the marsh surface which is associated with the vegetation cover may not be influencing the DSi export calculation strongly because during the July sampling the flooding water was confined into the creeks. The volume which was calculated with the DEM is therefore only sensitive to errors of the creek bed elevation.

The elevation bias was shown to be highest in tidal creeks where the real elevation is overestimated (Chassereau et al. 2011). That means that in reality the creek bed elevation is lower than represented in the DEM. Overestimation of the DEM elevation leads to an underestimation in the volume of the creek channel network. Because of the volume term in Eq. 3.2 the DSi export would also be underestimated. All in all the DSi export rates in this study seem to be underestimated, but nevertheless provide a first insight into the silica cycle of the Elbe estuary and add new data to the few yet existing marsh DSi export values.

3.6 Conclusion

For the first time the distribution and temporal variability of DSi and BSi along a salinity gradient in the same estuarine system was analysed. The combination of field sampling and GIS-calculations can be used to estimate potential DSi export fluxes from the dyke foreland of the estuary. Results suggest that specifically the export of DSi during seepage phase needs to be included in the calculations.

The complex relationship between abiotic and biotic factors, which influence the distribution of silica in watersheds lead to a textbook like distribution of BSi and DSi concentrations along the salinity gradient. The tidal exchange in the Elbe estuary seems

to play an important role as DSi supplier to the system and stress the importance of tidal marsh areas for the water quality in eutrophied estuaries.

4 The role of salt marshes in the silica budget of the North Sea

4.1 Abstract

Local studies showed that salt marshes are effective recyclers of silica and could significantly attenuate the DSi limitation in coastal waters during summer months by net-exports of DSi. These observations lead to the hypothesis that salt marshes can be significant sources of DSi to the North Sea during summer months also at the regional scale. To test this hypothesis, we extrapolate DSi fluxes reported by local studies to salt marsh areas adjacent to the North Sea. The resulting annual average contribution of salt marshes to the DSi budget of the North Sea amounts to 0.7% of the annual riverine inputs to the North Sea. During summer, this contribution still does not exceed 2.4%. Thus, the hypothesis is rejected for the North Sea, and it is concluded that salt marsh DSi fluxes need not to be included in DSi budgets of regional seas. However, for smaller regions with favourable geographic conditions of low river inputs and large marsh areas, like in this study the English Channel, salt marsh DSi exports can be a significant contribution to coastal DSi budgets during summer.

4.2 Introduction

Dissolved silica (DSi) is an important nutrient in coastal marine ecosystems (Schelske & Stoermer 1971, Officer & Ryther 1980). It originates from chemical weathering of silicate rocks (Derry et al. 2005) and is delivered to the oceans by rivers (Tréguer et al. 1995, Laruelle et al. 2009, Dürr et al. 2011). Silica can be retained in rivers and lakes (Lauerwald et al. 2013) before reaching estuaries, which can act as filters and also shift the seasonal distribution of DSi inputs into the oceans (e.g. Arndt et al. 2009). Particularly during the main growing season, when river DSi exports decline (e.g. for the Rhine (Hartmann et al. 2011)), the absence of DSi may lead to harmful blooms of non-diatom algae (Smayda 1990, Hallegraeff 1993).

Tidal marsh systems were hypothesized to function as buffer attenuating the seasonal DSi limitation in coastal marine environments (Hackney et al. 2000). This hypothesis is

supported by local studies showing that tidal marshes export DSi to the adjacent water bodies (Dankers et al. 1984, Struyf et al. 2005a, Struyf et al. 2006a, Vieillard et al. 2011, Müller et al. in press) because they are effective biogenic silica (BSi) recyclers. The BSi pool is built up during the growth of marsh vegetation and diatoms, and by the trapping of sediments containing BSi. The BSi accumulated in the marsh soils dissolves rapidly, because of its high dissolution rate compared to clay minerals (Fraysse et al. 2009). The resulting DSi accumulates in the pore water and is exported from the marsh via diffusive exchange during high water and most importantly by advective drainage through the tidal creeks (Struyf et al. 2005a). For example, the tidal marsh areas of the Scheldt estuary, Belgium, were reported to be able to deliver the total monthly DSi river load (minimum 1.78 kmol month^{-1}) in only a few days (marsh DSi export 0.35-0.71 kmol per tidal cycle) (Struyf et al. 2005a).

Continental to global scale studies on terrestrial DSi mobilization (Hartmann et al. 2010, Jansen et al. 2010, Moosdorf et al. 2011) or its input into coastal waters (Beusen et al. 2009, Dürr et al. 2011, Tréguer & De La Rocha 2013), as well as silica budgets of regional seas (Proctor et al. 2003) do not account for the effect of DSi fluxes from tidal marshes. The findings from local studies lead to the hypothesis that the DSi fluxes from salt marshes would be significant also on larger scales. In this study, we test this hypothesis for the North Sea.

4.3 Materials and Methods

Four local studies that quantify the area specific DSi exports from salt marshes can be used for upscaling to the salt marsh area around the North Sea coast (Table 4.1). These studies derived their DSi export fluxes from direct discharge and DSi concentrations measurements in tidal creeks over at least one tidal cycle. The average specific DSi flux of the studies is 0.14 Mmol km^{-2} a^{-1} (Table 4.1).

Three other works which report DSi exports from salt marshes were discarded from this selection, because the DSi fluxes from the salt marshes were blurred by external DSi inputs to the marsh areas (Daly & Mathieson 1981, Imberger et al. 1983, Poulin et al. 2009). These fluxes would have been very small (0.01 Mmol km^{-2} a^{-1} for the Pointe-aux-Epinettes salt marsh (Poulin et al. 2009) and 0.03 Mmol km^{-2} a^{-1} for the Crommet creek marsh (Daly & Mathieson 1981), and 0.004 Mmol Si km^{-2} a^{-1} for the Duplin River, Georgia

(Imberger et al. 1983)) Influxes by streams or groundwater render the salt marsh area not representative for the reported DSi flux. Further, studies quantifying diffusive DSi flux (Scudlark & Church 1989) cannot be used to represent total DSi fluxes (Struyf et al. 2005a) and were thus also not regarded in this study.

Table 4.1: Literature values of dissolved silica fluxes from salt marshes.

Reference	Location	Flux (Mmol km^{-2} a$^{-1)}$	Description
Dankers et al. (1984)	Ems-Dollard Estuary, The Netherlands	0.11	low marsh, on average slightly above high tide level
Struyf et al. (2006a)	Carmel Polder, France	0.33	young marsh, macrotidal waters
Müller et al. (in press)	Söhnke-Nissen Koog, Germany	0.09	low salt marsh (0.9 - 2.6 m NHN), high flooding frequency
Müller et al. (in press)	Dieksanderkoog, Germany	0.05	higher elevated salt marsh (1.2 - 2.8 m NHN)
Vieillard et al. (2011)	Rowley, MS, U.S.A.	0.04	fully established, large mature marsh; data only from July

The average specific DSi flux of the four included studies was extrapolated to the salt marsh areas tributary to the North Sea. To evaluate the significance of the DSi flux from salt marshes in the marine DSi budget, the DSi flux from salt marshes was included into an existing DSi budget of the North Sea (Proctor et al. 2003), which represents advective flux in the ocean, benthic flux, river transport, and internal fluxes within five "boxes" of the North Sea and the English Channel. The boxes were defined by Proctor et al. (2003) as regions with similar hydrodynamic behaviour, which are:

"1. The area of the northern North Sea between the Dooley current (57.758 N) and north of the Dogger Bank, all stratified water;

2. Stratified water around the Dogger Bank, bounded in the north by Box 1, in the south by the tidal front, and in the east by the coastal area affected by the river discharges;

3. Well-mixed waters of the southern North Sea;

4. The river plume dominated areas of the German Bight; and

5. The well-mixed English Channel"

The spatial extent of the Boxes is shown in Figure 4.1. Salt marsh areas were taken from the European EEA CORINE land cover 2006 data. Data for Great Britain was added from originally gridded CORINE land cover 2005 data from (CLC2000 100x100 m version 8/2005). No data on salt marshes were available for Norway. However, due to the small contribution of Norway to the total considered coast area, and due to the predominantly steep rocky shoreline (Lundberg 1996), preventing extensive salt marsh formation, the resulting underestimation of salt-marsh derived DSi in Box 1 is expected to be minor. The salt marshes were manually attributed to the boxes of Proctor et al. (2003) using the software ArcGIS 10 (ESRI®). In total, the salt marshes in the North Sea tributary area and the English Channel amounted to an area of 809 km².

To quantify the relative contribution of salt marshes to the DSi budget in coastal waters during the growing season, we analysed monthly riverine DSi exports using data from the GLORICH river chemistry database (containing published data from the DEFRA Monitoring Scheme and published studies (Krinitz 2000, Deutsche Kommission zur Reinhaltung des Rheins (DK Rhein) 2008)). In total, 65 rivers were included in the seasonality analyses (63 British rivers, the Elbe River and Rhine River). Only sampling locations close to the river mouths were included. To assess the seasonality of individual boxes, the annual average river DSi exports of Proctor et al. (2003) were corrected by a seasonality factor based on the maximum reduction in summer of the river dataset that was considered representative for the individual boxes (English rivers: Box 1, 2, 5; Rhine: Box 3; Elbe: Box 4). The seasonality factor was calculated as:

$$SF_{BoxNr} = FDSi_{min} / FDSi_{avg}$$

Where SF_{BoxNr} is the seasonality factor for each box number, $FDSi_{min}$ is the minimum monthly DSi flux of the river dataset representing that box number and $FDSi_{avg}$ is that dataset's annual average monthly DSi flux. For the North Sea, the average SF of all three datasets was used.

4.4 Results and Discussion

Extrapolating the specific DSi flux of 0.14 Mmol km^{-2} a^{-1} (=3.95 t Si km^{-2} a^{-1}) to the 809 km² salt marshes adjacent to the North Sea results in a total annual flux of 113 Mmol Si a^{-1} (3.2 kt Si a^{-1}). This equals 0.7% of the annual riverine DSi inputs to the

North Sea area reported by Proctor et al. (2003). The comparison to rivers is justified by the spatial connection of both inputs and because previous comparisons in local studies highlighted that DSi fluxes from rivers and tidal marshes were in the same magnitude locally (Struyf et al. 2005a, Struyf et al. 2006a, Vieillard et al. 2011). From the distinguished regions of the North Sea, the Boxes 4 and 3, the German Bight, and the well mixed waters of the southern North Sea, have the largest salt marsh areas (Box 4: 275 km²; Box 3: 218 km²) and consequently the largest total DSi fluxes from salt marshes (Figure 4.2). However, because they also receive the most DSi from riverine input, the relative DSi flux from salt marshes compared to rivers remains small (0% (Box 4) and 1% (Box 3), Figure 4.1). The relative contributions of annual DSi fluxes from salt marshes rise to 3% and 6% in the Boxes 1 and 5 (salt marsh area: 150 km² and 162 km², respectively), the stratified water north of the Dogger Bank and the English Channel, which have smaller river contributions (Figure 2). Box 2, the stratified waters around the Dogger Bank, has the smallest river contributions but also only 4.5 km² of mapped salt marsh area, resulting in very low DSi fluxes from these sources. This shows that on annual average, the contribution of salt marsh areas to the DSi fluxes is small for the North Sea and does not exceed 6% of river fluxes even under favourable geographic conditions.

However, for DSi consuming marine organisms (e.g. diatoms) the DSi fluxes during times of silica scarceness, which is usually spring to summer, are likely more important than annual fluxes. In summer, regional scale riverine DSi exports are on average reduced to 30% of their annual average monthly flux (Figure 4.3). The seasonal behaviour of DSi fluxes from salt marshes is less clear. While they were reported to remain constant in two salt marshes in the lower St. Lawrence estuary (Poulin et al. 2009), doubling of DSi fluxes from tidal marshes during summer months was also reported (Scudlark & Church 1989, Struyf et al. 2006a). In the studies analysed here, no clear seasonal pattern was visible for DSi fluxes from salt marshes (Figure 4.3). Thus, with assumed constant DSi fluxes and the river flux decrease, the proportion of DSi from salt marshes does not exceed 2.4% of the riverine exports to the North Sea in summer. In addition, the summer decrease of riverine DSi is accompanied by an increase of exported BSi (Conley 1997, Roubeix et al. 2008b), of which a substantial proportion can be redissolved in the coastal zone (Yamada & D'elia 1984, Anderson 1986).
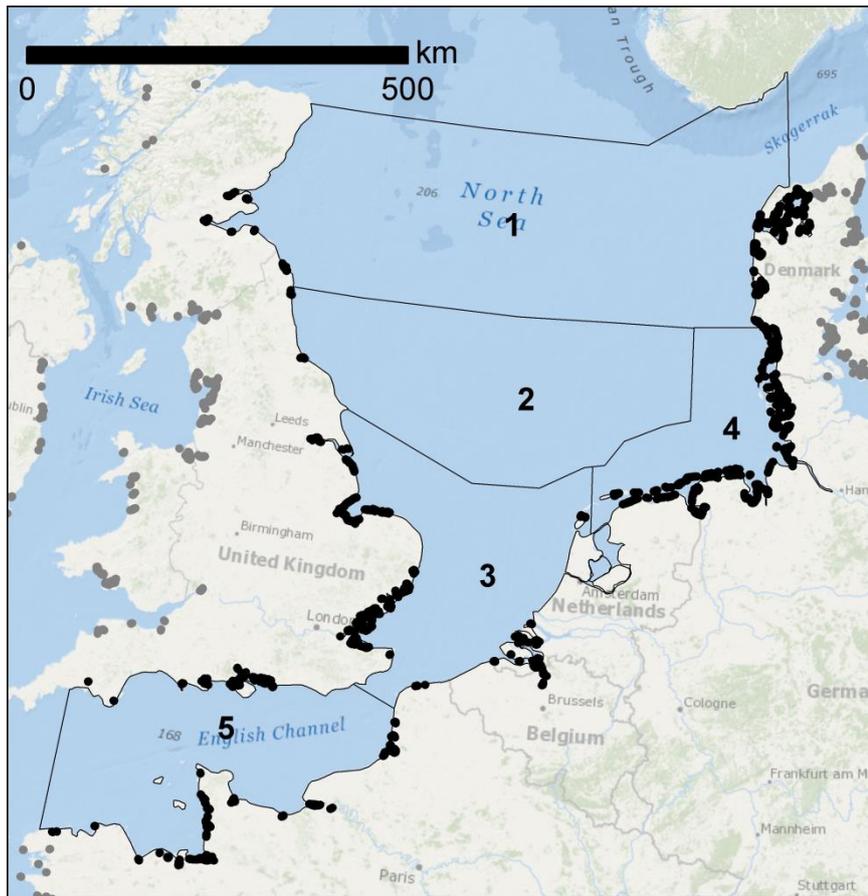
Figure 4.1: Location of salt marshes and numbers of the boxes defined by Proctor et al. (2003). Salt marshes around the North Sea and English Channel are highlighted in black, salt marshes outside that area are marked in grey. The figure exaggerates the area of the salt marshes for visibility reasons. Base map is the "Oceans Basemap" by ESRI® ArcGIS Online, updated January 2013.

This effect further reduces the relative proportion of DSi exports from salt marshes. However, in favourable regions like the English Channel (Box 5), where small river inputs meet large salt-marsh areas, DSi flux from salt marshes can account for up to 15% of the riverine inputs during summer. In that area, the lateral advective DSi inputs with marine currents is about four times higher compared to rivers (Proctor et al. 2003).

Comparing the salt marsh fluxes with the benthic fluxes highlights that the benthic component is the most important recycling based system in the North Sea, due to the large area. However, the benthic fluxes are tightly coupled to the siliceous water column primary production (Grunwald et al. 2010), i.e. the fluxes are highest after deposition of fresh diatom frustules (Gehlen et al. 1995). The salt marsh fluxes on the other hand are decoupled from the water column primary production. In areas, where the benthic - pelagic coupling is reduced due to deeper water depth, weaker vertical mixing or a
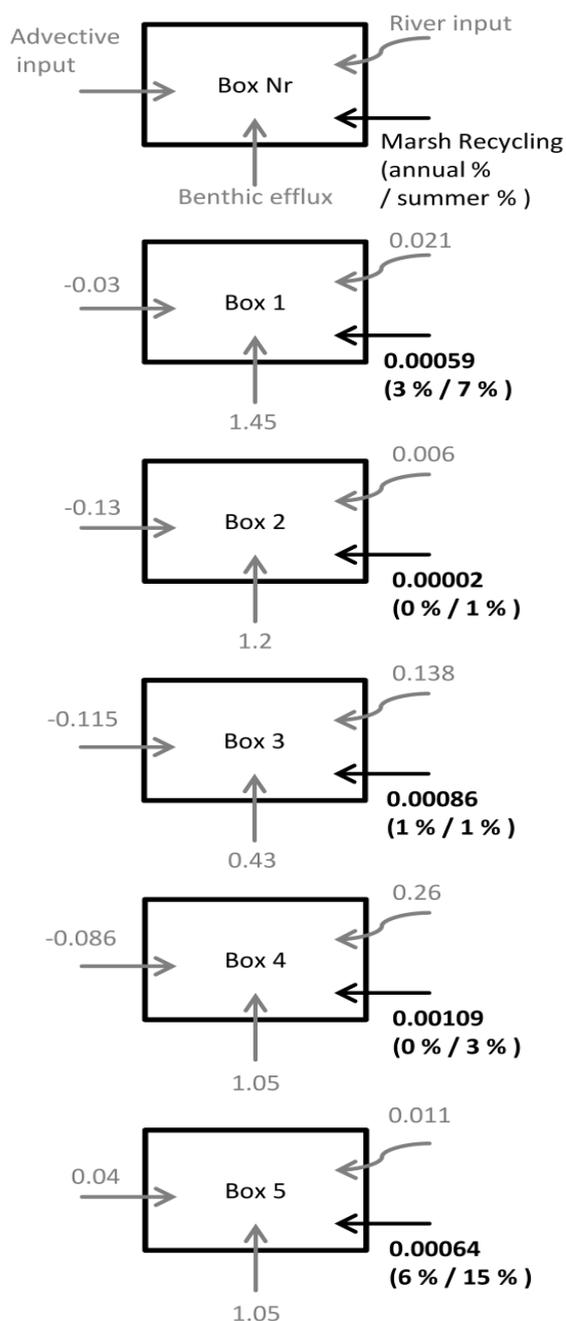
Figure 4.2: DSi fluxes (t Si a-1) from salt marshes compared to advective input, benthic efflux and river input taken from Proctor et al. (2003). The percentages compare the DSi flux from marshes and rivers (% of annual river fluxes / % of summer river fluxes). The extent of the individual boxes is provided in Figure 4.1. Only the bold black DSi fluxes from salt marshes are results from this study; the grey DSi fluxes were quantified by Proctor et al. (2003).

combination of both, the salt marsh DSi flux may bemore important for the marine DSi budget, especially during the diatom blooming season.

Although the total DSi export from salt marshes is small compared to the riverine export at the regional scale, the specific fluxes (regarding the area) are high. In the North Sea tributary area, the average specific DSi flux from rivers is 0.04 Mmol DSi km^{-2} a^{-1} (Dürr et al. 2011); the assumed specific DSi flux from salt marshes is 3.5 times higher. For comparison, the assumed specific DSi flux from salt marshes equals 2.5 times the global average specific DSi fluxes from the continents (Dürr et al. 2011). It is 3.7 times above the average specific DSi mobilization into rivers by chemical weathering in North America (Moosdorf et al. 2011), but less than the specific DSi mobilization on the highly active Japanese Archipelago (Hartmann et al. 2010). The high specific DSi fluxes from salt marshes imply that the reduction of salt marsh areas by levee construction along the coast of the North Sea and the canalization of European estuaries heavily impacted the DSi supply of coastal waters. The historic salt marsh area, before embankment of tidal areas started, was reported as about ten-fold larger than today along the coast of the Wadden Sea

(Reise 2005). If the specific DSi export from these salt marshes followed the same patterns as today, the embankment substantially decreased the seasonal DSi supply to the North Sea coastal waters.
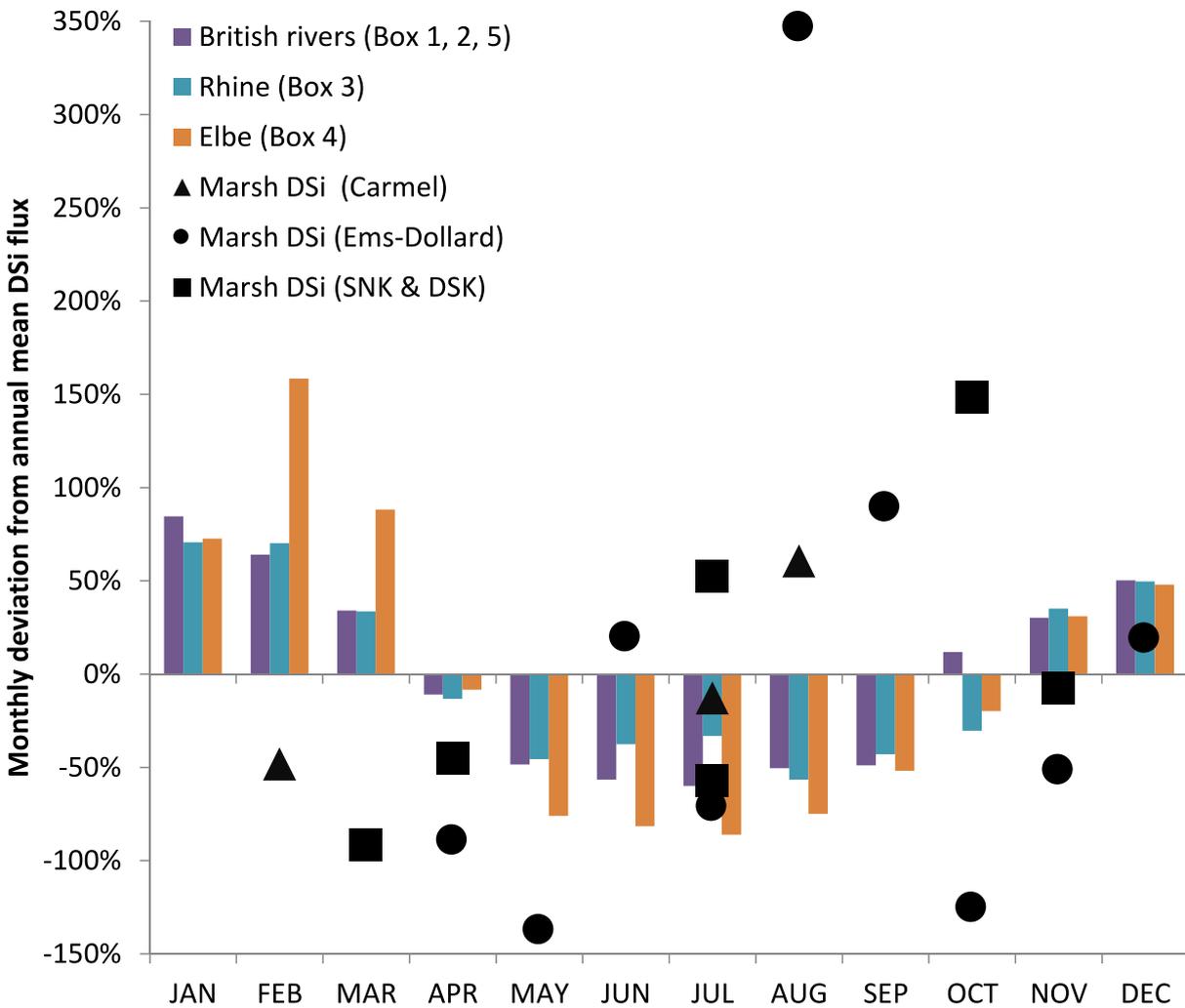

Figure 4.3: Deviation of monthly average DSi flux from annual average DSi flux for river (bars) and salt marsh (point markers) DSi exports. In Brackets, the corresponding North Sea regional boxes (after Proctor et al. (2003)) are provided , as well as the salt marshes from which the DSi is exported: Carmel Polder (Struyf et al. 2006a), the Ems-Dollard estuary (Dankers et al. 1984) and the Söhnke-Nissen Koog (SNK) and Dieksander Koog (DSK) from (Müller et al. in press). For the salt marshes, all available months were taken as annual average, despite not representing a complete annual cycle.

4.5 Conclusions

For the North Sea as a whole, the contribution of the salt marshes to DSi inputs is small annually (0.7% of riverine inputs) and even in summer (2.4% of riverine inputs), when river DSi fluxes are low. However, in smaller subsections where small river inputs meet large salt marsh areas, like in the English Channel, the summer DSi fluxes from salt marshes

can exceed 15% of the riverine DSi exports, leaving salt marshes a seasonally significant source of DSi to coastal waters.

Concluding, for the North Sea as a whole, the hypothesis of major impact from salt marshes on DSi seasonality can be rejected, and we conclude that salt marshes do not need to be included in models of dissolved silica fluxes from the regional sea scale (e.g. Meybeck et al. 2007) to global scale (e.g. Tréguer & De La Rocha 2013). However, we confirm the local results of (Struyf et al. 2006a), who showed that for certain areas, like in the here presented case of the English Channel, salt marshes should not be ignored in seasonal DSi budgets. Thus, in studies which resolve individual coastal segments ("COSCATS" (Meybeck et al. 2006, Beusen et al. 2009, Garnier et al. 2010)), the consideration of salt marshes may be relevant for the representation of the annual DSi supply and its seasonality.

5 Silicon Isotopes in the Elbe estuary

5.1 Abstract

The distribution of DSi and δ^{30}Si where studied in the Elbe estuary, Germany and its tidal marshes. Water samples from three tidal marsh areas along the estuarine salinity gradient where taken over one tidal cycle. All three sites were sampled in November, whereas extra samplings were carried out in May and July at the brackish marsh. Additionally, two cruises along the main axis of the estuary where conducted in October and December to gain insight in the estuarine distribution of δ^{30}Si. Tidal marsh samples were characterised by high DSi concentrations during seepage phase and low DSi concentrations during bulk phase. The δ^{30}Si values showed site specific tidal patterns. At the freshwater site the seepage and bulk samples only differed by 0.1‰ (range 1.71 ± 0.08‰ to 1.87 ± 0.13‰) with lower values during the seepage phase. At the salt marsh the seepage water had lower values than the bulk water (range 1.81 ± 0.03‰ to 2.59‰). The tidal pattern of δ^{30}Si values at the brackish marsh was similar during May, July, and November with higher values in the seepage phase than during the bulk phase. Highest absolute values were 3.26 ± 0.10 ‰, 2.98 ± 0.15‰, and 2.78 ± 0.11‰ in May, July, and November respectively. The isotopic signatures were always positive and ranged between 1.71 ± 0.08‰ and 1.87 ± 0.13‰ at the freshwater site. At the brackish site highest δ^{30}Si values were observed (1.97 ± 0.08‰ − 2.78 ± 0.11‰). The October cruise showed DSi uptake by diatoms which decreased concentrations in the freshwater part of the estuary. The δ^{30}Si values increased from 1.64 ± 0.02‰ to 2.21 ± 0.08‰, which was best explained by open system fractionation. In December DSi was added to the estuary, most probably by tributaries. The δ^{30}Si values were lower than in November (0.85 ± 0.08‰ to 1.61 ± 0.08‰), reflecting the absence of biologic activity. The δ^{30}Si values were heavily altered in the freshwater part, possibly due to the combined effect of mixing with tributary water and fractionation.

5.2 Introduction

The average silicon isotopic composition (δ^{30}Si) of seawater represents the balance between river and hydrothermal inputs of dissolved silicon (DSi) to the ocean. The oceans have an average δ^{30}Si (around +1‰) that is much closer to typical riverine values

(+0.5‰ to +2‰) than to deep sea hydrothermal DSi (-0.4‰), reflecting the much greater input of river Si than hydrothermal Si (Tréguer & De La Rocha 2013). There are severe weaknesses in our elemental and isotopic budget for Si in the ocean. We have only rough estimates for how much river DSi is removed in estuaries and therefore never input into the ocean (Tréguer et al. 1995, Tréguer & De La Rocha 2013) and next to no idea to what extent the estuarine Si cycling alters the δ^{30}Si before it reaches the sea. Also, currently unknown and unaccounted for is the diffuse input of hydrothermal DSi through ridge flanks (Wheat & McManus 2005), although it may be an order of magnitude greater than the current estimate for hydrothermal inputs. Better constraining the impacts of the estuaries on the riverine inputs and δ^{30}Si would not only allow us to improve the global budget for the Si cycle, it would help us to constrain the size and isotopic input of the ridge flank hydrothermal flux of Si (and Si isotopes) into the ocean.

Estuaries serve as the interface through which solutes delivered to the ocean from the terrestrial biogeosphere must pass. These estuaries are complex environments, showing stark river to ocean gradients in turbidity, salinity, and pH (Bianchi 2007). Through colloid formation, scavenging, reverse weathering, and the production and sedimentation of biogenic materials, significant quantities of river borne solutes are retained in estuaries (Bianchi 2007), severely diminishing the input of these salts to seawater. Likewise, dissolution of estuarine materials may at times serve as a source of solutes, as shown for calcium in the Gironde estuary (Abril et al. 2003).

This is especially true for Si in tidal marshes (Struyf & Conley 2009). Numerous studies (Struyf et al. 2005a, Struyf et al. 2006a, Struyf et al. 2007, Jacobs et al. 2008) have demonstrated that biogenic silica (phytoliths from marsh plants and frustules of diatoms) in marsh serves alternately as a net sink and a net source of Si to adjacent estuarine waters, varying over seasons and tidal cycle. As both silica production (De La Rocha et al. 1997, Opfergelt et al. 2006, Ding et al. 2008a, Ding et al. 2008b) and dissolution (Demarest et al. 2009) fractionate silicon isotopes, this cycling of (and retention of a portion of) riverine DSi in tidal marshes likely alters the δ^{30}Si of DSi delivered to the ocean, and therefore plays a key role in controlling whole ocean δ^{30}Si. We propose to take the first look at the cycling of Si isotopes in tidal marshes to begin to quantify this effect.

5.3 Material and Methods

5.3.1 Sampling

Silicon isotope samples of the Elbe estuary were taken from surface water during two cruises along the main axis of the Elbe estuary in October and December 2011. Samples from the tidal marsh areas were obtained in November 2011 at all three sampling sites and additionally at the brackish site in May and June 2011. For 7-12 hours every hour superficial water was taken with a plastic bottle attachted to a telescope bar. The phyical parameters pH, temperature, dissolved oxygen (DO) and salinity were measured with a handheld sensor (pH, temperature: Methrohm pH 827, Primatrode 6.0228.020 or Aquatrode 6.0257.000; salinity and oxygen: WTW 350i ConOX). Tidal marsh DSi samples were filled into acid cleaned plastic bottles and stored in a cool-box. In the laboratory the samples were vacuum filtered through 0.45 µm PC filter (Sartorius). The filtrate was stored in acid cleaned plastic bottles until analysis. The estuarine samples were filtered on board of the research vessel and stored at 4°C.

The dissolved silica (DSi) concentrations in the samples were measured using standard colorimetric techniques (Strickland & Parsons 1972).

5.3.2 Isotopic measurement

All work described here was carried out using Suprapur (Merck) grade acids, deionized distilled water (18.2 MΩ cm^{-1}), and acid-cleaned labware (PTFE and LDPE).

Dissolved silicon was precipitated from the samples applying the Triethylamine Molybdate (TEA-Moly) method as described in (De La Rocha et al. 1996). Firstly, the DSi was precipitated over night in TEA-Moly solution and then filtrated on 0.6 µm PC filter. The filtrate was then combusted in two steps in a muffle furnace using platinum crucibles. To remove organic compounds the samples were brought to 500°C for two hours. In the second step the temperature was ramped up to 1000°C for ten hours.

The silicon recovered as silica was dissolved in 40% HF to 229.855 mmol L^{-1} (4 µmol Si in 17.4 µl). Samples were diluted to a concentration of 518.3 µmol Si L^{-1} then loaded onto ion exchange columns filled with 1 X-8 resin (Eichrom) following the protocol outlined in Engström et al. (2006) and utilized previously in the lab (De La Rocha et al. 2011). A

47

solution of 95 mM HCl plus 23 mM HF was used to elute matrix elements while Si eluted with a solution of 0.14 M HNO_3 plus 5.6 mM HF.

Silicon isotope abundances in the samples were measured using a Neptune multi-collector inductively coupled plasma mass spectrometer (MC–ICP–MS) (Thermo Scientific). Settings are given in Table 5.1. Samples were diluted with 0.16M nitric acid to 2 ppm Si and sample and standard beam intensities and HF concentrations (~1 mM HF) were matched within 10%. The standards used were NBS28 and a laboratory working standard of 99.995% pure silica sand (Alfa Aesar). A final concentration of 0.1 ppm magnesium was added to the samples and the standards to allow monitoring of mass fractionation during the isotopic measurements. For each measurement, beam intensities at masses 25 and 26 (Mg), and 28, 29, and 30 (Si) in dynamic mode were monitored for 1 block of 25 cycles of 8 second integrations. Roughly 5 minutes of rinse with 2% nitric acid occurred between silicon-containing solutions (i.e. samples and standards).

Magnesium correction was used to correct the measured silicon isotope ratios ($^{30}Si/^{28}Si$ and $^{29}Si/^{28}Si$) for mass bias within the mass spectrometer following Cardinal et al. (2003). The corrected ratio ($^{30}Si/^{28}Si$)$_{corr}$ is:

$$\left(\frac{^{30}Si}{^{28}Si}\right)_{corr} = \left(\frac{^{30}Si}{^{28}Si}\right)_{meas} \times \left(\frac{^{30}Si_{AM}}{^{28}Si_{AM}}\right)^{\varepsilon_{Mg}}$$

Eq. 5.1

where ($^{30}Si/^{28}Si$)$_{meas}$ is the ^{30}Si to ^{28}Si ratio measured and $^{28}Si_{AM}$ and $^{30}Si_{AM}$ are the atomic masses of ^{28}Si and ^{30}Si. The beam intensities on masses 25 and 26 allow estimation of ε_{Mg}:

$$\varepsilon_{Mg} = \ln\left[\frac{\frac{^{25}Mg_A}{^{26}Mg_A}}{\left(\frac{^{25}Mg}{^{26}Mg}\right)_{meas}}\right] \div \ln\left[\frac{^{25}Mg_{AM}}{^{26}Mg_{AM}}\right]$$

Eq. 5.2

where ($^{25}Mg/^{26}Mg$)$_{meas}$ is the ratio measured, $^{25}Mg_A/^{26}Mg_A$ is the ratio expected based on the natural abundances of the isotopes, and $^{25}Mg_{AM}$ and $^{26}Mg_{AM}$ are the atomic masses of ^{25}Mg and ^{26}Mg.

The corrected silicon isotope ratios obtained from a set of bracketed standard-sample-standard measurements consisting of 2 blocks of the sample ratio and 3 of the standard ratio were used to calculate the average $\delta^{30}Si$ and $\delta^{29}Si$ values for each sample:

$$\delta^x Si = \frac{R_{sam} - R_{std}}{R_{std}} \times 10^3$$

5.3

where $\delta^x Si$ is $\delta^{29}Si$ or $\delta^{30}Si$, and R_{sam} and R_{std} are the $^{29}Si/^{28}Si$ (for $\delta^{29}Si$) or the $^{30}Si/^{28}Si$ (for $\delta^{30}Si$) of the sample and standard.

The precision for individual measurements of $\delta^{30}Si$ was generally ± 0.04‰ (1σ standard deviation) on $\delta^{30}Si$. The long term precision (also 1σ SD), including the column chemistry, was ±0.07‰, based on 22 separate samples of the standard measured between July 6, 2009 and September 1, 2010. Both the backgrounds during analysis and the procedural blanks were normally less than 1% of the sample signal. Final values obtained fell along the mass dependent fractionation line expected for silicon of $\delta^{30}Si = 1.93 * (\delta^{29}Si)$ (see Appendix 5).

Table 5.1: Operating conditions for the Neptune MC-ICP-MS

resolution	medium
sensitivity	~6 V ppm^{-1}
forward power	1200 W
accelerating voltage	10 kV
cool gas	15.5 L min^{-1}
auxiliary gas	0.8 L min^{-1}
sample gas	1 L min^{-1}
sampler cone	standard Ni cone
skimmer cone	standard Ni cone
desolvator	Apex (ESI)
nebulizer	60 µl min^{-1} PFA microconcentric

5.4 Results

5.4.1 Tidal marsh areas

The δ^{30}Si values of the tidal marsh samples lay between 1.71 ± 0.08‰ and 3.26 ± 0.10‰ (Figure 5.1). They showed different tidal signals at each sampling location. At HDM δ^{30}Si values were similar during the seepage and the bulk phase (1.71 ± 0.08‰ to 1.87 ± 0.13‰) and the lowest of all three sampling stations. At NF seepage values were always higher than the bulk values. They also differed seasonally, with highest values in May and lowest in October. At DSK the pattern was reversed and bulk δ^{30}Si values were higher than in the seepage phase. DSi concentrations on the other hand were at all sites always higher during the seepage phase than during the bulk phase which led to distinct correlations between δ^{30}Si and DSi concentrations (Figure 5.2). A positive correlation was present at NF (Pearson's r^2 = 0.59) while at DSK the values were negatively correlated Pearson's r^2 = 0.64). At HDM no correlation was found (Pearson's r^2 = 0.09).
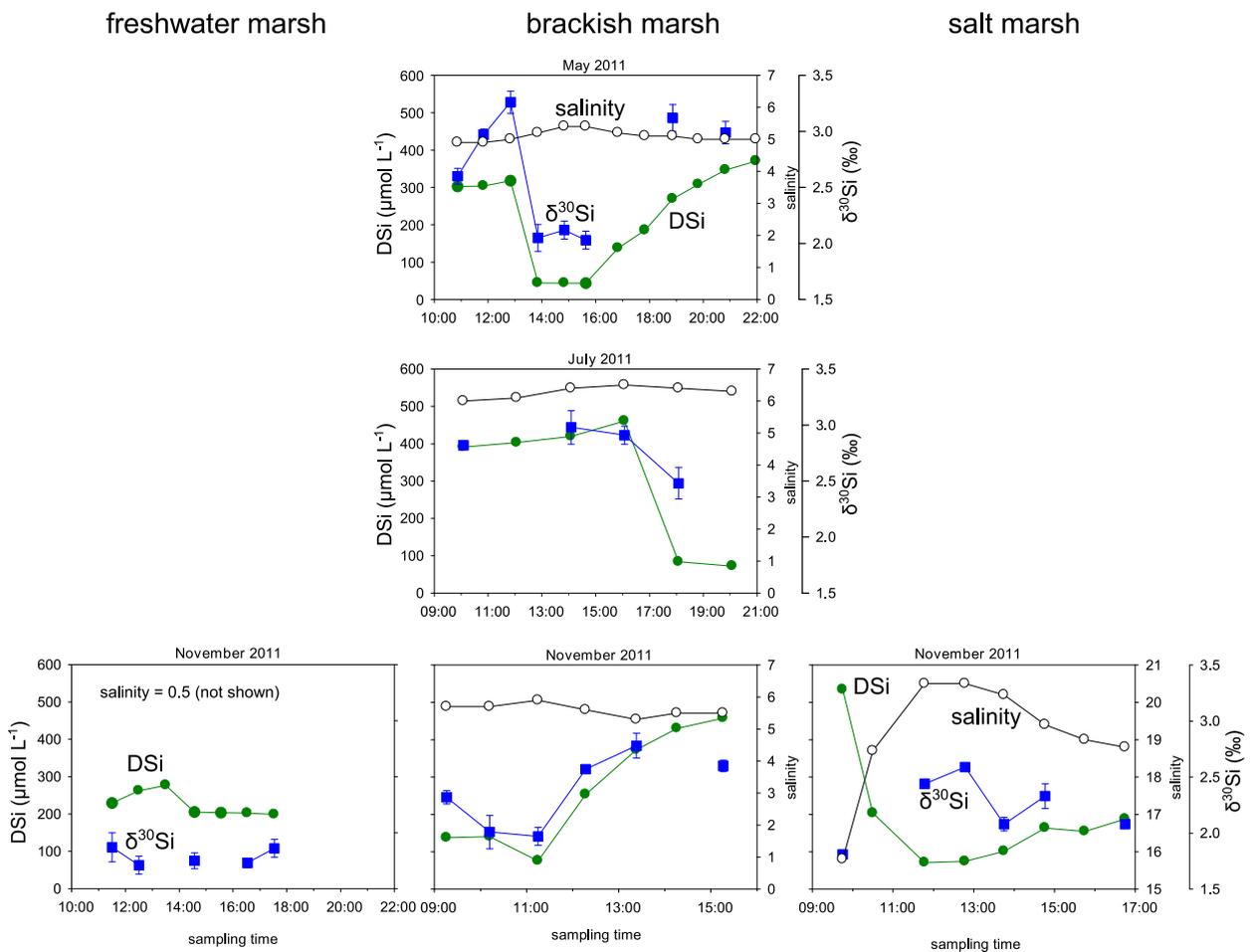

Figure 5.1: Overview of DSi concentrations, d30Si values and salinities in the fresh, brackish and salt marsh sampling sites. DSi concentrations were highest during seepage phase and lowest during bulk phase. Error bars on the δ^{30}Si data points are 1 σ standard deviation.

50

5.4.2 Estuarine transects

Physico-chemical parameters

During the October and December the monthly mean river discharge was 572 m^3 s^{-1} and 604 m^3 s^{-1} respectively, which differed not much from the discharge on the sampling day (638 and 674 m^3 s^{-1} for the October and December cruise, respectively). Also of similar magnitude and distribution along the estuarine transect were the DO saturation and pH values (Figure 5.4, A and B). At km 609 both DO saturation values were in equilibrium with the atmosphere and decreased by about 14% towards km 659 (see section 2.1 for a more detailed description of the biogeochemical zonation of the Elbe estuary). The pH was also highest at km 609 and decreased slightly towards km 659. In December the DO saturation and pH values had another minimum at km 724. The water temperature was higher in October and increased towards the estuarine mouth. In December temperatures were around 4°C with only a minor downstream increase.

SPM concentrations showed that the maximum turbidity zone was located between km 649 and km 699 during both cruises (Figure 5.4, C and D). Maximum concentrations were higher in December, reaching 364 mg L^{-1}. The first SPM maximum coincided with the location of the DO minimum.
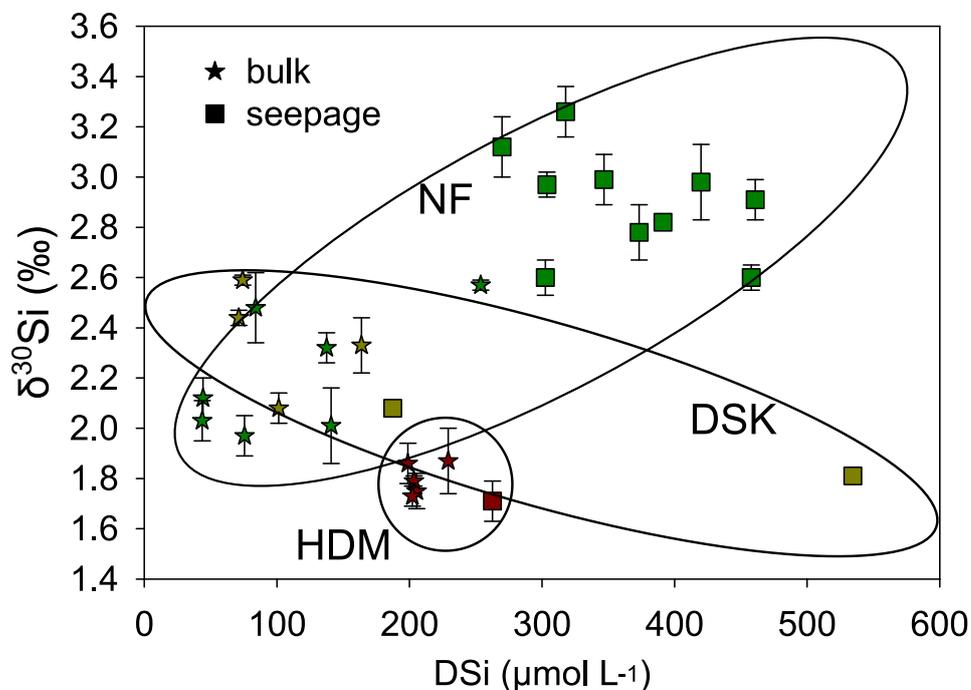

Figure 5.2: δ^{30}Si as a function of DSi concentrations for all three sampling locations. The samples of one sampling station are enclosed in one ellipsis. HDM = red, NF = green, DSK = dark yellow. Stars denote seepage samples, squares bulk samples. Error bars are 1 σ standard deviation.

DSi concentrations and δ³⁰Si

October

DSi concentrations decreased non-conservatively over the whole transect from about 165 µM to 52 µM at the estuarine mouth (Figure 5.3), with significant quantities removed only after km 639 (Figure 5.4, C).

The $\delta^{30}Si$ values increased stepwise from 1.43 ± 0.11‰ at km 609 to about 1.63‰ until km 639 and again to about 2.02‰ at km 659 after which they stayed constant with the exception of the value at km 699 (Figure 5.4, C). The increase after km 639 coincided with the increase of SPM concentrations (Figure 5.4, A, C).
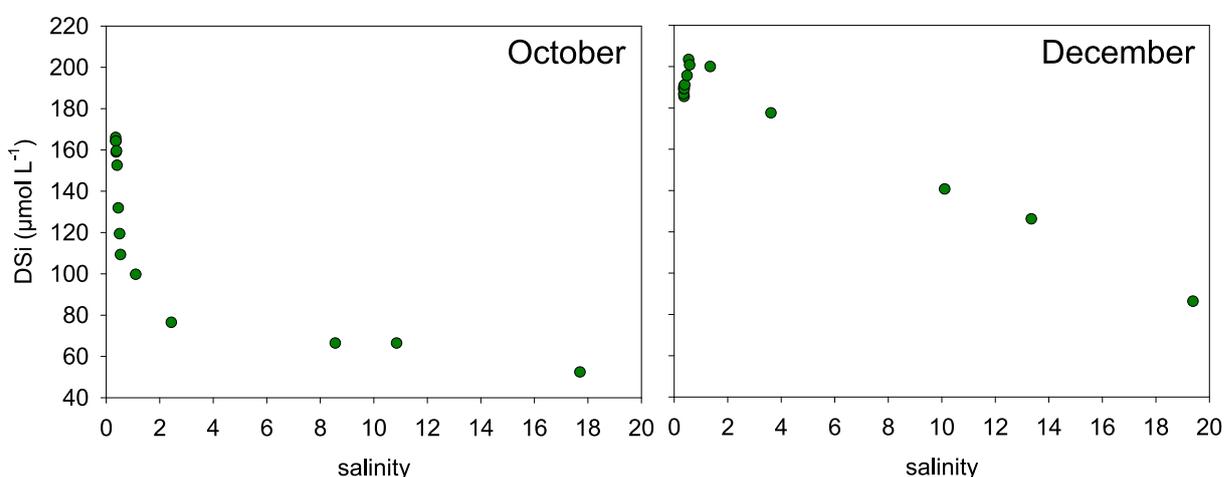
Figure 5.3: Distribution of DSi along the estuarine salinity gradient during the October (left) and December (right) cruise.

December

In December, DSi concentrations increased from 184 µM at km 609 to 202 µM at km 669 (Figure 5.4 D) after which they were mixed conservatively with salinity (Figure 5.3). The increase of DSi concentrations at km 724 is due to the change of tides during the cruise, as indicated by the decrease of salinity at this sampling point. The $\delta^{30}Si$ values decreased gradually from 1.47 ± 0.12‰ at km 609 to 0.85 ± 0.08‰ at km 629. After the minimum the values increased together with SPM concentrations to about 1.54‰, with the exception km 679.

5.5 Discussion

5.5.1 Tidal marshes

The δ^{30}Si values measured in the seepage water of the brackish marsh are the highest reported so far for soil solutions (Opfergelt & Delmelle 2012) and on the upper end of those reported for rivers, lakes and the ocean. Several factors affect the isotopic signature in soil solutions, including liquid-solid exchanges between monosilicic acid (H_4SiO_4) and neoforming minerals, such as clays and oxy-hydroxides (Basile-Doelsch 2006, Opfergelt & Delmelle 2012). The fractionation associated with these exchange processes is augmented by successive dissolution/precipitation or adsorption/desorption cycles (Opfergelt & Delmelle 2012). Additionally, plant mediates processes also affect the isotopic composite on of the soil porewater and the seepage water (e. g. De La Rocha et al. 1997, Ding et al. 2005). Finally, the soil hydrology also plays its part in the distribution of δ^{30}Si signatures in soil, due to its influence on mixing processes of different water masses which can have distinct isotopic signatures. Detailed knowledge of the rates and the isotopic composition of the endmembers present in the marsh soil would be necessary to quantify each of the
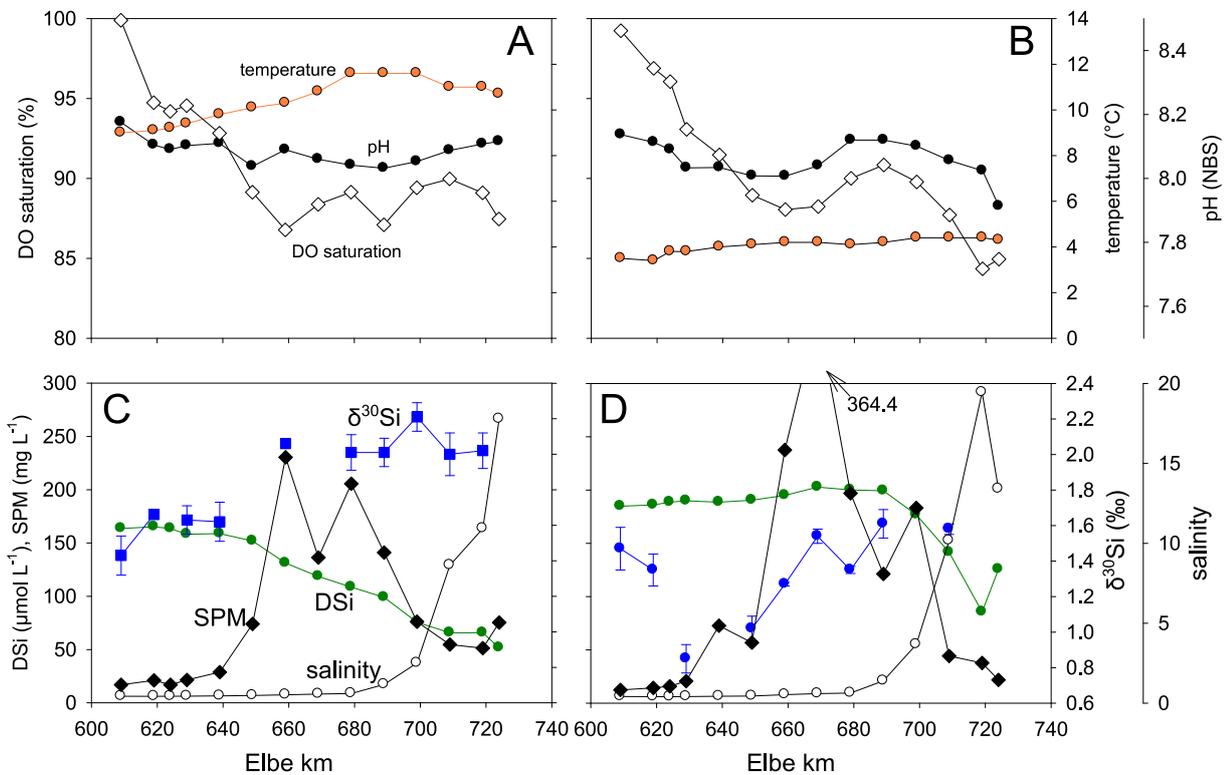

Figure 5.4: Overview of temperature, pH and DO saturation (panel A and B) and DSi concentrations, δ^{30}Si values and salinity (panel C and D) distributions along the main axis of the Elbe estuary in October 2011 and December 2011. Elbe km denotes the distance from the Czech border. Errors bars are 1 σ standard deviation

53

above mentioned process Because the here presented dataset lack these requirements the following discussion will focus on a qualitative description of processes important for the silica cycle in tidal marshes.

Hydrology

The occurrence of regular and irregular flooding events distinguishes tidal marsh soils from terrestrial soils. The Elbe estuary has a semidiurnal flooding regime with two tides approximately every 25 h (BSH 2010). Most of the tides flood only the tidal creeks and do not inundate the marsh surface. Between September and March the probability of storm surges is increased. Such events flood the complete marsh surface to a depth of several decametres to metres. During inundation events estuarine water infiltrates into the marsh soil over the whole marsh area, while during the regular tides the infiltration is confined to the creek bed or even non-existent. The hydraulic pressure gradient between the soil and the creek allows infiltration of inundation water only if the water level exceeds the marsh surface (Gardner 2005a). Infiltration is further positively correlated with the soil permeability.

The seepage water, which drains into the tidal creek, is drawn from the pool of soil porewater only several metres away from the edge of the tidal creek (Gardner 2005a). Because of the constant drainage, this water has shorter turnover times than the soil porewater in the centre of the marsh. The seepage water can thus be seen as a representation of the soil porewater close to the creek edge.

The fact that the seepage sample at HDM did not differ from the bulk samples could be explained by the hydrological conditions of the sampling site. The sampling site has high saturated water conductivity (see section2.2.2) and was also flooded before the sampling day. Between November 26 and November 28, the marsh site was inundated to a depth between 0.55 to 1.7 m. The high water 4.5 hours before the sampling inundated the marsh surface to a depth of 0.5 m. These flooding events allowed the infiltration of estuarine water into the soil. The comparison of sampling days without prior flooding and this sampling day, showed that the water discharge during the seepage phase was visibly much higher (A. Weiss, pers. obs.), which corroborated the hypothesis that the infiltration of estuarine water into the marsh soil occurred, because during the seepage phase that water is released back from the marsh soil. This so called sponge effect of marsh soil was

also reported from another study of tidal marshes in the German Wadden Sea National Park (Müller et al. in press). The infiltration of estuarine water shifted the δ^{30}Si values of the porewater to the estuarine signature, resulting in the observed similar δ^{30}Si signal during the whole sampling. For the here presented data hydrology can be considered as the dominant factor for the isotopic signal at the freshwater site. The brackish and the salt marsh were not affected by inundation events 68 and 70 days prior to the respective sampling day. Therefore the patterns observed at these sampling sites are most likely the result of the interplay between hydrology and other factors.

Brackish (NF) and salt (DSK) marsh

Vegetation

The importance of vegetation for the cycling of silicon through tidal marshes was recently highlighted in several studies (Struyf et al. 2005b, Struyf et al. 2006b, Struyf et al. 2007, Struyf & Conley 2009, 2011).

Tidal marshes are grassland ecosystems, dominated by species like *Phragmites australis*, *Elymus athericus*, *Thypha* spp., *Spartina spp.* and *Phalaris arudinace*, which all are silica accumulation species (Raven 2003). In the plant the DSi is partly precipitated as biogenic silica (BSi), which is a form of amorphous silica. These BSi structures in plants are called phytoliths (Kaufman et al. 1981). The BSi content of tidal wetland plants can reach values of about 70 mg g^{-1} dry weight, which is comparable to that of rice (Struyf and Conley (2009), electronic supplemental material).

Especially *P. australis* has high BSi contents. The storage of BSi in *P. australis* in a tidal freshwater marsh in the Scheldt estuary, Belgium accounted for 90% of all BSi found in the vegetation (Struyf & Conley 2009). This BSi is several orders of magnitude more soluble than clay minerals, primary mafic silicates and feldspars (Fraysse et al. 2009). As a result it is has short turnover times compared to other particulate silica components. It was shown for a tidal freshwater marsh that 50% of all BSi in litter of the common reed *P. australis* were dissolved after only 20 days, after one year 98% of the BSi was leached from the samples (Struyf et al. 2007).

Monocotyledonic plant species favour the incorporation of light silicon isotopes during the uptake of DSi, as was shown for several species like, banana (Opfergelt et al. 2006),

bamboo (Ding et al. 2008b), rice (Ding et al. 2008a) and wheat and corn (Ziegler et al. 2005). The fractionation factor of the DSi uptake seems to be very similar for all these species, with a value of about 1‰. Additionally, isotopic fractionation occurs during the formation of phytoliths in the plant along the root – shoot transport path (Opfergelt et al. 2006, Ding et al. 2008b) This results in higher δ^{30}Si values in phytoliths located in the upper parts of the plant (Ding et al. 2005, Ding et al. 2008a, Opfergelt et al. 2008). The highest δ^{30}Si values were in general observed in the leaves (excluding husks and seeds).

Especially *P. australis* has the potential to create very high δ^{30}Si values in the soil solution. The plant is known for its very high transpiration rates, which can exceed the annual precipitation of the habitat (Herbst & Kappen 1999). The very high water throughput is accompanied by the uptake of DSi, which, together with the above mentioned fractionation, would results in the enrichment of heavy Si isotopes in the remaining soil porewater. Additionally, the plant can reach heights of 3-4 m which could create highly enriched BSi in the plant leaves and a lighter pool in the culms. The time lack of complete BSi dissolution in the culms compared to leaves (see above) would trap the reservoir of light Si isotopes in the plant material could contribute to the δ^{30}Si enrichment of the soil porewater and explain the high values observed at NF. The differences between δ^{30}Si values at DSK and NF in November could indicate a weaker influence of the vegetation on the isotopic composition in the seepage water. At DSK *E. athericus* dominated the vegetation. This grass does not grow high stems like *P. australis,* but forms a dense leave cover of about 0.3-0.5 m in height. It also tends to have lower BSi concentrations compared to *P. australis* (Chapter 3, Table 3.3), which may be the result of lower transpiration rates compared to *P. australis,* caused by self-shading due to its growth form.

Adsorption/desorption processes
It has been shown that the adsorption of DSi onto iron oxides is accompanied by isotopic fractionation (Delstanche et al. 2009). Lighter isotopes are preferentially adsorbed, which results in the decrease of δ^{30}Si. The adsorption is pH dependant and reaches its maximum around pH 9 (Jones & Handreck 1963, Hiemstra et al. 2007).

The redox state of tidal marsh soils and therefore the availability of Fe oxides are governed by hydrological and biogeochemical factors which interact in a complex way.

For example, on the one hand inundation reduces the oxygen availability due to the low oxygen diffusion in water compared to a porous medium like drained soil (c.f. Mitsch & Gosselink 1993, p. 120), resulting in reducing conditions favouring the formation of iron sulphides. On the other hand infrequent flooding paired with low precipitation and high temperatures cause the drying of the marsh soil which can cause desiccation cracks. Under these conditions atmospheric oxygen can penetrate into the soil. As a result the oxidation of iron sulphides to iron oxides is favoured. Furthermore, availability of iron oxides is regulated by plants, via the effect of root aeration on the availability of poorly crystalline iron for microbial iron reduction (Weiss et al. 2004). As the fractionation factor of iron oxides is positively related to their cristallinity (Delstanche et al. 2009), the presence of plants may decrease the influence of adsorption on the δ^{30}Si signature in the soil porewater.

It can be assumed that the factors which increase the availability of iron oxides in the marsh soil are more prevalent in warmer month, because conditions favour the processes that are responsible for oxygenation of the soil (dense vegetation cover, better soil drainage, desiccation cracks) and thus oxidation of iron. Hence, the influence of adsorption on δ^{30}Si values of the marsh porewater in the here presented November sample was most likely small. However detailed studies are needed to quantify the effect of the adsorption/desorption process on the δ^{30}Si signatures in pore and seepage waters in tidal marshes. Additionally, these studies should include the effect of aluminium oxides because they are twice as effective in sorbing Si than iron oxides (Jones & Handreck 1963).

5.5.2 Elbe estuary

Both Elbe cruises showed that in the freshwater zone of the estuary modifications of the δ^{30}Si ratios of DSi occur. In the salinity gradient on the other hand, conservative mixing seems to be the only active process as indicated by stable δ^{30}Si ratios. Until now only two published datasets of δ^{30}Si values from estuaries exists. In the Tana River estuary, Kenya (Hughes et al. 2012), DSi was only affected by conservative mixing. The second dataset is from the Yangtze River, China (Ding et al. 2004) and includes only five δ^{30}Si values from the tidally influenced freshwater part of the river which were sampled on different days.

There, the increase of δ^{30}Si ratios (up to 3.4‰) was explained with the presence of rice paddies and wetlands.

October cruise modelling and interpretation

Uptake of DSi by diatoms

Diatoms need Si to build up their frustules. The uptake of DSi is associated with a fractionation factor of about -1.1‰ (De La Rocha et al. 1997, Milligan et al. 2004). Benthic diatoms are abundant on the tidal flats of the Elbe estuary and have been shown to alter nutrient fluxes in the coastal zone (Sigmon & Cahoon 1997). However they only create negative DSi fluxes during a short period of the day (Ní Longphuirt et al. 2009) and most likely assimilate DSi directly from the sediment porewater (Ní Longphuirt et al. 2009), which rules out than benthic diatoms are the main sink for DSi in the water column. Their activity however, can influence the δ^{30}Si value, due to the fractionation during DSi uptake.

Pelagic diatoms in the Elbe estuary can reach primary production rates between 20-50 mg C m^{-2} d^{-1}, even in the maximum turbidity zone (Goosen et al. 1999). The pelagic plankton community during late summer/autumn only partly consist of diatoms, why the diatomaceous primary production rate is lower than the above mentioned values. To account for that in the calculation of theoretical DSi uptake rates by pelagic diatoms this values is assumed to be 50% smaller. Together with SiO_2:C ratios (weight based) for freshwater diatoms of 1.89 (lowest value, Sicko-Goad et al. (1984)) and the water surface area between km 639-680 (63.4 km^2) the pelagic DSi uptake is 19.9-49.9 kmol Si d^{-1}. These values could explain the loss of 28.6 kmol Si observed in this zone and also the change of the δ^{30}Si signature.

Based on the assumption that DSi is taken up by diatoms the data can be interpreted as a combination of open system fractionation and conservative mixing between the estuarine and North Sea water. However, two assumptions must be made. Firstly, that the δ^{30}Si value of 2.21 ± 0.08‰ at km 699 is correct and the value of 1.43 ± 0.11‰ at km 609 is too small. The assumptions have to be checked by re-measuring these samples. These checks could not be included into this work, because practical constrains in the isotopic laboratory delayed the measurements until after the submission deadline of this thesis.
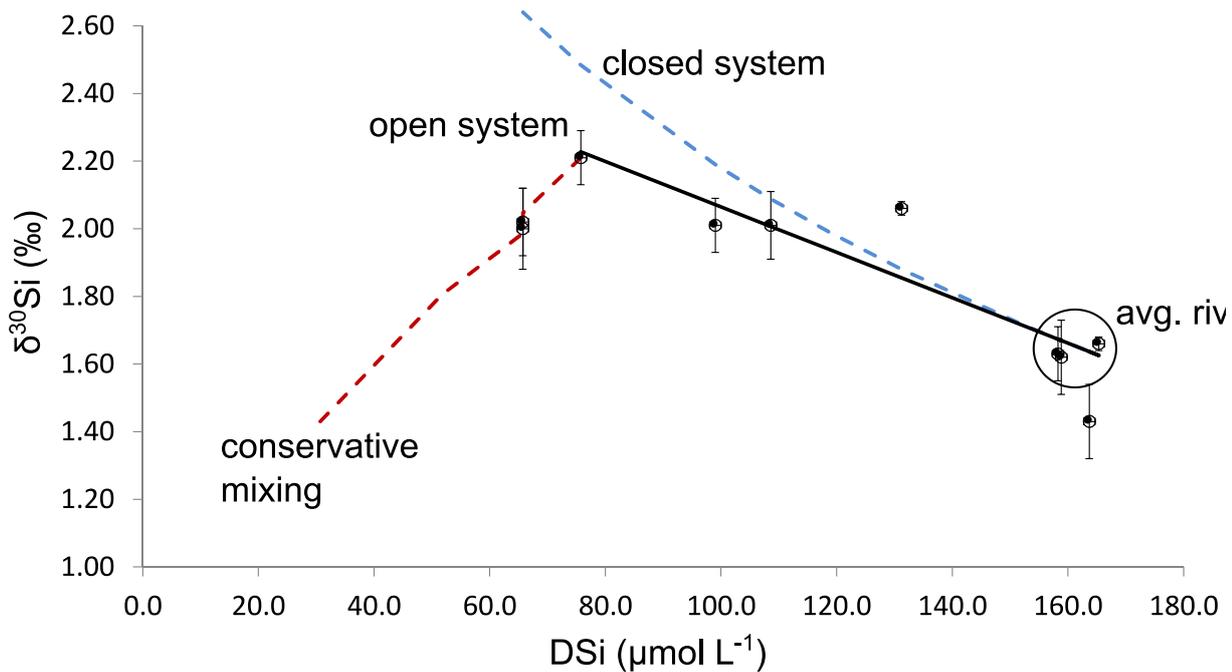
Figure 5.5: δ^{30}Si as a function of DSi. The blue dotted line represents the closed system model fractionation, the solid black line is the open system model fractionation. The conservative mixing between a seawater endmember of 1.4‰ and 29 µmol L^{-1} DSi is indicated by the red dotted line. The average δ^{30}Si value of the river endmember is the mean of the encircled data points, yielding 1.64‰.

The spatial distribution of DSi shows three distinct zones (Figure 5.4). Zone 1 between km 609-639 where DSi concentrations and δ^{30}Si values are constant, if the δ^{30}Si value of 1.43 ± 0.11 ‰ is excluded. Zone 2 after km 639 to km 699 where DSi is significantly removed and δ^{30}Si values increase. Finally, zone 3 where DSi is mixed conservatively with seawater.

If the light δ^{30}Si value in zone 1 is excluded the freshwater endmember is 1.64‰. The increase of the δ^{30}Si signal in zone 2 from 1.64‰ to 2.21‰ can then be best described as an open system model fractionation (Figure 5.5). One δ^{30}Si value falls off the modelled fractionation line by about 0.2‰. It could indicate that at this sampling location input of enriched DSi occurs. However, due to the lack of isotopic data from tributaries, a possible source for enriched DSi, this interpretation remains speculative.

Absorption onto clay minerals

The coincidence of the DSi and δ^{30}Si changes with increase in SPM concentrations could indicate that Si adsorption onto particles caused the shift of the isotopic composition. Suspended matter in the Elbe estuary consists to 70% of silt particles < 20 µm, the clay fraction (<2 µm) makes up about 30% (Schwedhelm et al. 1988). illite is the dominant

mineral (~50%) in the 2-20 µm fraction, followed by kaolinite and chlorite (~20%, respectively). The clay fraction < 2 µm also consists of illite (~45%), kaolinite (~20%) and chlorite (~10%), but also contains smectite in considerable amounts (~20%) (Schwedhelm et al. 1988). The SPM composition has thus the prerequisites for DSi adsorption onto aluminium oxide surfaces of the clay minerals. Assuming the removal of DSi is solely due to the adsorption of DSi on clay mineral surfaces, the adsorption capacity of the SPM must be as high as 309 mmol kg^{-1} to account for the loss of 28.6 Mmol Si. This calculation is based on a mean tidal volume of 571 x 10^6 m^3, an average SPM concentration of 161.6 mg L^{-1} and a DSi loss of 50 µmol L^{-1} between km 639 and km 679. The value of 309 mmol kg^{-1} exceeds by far all adsorption capacity measurements made for metal ions (e.g. Manning & Goldberg 1996) or dissolved silica (Delstanche et al. 2009) by at least 3 orders of magnitude. To come close to the adsorption capacity cited in the literature the SPM concentration in this zone must be > 1000 mg L^{-1}. These values do occur in nature but only in fluid mud systems as shown in the Gironde estuary (Abril et al. 2000). SPM concentrations in the Elbe estuary seldom exceed 300 mg L^{-1} (FGG Elbe 2012) in the surface water but can be up to six times higher near the sediment (Goosen et al. 1999). However, the zones with such high SPM concentrations are confined to a small fraction of the total water column, which limits their contribution to the adsorption processes. Adsorption on sediment particles is thus most likely not the main cause for the decline of DSi concentrations and the increase of δ^{30}Si values in the freshwater part of the estuary.

Dilution

The DSi concentrations and δ^{30}Si values in the main stream of the Elbe could also be changed by input of tributary water. These waters must have lower DSi concentrations than the main stream to decrease its DSi concentration. However, during this time of the year, the tributary DSi concentrations are equal or even higher than in the main stream (FGG Elbe 2012), ruling out dilution as a reason for the DSi concentration decline.

December cruise interpretation

The distribution of DSi during the December cruise was typical for this time of the years as shown by monitoring data from 1992-2009 (FGG Elbe 2012). Due to the lack of biotic activity, high DSi concentrations are delivered from the non-tidal river to the estuary where they are further increased, most probably due to tributary input.

The tributaries of the estuary have higher DSi concentrations than the main stream (FGG Elbe 2012). Due to the distribution of the main tributaries the cumulative discharge increases gradually along the estuarine axis (Figure 5.6) Because the water residence time also increases towards the mouth (Figure 5.6), more DSi from tributaries input may accumulate in the same water body as further upstream, causing the slight DSi increase in the estuary. Additional DSi input along the estuarine axis may come from the tidal marshes as described in chapter 3. Their spatial extend increases drastically after km 640.

The δ^{30}Si signal (Figure 5) is lower than during the October cruise, corroborating the hypothesis that uptake of DSi by diatoms caused the decrease in October. Due to the DSi distributions the estuary can be separated into two zones. Firstly, zone 1, the DSi gain zone, between km 609-669 and secondly, zone 2, where DSi concentrations decrease due to conservative mixing. In zone 1 the δ^{30}Si values decrease and then increase again. Finding an explanation for the observed pattern, however, is much more difficult than for the October data. It seems to be that a combined effect of mixing with tributary water and fractionation due to a liquid-solid exchange is responsible for the observed pattern.
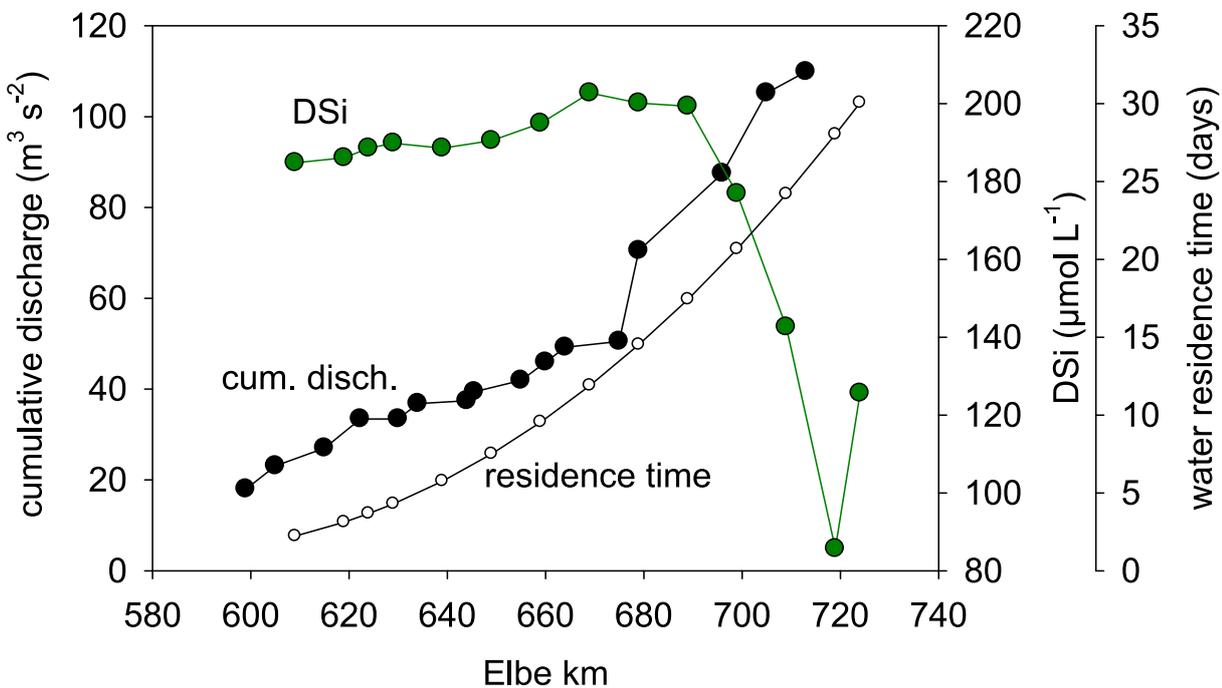
Figure 5.6: cumulative discharge of tributaries along the estuary in relationship with DSi concentrations and water residence time. The cumulative discharge was calculated with the long term annual mean discharge of the individual tributaries. The water residence time is based on the Elbe discharge at Neu Darchau and the empirical relationship $W_T = a*discharge^2 + b * discharge + c$, which was derived from figure 3 in Bergemann et al. (1996).

61

The decrease in the first half of zone 1 coincides with the harbour area of the city of Hamburg. There one tributary, the Alster, enters the main stream of the Elbe at km 615. Additionally, the inlet of the sewage treatment plant is located at km 620. This could indicate the mixing of isotopic lighter water to the main stream, which could have caused the drop of δ^{30}Si. A back of the envelope calculation, with mean DSi concentrations, discharge data from the tributaries and the sewage treatment plant, as well as assumed d^{30}Si values (Table 5.2), reveals that the input of DSi by the tributaries is unable to explain the observed drop of δ^{30}Si in that area. The tributary input would lower the δ^{30}Si signature from 1.47‰ to only 1.28‰, which is not even near the observed 0.85‰. Because until now no δ^{30}Si measurements exists for the tributaries in question and the discharge data was not recorded during the sampling period it is not possible to make a quantitative estimation of the inputs and the answer to the hypothesis remains speculative.

The subsequent increase of δ^{30}Si from the local minimum at km 629 to 1.54‰ could reflect the input of water with higher δ^{30}Si values and DSi concentrations coming either from seven tributaries which discharge into the estuary between km 630-660 and/or from the tidal marsh areas. As showed in Figure 5.2, the δ^{30}Si values and DSi concentrations

Table 5.2: Overview of discharge, long term mean DSi concentrations from December, and δ^{30}Si values of tributaries used in the probability check calculation (explanation see text). Discharge is the long term mean for December plus its standard deviation to yield a maximum estimate (data from FGG Elbe (2012)). The same procedure was applied to the DSi concentrations. The DSi concentration of the Alster was set to 200 µmol L^{-1}, due to lack of data. The δ^{30}Si values of the tributaries were assumed to be 0‰, the lowest values measured in rivers (Opfergelt & Delmelle 2012). The DSi concentration of the sewage treatment input was assumed to be 1000 µmol L^{-1}, which was based on measurements of tap water in the author's laboratory in Hamburg. For the δ^{30}Si signature, the lowest value measured in groundwater was used (Opfergelt & Delmelle 2012).

	location of tributaries (Elbe km)	Discharge (m^3 s^{-1}) mean	stdev	Dsi (µmol L^{-1}) mean	stdev	δ^{30}Si (‰)
Ilmenau	599	9.2	2.7	262.3	36.3	0
Seeve	605	4.6	1.2	193.6	90.3	0
Dove Elbe	615	2.6	1.2	244.5	11.4	0
Alster	622.3	6.4		200.0		0
Sewage treatment plant	623	5.1		1000.0		-1.43

from the marsh side all exceed the δ^{30}Si values from the estuary and especially the low value of 0.85‰ of the harbour region. If the δ^{30}Si signature of the marsh water is the same in December as in November, input of this water into the estuary thus might as well increase the δ^{30}Si value. Another process that might increase δ^{30}Si values is the fractionation due to solid-liquid exchange on clay minerals or biological uptake as described above. Under the temperature and light conditions the latter process would be severely down regulated. The solid-liquid exchange would be favoured by the increase of the SPM concentrations from 20.7 to 364 mg L^{-1}, but would not explain the increase of DSi concentrations. Only a combination of the before mentioned processes could explain the changes of δ^{30}Si in zone 2. Yet, to answer the open questions, future sampling campaigns must be carried out, including all possible DSi sources, such as tributaries, groundwater and the sewage treatment plant discharge. Additionally, the role of the harbour basins in altering DSi and δ^{30}Si signals should be analysed to quantify the influence of anthropogenic disturbance on the distribution of δ^{30}Si in the estuary.

5.6 Conclusions

The Elbe estuary is a location where alteration of the isotopic signal of DSi takes place. This finding is new in silica isotope related studies and underlines the role of estuaries for the alteration of the riverine δ^{30}Si signal. Especially in the tidal freshwater zone the changes of δ^{30}Si signatures can be huge, which highlights the importance of this zone for biogeochemical transformations of silica in tidal estuaries. However the lack of knowledge about the DSi and δ^{30}Si dynamics of external sources prevents a detailed quantification of the isotopic landscape. This, however, is a prerequisite for the understanding of the influence estuaries have on the isotopic silica cycle in the land ocean transition zone and thus the marine cycle. Future studies of estuarine silica dynamics should therefore include isotopic sampling of all possible endmembers as well as seasonal sampling to promote our understanding of the processes which influence the silica cycle in estuaries, which, in face of anthropogenic disturbance of the two elemental cycles and the consequences for the global climate, is an important undertaking.

6 Sources and export of DIC and TA from tidal creeks along a salinity gradient in the Elbe estuary, Germany

6.1 Abstract

Tidal marshes are direct sources of DIC and TA to adjacent water bodies due to advective transport of highly enriched soil porewater from the marsh area. Based on studies conducted on the east coast of the USA, the main source of DIC and TA is thought to be sulfate reduction. In north European tidal marsh systems, however, it is possible that $CaCO_3$ dissolution may be an important source of DIC and TA, because hydrological and morphological conditions of the coastal zone favour the import of $CaCO_3$ rich sediments to the tidal marsh areas. In this study the spatio-temporal variability of the carbonate system and the DIC export fluxes from three tidal marshes along a salinity gradient in the Elbe estuary, Germany were studied. DIC and TA concentrations together with major ion concentrations were measured over one tidal cycle in different seasons in the main creek of the sampling location. The mean DIC and TA concentrations increased from the freshwater to the two brackish sampling sites by more than 2-fold. They were the highest concentrations measured in tidal marsh studies reaching 14237 μmol kg^{-1} at the brackish sampling site in summer. The tidal variability was also high, showing a 1.7 to 3.2 fold difference between low and high tide concentrations. Mixing analysis revealed that carbonate dissolution is the dominant source for TA in these systems, as opposed to tidal marshes in the USA, where sulphate reduction is the main TA generating process. Export fluxes of DIC and TA were similar due to the low percentage of CO_2 in the water (< 4.4%). The export fluxes ranged from 0.06 ± 0.03 to 0.24 ± 0.07 mol m^{-2} d^{-1} with no apparent seasonal pattern. The lowest but also the highest flux was calculated for the freshwater sampling site. DIC export from the whole tidal marsh areas could account for 7.5-27.8% of the excess DIC (i.e. DIC in excess of that expected from conservative mixing

between seawater and freshwater and equilibrium with the atmosphere) measured in the estuary. The area weighted fluxes are 194 to 621-fold higher than the DIC export from the Elbe watershed, stressing the importance of these areas in estuarine and even regional land-ocean DIC fluxes.

6.2 Introduction

Studies of estuarine carbon dioxide (CO_2) and dissolved inorganic carbon (DIC) dynamics have shown that inner estuaries exhibit high rates of net heterotrophy, i.e. respiration exceeds primary production in this systems, and are generally supersaturated with respect to CO_2 (Smith & Hollibaugh 1993, Frankignoulle et al. 1998, Gattuso et al. 1998, Borges 2005). Sources of the net heterotrophy in estuarine systems include water-column and benthic respiration, groundwater inputs (Kempe et al. 1991), photo degradation of dissolved organic matter (Tzortziou et al. 2007), and inputs of inorganic carbon from intertidal marshes (Cai & Wang 1998).

Tidal salt marshes play an important role as a source for DIC and TA in marsh dominated estuaries along the east coast of the United States (Cai & Wang 1998, Cai et al. 1999, Cai et al. 2000, Cai et al. 2003a, Jiang et al. 2008). Studies showed that the export of DIC and TA from the marsh areas can account for a major fraction of the net heterotrophy observed in the estuarine systems. In the York River estuary, for example, the tidal marsh export of DIC could account for 47 ± 23% of its excess DIC production (i.e. DIC in excess of that expected from conservative mixing between seawater and freshwater and equilibrium with the atmosphere) (Neubauer & Anderson 2003). On a regional scale it has been shown that the DIC export flux from tidal marshes contribute about 58 Tmol C yr^{-1} to the total DIC flux to the continental shelf in the U.S South Atlantic Bight of 108 Tmol C yr^{-1} (Cai et al. 2003a).

Considering European estuaries, there exist only a few studies about the sources and the influence of tidal marshes on the estuarine carbonate system, with a regional focus on the Mediterranean tidal marsh systems. For example, Forja et al. (2003) showed that the circulation of coastal water from the Bay of Cádiz through a salt marsh system increased the DIC flux by a factor of 2.8. Also in the Bay of Cádiz La Paz et al. (2008) showed that Rio San Pedro, a tidal creek influenced by fish farming activities, exported DIC to the adjacent coastal area. Only one study examined the origin of DIC interstitial waters of

tidal freshwater marshes (Hellings et al. 2000), without addressing the influence of the marsh areas on the carbonate system of the estuary.

The processes which create DIC and the TA in marshes (salt and freshwater) are manifold. Under anoxic conditions, as frequently present in the water logged marsh soils, nitrate, manganese, iron, and sulphate reduction are the main respiratory pathways (Mitsch & Gosselink 1993) which all produce DIC and TA. The contribution of each process to the total soil respiration is governed by various factors such as temperature, water-table level, reduction-oxidation potential, pH (Mitsch & Gosselink 1993), plant growth (Neubauer et al. 2005, Keller et al. 2012) and the availability of electron donors and electron acceptors (Sutton-Grier et al. 2011). All of these processes haven been frequently used to explain the excess DIC and TA concentration, i.e. DIC in excess of that expected from conservative mixing between seawater and freshwater and equilibrium with the atmosphere, in the above mentioned studies of the marsh dominated estuaries (Raymond et al. 2000).

Additionally, DIC and TA can be produced by the dissolution of calcium carbonate ($CaCO_3$), a process widely recognized in marine sediments (c.f. Morse et al. 2007 and references therein) which has never been reported to play an important role in the TA generation in tidal marsh sediments or marsh-estuarine systems. In the Elbe estuary the calcite content of suspended matter ranges between 3-17%-wt. which is mainly of marine origin (Schwedhelm et al. 1988). The tidal marshes of the Elbe estuary trap the $CaCO_3$ rich sediments resulting in $CaCO_3$ bearing marsh soils. The production of protons during the anaerobic degradation of organic carbon can thus be buffered by the dissolution of $CaCO_3$, increasing the DIC and TA concentration in the soil porewater. Surprisingly, this process has been mentioned as a DIC and TA source only episodically for environments such as estuaries (Kempe 1982, Hellings et al. 2000) and submarine groundwater estuaries in a salt marsh environment (Cai et al. 2003b).

In this study the carbonate system of tidal creek water of three sampling sites along an estuarine salinity gradient of the temperate Elbe estuary is analysed. It is hypothesised that a major part of the alkalinity stems from $CaCO_3$ dissolution. The export of DIC and TA from the tidal creek systems is assessed combining geographic information systems (GIS) with field measurements.

6.3 Material and Methods

6.3.1 Study area

The Elbe estuary in northern Germany is the connection to the North Sea for the fourth largest river basin in Europe and heavily influenced by human activities. It underwent a phase of extensive anthropogenic pollution from the 50s to 80s but is now recovering from this eutrophication (Adams et al. 2002, Amann et al. 2012). The anthropogenic influence is still high due to river engineering, e.g. dyke construction, bank protection measures and the deepening of the shipping channel, which lead to the loss of tidal marshes in the estuary. The tidal influence reaches 142 km inland to the city of Geesthacht where a weir stops the tidal wave. Tides are diurnal with mean tidal amplitudes of 3 m at the mouth and 3.6 m at the harbour region of the city of Hamburg (for more details see section 2.1).

Three sampling sites in the dyke foreland of the Elbe estuary were chosen along its longitudinal axis to represent three different salinity zones of the estuary. One freshwater site and two mixo-mesohaline sites, with a long term salinity range of 5-18 and 5-30, respectively. The sites differ in their dominant vegetation as well as in their hydrology. A detailed description can be found in section 2.2.2.

6.3.2 Sampling and analysis

Sampling was carried out seasonally in 2010 and 2011. At each sampling day, water samples were taken in hourly intervals for 7-12 hours to obtain water from the seepage phase as well as the bulk phase of the tidal cycle. The seepage phase represents soil pore water which drains from the marsh area during ebb tide. The bulk phase is defined as the period of time where estuarine water is flowing in or out of the tidal creeks in great volume. During this period the water depth in the creek is several decametres high. At high tide the creek is normally filled up to its edge. The bulk water mass is dominated by the estuarine endmember. The seepage phase is the period of time were gravitational drainage of soil pore water from the marsh occurs. During this phase generally only a small central channel of about 15-40 cm in width and about 5-10 cm in depth was filled with water. The water mass during this period is dominated by the soil pore water from the marsh area. Occasionally the water level during the seepage phase was higher than

67

several cm because of an intense flooding event during the previous flood, which led to infiltration of high amounts of flooding water into the marsh soil. This water was then released during the seepage phase in which sampling occurred.

pH, temperature, salinity ,and oxygen

Temperature, salinity, pH and oxygen were measured with handheld sensors (pH, temperature: Methrohm pH 827, Primatrode 6.0228.020 or Aquatrode 6.0257.000; salinity and oxygen: WTW 350i ConOX) after the DIC samples were taken. Therefor the plastic cylinder was carefully filled to avoid bubble formation and turbulence. The cylinder was then placed on a magnetic stirrer which was set on slow rotation. This was done to avoid the formation of a stagnant layer around the sensors that would otherwise have caused erroneous measurements of the oxygen concentrations and the pH. A three point calibration with NBS standards was performed in the morning of every sampling day. The oxygen sensor was calibrated at the same time using the calibration chamber provided by WTW.

To calculate average pH values the pH was first converted to H^+ concentrations, averaged and converted back to pH, to avoid errors that are associated with the averaging of logarithmic data, such as pH. The error can be as high as 0.2 pH units which is a significant value when calculating pCO_2 and TA from pH and DIC concentrations (Dickson et al. 2007).

Nutrients, major Ions

Water was sampled with a plastic cylinder attached to a telescope bar. The water from the cylinder was transferred to a syringe and filtered through 0.45µm nylon filters (Minisart®). Aliquots of the filtered water were used for metal, nutrient and major ion samples. The cation samples were acidified (2 vol-% concentrated HNO_3) and nutrient samples poisoned with $HgCl_2$ to suppress microbial activity. All samples were stored in a cool box. In the laboratory they were stored at 4 °C until analysis.

Concentrations of nitrate, nitrite, phosphate, and ammonium were measured with a Technicon AutoAnalyzer System III, silicate was measured manually. Both, automatic and manual measurements followed standard colourimetrical techniques (Hansen & Koroleff 1983).

The concentrations of Ca^{2+} and Mg^{2+} were measured after appropriate dilution by inductively coupled plasma (ICP) optical emission spectrometry (at the Institute of Baltic Sea Research, IOW) with IAPSO low salinity seawater standard (OSIL Ltd.) as internal standard, Cl^- and SO_4^{2-} were measured chromatographically on a Metrohm 881 Compact IC Pro system. The recovery for the determination of Cl^- and SO_4^{2-} were 99.0 ± 1.7 % and 97.5 ± 3.3 %, respectively. The precision for the determination of duplicate samples was better than 1% for both ions

Dissolved inorganic carbon

DIC samples were taken in duplicates with 250 ml glass bottles (Schott Duran®) using the telescope bar. The bottles were filled slowly at the water surface to reduce turbulent mixing and to prevent bubble formation, which would have caused outgassing of CO_2. Immediately after filling 120-360 µl saturated $HgCl_2$ was added and the bottles were capped with screw caps holding gas tight PTFE septa. The samples were stored at 4°C in the laboratory until analysis.

DIC samples were measured with a Marianda VINDTA 3D automated DIC analyser at constant temperature of 25°C. The system was calibrated using certified reference material (CRM, Dickson). The same material was used as an internal check standard during measurements. The mean accuracy of the measurements was 0.37% (0.001%-1.590%).

Calculation of the carbonate system

The excel macro of the CO2sys program (Pierrot et al. 2006) was used to calculated the TA and the pCO_2 as well as the saturation state of calcite and aragonite, correcting for dissolved silica and dissolved phosphorous. The following settings were used:

1. Constants: Cai & Wang 1998
2. $KHSO_4$: Dickson
3. pH scale: NBS
4. input parameter case: DIC and pH

For each parameter of the carbonate system the average of the duplicate samples was calculated and used in the data analysis.

6.3.3 DEM Modelling

Digital elevation model

To quantify the DIC export from the sampling sites geographic information systems (GIS) a slightly modified methodology as described in chapter 3 was used.

The DEM was provided by the State Office for Agriculture, Environment and Rural Areas, Schleswig-Holstein, Germany (Amtliche Geobasisdaten Schleswig-Holstein, © VermKatV-SH). It was obtained with LIDAR technique in 2007 and included corrections for different vegetation cover, leading to an overall vertical accuracy of ± 20 cm. The resolution of one raster cell was 1 x 1 m. To assure that the creeks visible in the DEM were consistent with the creeks at the sampling site the DEM was compared with the Microsoft Virtual Earth (© 2009 Microsoft Cooperation) satellite map which was linked into the ArcGIS software (ESRI ® Version 10.0).

To be able to calculate the flooding volume of the tidal creeks on the sampling area, the tidal creeks were cut manually from the DEM using the ArcGIS software (ESRI ® Version 10.0). This new dataset was used together with the water level data from the nearest gauge station (obtained from the Waterways and Shipping Administration of the Federal Government (WSV), subdivision Cuxhaven and Schleswig-Holstein). The vertical accuracy of this data was ± 2 cm.

Export calculations

For each set of adjacent sampling time point during ebb tide t(i) and t(i+1) the average DIC enrichment taking the Elbe river water as reference (DIC_{enrich}, mmol m^{-3}) was calculated (Eq. 6.1),

$$DIC_{enrich} = DIC_{marsh,t(i)} - DIC_{river} \qquad \text{Eq. 6.1}$$

where $DIC_{marsh,t(i)}$ is the DIC concentration measured in the tidal creek at time point t(i) and DIC_{river} is the DIC concentration in the estuary. The latter concentration was calculated from DIC concentrations of samples taken in the same month in the shipping channel of the Elbe estuary. Therefor spatial intervals were defined for each marsh sampling location and the DIC_{river} concentration was calculated from all sampling points in these intervals. To account for natural variability of the DIC concentrations in the estuary

the "average + standard deviation" and the "average − standard deviation" were used to calculate the DIC enrichment.

To calculate the DIC export per ebb tide (DIC_{export}, mmol tide^{-1}) the DIC_{enrich} was multiplied by the change in volume (V, in m^3) (Eq. 6.2) between two sampling time points. The water volume at each sampling time point was calculated for each sampling site with the DEM and the water level data using the build in function "surface volume" of the ArcGIS software. This calculation was done with the original DEM elevation and an elevation which was 20 cm lower to account for the uncertainty in elevation due to vegetation cover.

$$DIC_{export} = \frac{DIC_{enrich,t(i)} + DIC_{enrich,t(i+1)}}{2} * (V_{t(i)} - V_{t(i+1)}) \qquad \text{Eq. 6.2}$$

With this procedure six DIC export values were produced for one sampling day, i.e. one set of the above mentioned three estuarine DIC concentrations for the original DEM and one set of three for the -20cm DEM. To get the DIC flux from the sampling sites the average of the six DIC export values were taken and divided by the area of the sampling locations.

To account for the seepage phase, which is not represented by (Eq. 6.2), seepage discharge measured in July 2011 at NF and DSK was used. Seepage discharge was measured during this sampling days by stopping the time which floating particles on the water surface needed to travel a certain distance. To account for the bias induced by wind friction, which lowered the water velocity at the surface of the seepage stream, this value was multiplied by 1.3. Additionally, one seepage discharge value reported for a brackish marsh (Duve 1999) was also taken Into account. From the six numbers the mean and the standard deviation was computed and a minimum and maximum calculated by adding or subtracting the standard deviation from the mean. The two values were then used to calculate a range of the seepage DIC flux from the mean seepage DIC concentration of all samples of the respective sampling location (Appendix 6).

6.3.4 Ca²⁺ excess and SO₄²⁻ depletion

The excess Ca²⁺ concentration in the seepage water samples were calculated by subtracting the theoretical Ca²⁺ concentration of the estuary for the sample salinity from the Ca²⁺ concentration measured in the sample (Eq. 6.3),

$$[Ca^{2+}] \; excess = [Ca^{2+}]_{sample} - [Cl^-]_{sample} * \frac{1}{R} Elbe \qquad \text{Eq. 6.3}$$

where $[Ca^{2+}]_{sample}$ and $[Cl^-]_{sample}$ are the ion concentrations in the seepage water samples and R the Cl^-:Ca^{2+} ratio of the Elbe estuary at seepage sample salinity. R was computed from the best fit solution of a non-linear regression function using Ca^{2+}, Cl^- and salinity data obtained during 12 cruises in 2009-2010 (see Appendix 2).

Sulphate depletion in the seepage water samples was calculated in the same manner according to the formula,

$$[SO_4^{2-}] depletion \; = [Cl^-]_{sample} * \frac{1}{R} Elbe - [SO_4^{2-}]_{sample} \qquad \text{Eq. 6.4}$$

where $[SO_4^{2-}]_{sample}$ and $[Cl^-]_{sample}$ are the ion concentrations in the seepage water samples and R the Cl^-:SO_4^{2-} ratio of the Elbe estuary at seepage sample salinity. The ratio was computed from the best fit solution of a non-liniear regression function using SO_4^{2-}, Cl^- and salinity data obtained during 18 cruises in 2009-2011 (see Appendix 3

From the Ca²⁺ excess and the SO₄²⁻ depletion, the percentage contribution of CaCO₃ dissolution and SO₄²⁻ reduction to the measured DIC and TA concentrations were calculated.

6.4 Results

6.4.1 Water column conditions

Sampling was conducted during astronomical neap or mid tides with the exception of the sampling at NF on the 2011-05-18 which fell on a spring tide. The water was normally confined in the creek and only on two occasions the marsh surface was inundated. During the HDM150910 sampling strong winds led to an intense flooding which lasted
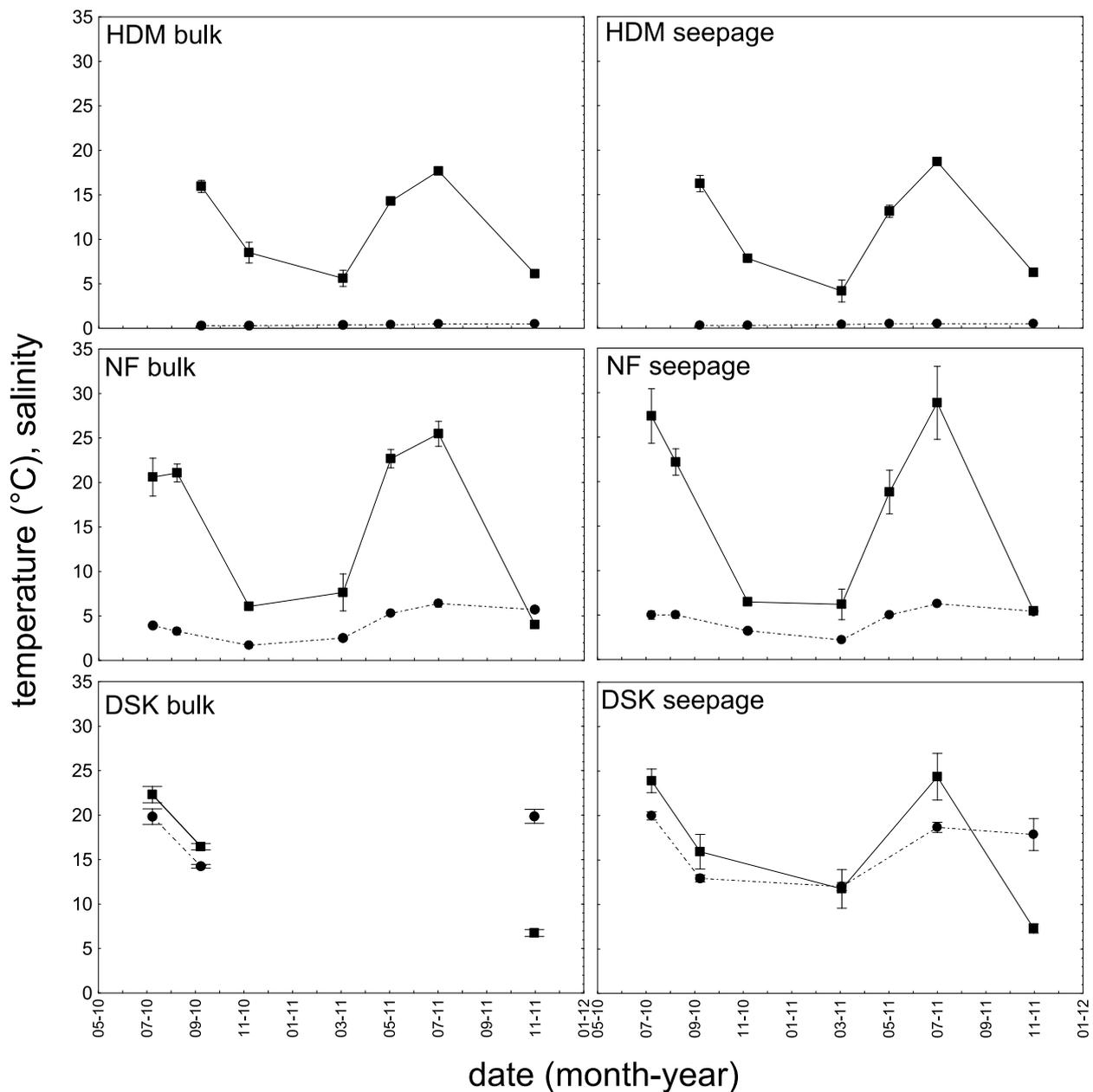
Figure 6.1 Seasonal variation of temperature and salinity in the bulk and seepage water of all three sampling sites. At DSK in March and July no bulk phase occurred due to low high water levels.

for approximately two hours and lead to the inundation of the marsh surface of approximately 0.5 m height. The sampling was conducted after the water retreated from the marsh surface. On 2011-03-11 the sampling site at NF was flooded for approximately 20 minutes. The water depth on the marsh surface during the event was about 0.05 m. During this event sampling continued during the flooding.

Physico-chemical parameters, namely salinity, temperature, pH, and DO showed variations depending on the sampling location, the season, and the tidal stage. The water temperature showed a clear seasonal signal at all three sampling site with slightly lower

mean temperatures (significant with p <0.01, Mann-Whitney U-Test) at the freshwater site than at the brackish or saline site. The lowest mean temperatures were observed in November 2010, and March and November 2011 (Figure 6.1). July temperatures were highest throughout the year.

The tidal variation of temperature could be substantial, especially in summer. A temperature increase of 11.5°C from 18.7 to 30.2°C between the inflowing bulk water and the nearly stagnant seepage water was measured during the NF sampling in 2010-07 (data not shown). Salinity measurements confirmed the existence of a salinity gradient along the estuary. At HDM salinities never exceeded 0.5 units (Figure 6.1). At NF mean values ranged between 2.3 and 6.8 whereas salinities at DSK lay between 12.0 and 19.9 (Figure 6.1). The tidal variation was small and never exceeded 1.7 units at NF and 2.0 units at DSK. The pH range observed during the sampling period ranged from 7.51 to 8.93 (Table 6.1). Averaged over all sampling dates NF had a significantly higher pH than DSK or HDM (Mann-Whitney U Test, p <0.001). The pH between the latter locations was not significantly different from each other (p = 0.96). On a monthly basis the, average pH values at HDM were in general the lowest of the three sampling site and lay between 7.72 ± 0.14 and 7.92 ± 0.13, except in 2011-03 where it reached 8.36 ± 0.26 units.

The DO saturation was positively correlated with the pH. Spearman's rank correlation computed for each sampling date revealed that at HDM the DO saturation and the pH were in all cases significantly dependent (R ≥ 0.81) (Table 6.1). At DSK, the correlation coefficients above 0.58 indicated a lower dependence between pH and DO saturation than at HDM. At NF In four three of seven samplings the correlation coefficient ranged between 0.50 and 0.97. The other cases exhibited correlations coefficients below 0.3 or were even negative in one case.

Absolute DO saturation values ranged between 30.2% and 212.8% which were measured at NF in 05/2011 during one tidal cycle. At the same location mean values were highest in 07/2010 with 123.2 ± 43.7%. At HDM and DSK mean DO saturation was highest in 03/2011 with 131.7 ± 19.2% and 113.7 ± 33.70%, respectively. The tidal variability of the DO saturation was also higher than the seasonal variation, as previously described for the pH data.

6.5 Carbonate system

6.5.1 Spatial and temporal patterns

Between site comparison

Mean DIC and TA concentrations as well as pCO_2 revealed a gradient from the freshwater to the brackish and saline site with lower mean concentrations and partial pressures in the freshwater marsh (Figure 6.2, A,B,C). For each sampling station, seepage concentrations were always higher than bulk concentrations (Figure 6.2, Mann-Whitney-U Test, p ≤ 0.01) with a maximum difference of the means at NF. There a 3.2-fold and 5.9-fold difference between the mean seepage and bulk DIC concentration and pCO_2 was observed.

Seasonal variation

Considering the maximum seepage DIC concentration as a proxy for the marsh pore water concentration no apparent seasonal pattern were visible. At HDM seepage DIC

Table 6.1: Summary of pH and DO statistics of all sampling dates. Spearmann's Rank correlation (R) was calculated for pH vs. DO saturation values. Numbers printed in bold indicate statistically significant correlations for p < 0.05.

| Location | Date | N | pH (NBS) | | | | | | DO saturation (%) | | | | R |
			mean	stdev	min	max	Overall mean	Overall stdev	Mean	Stdev	Overall mean	Overall stdev	
HDM	09-10	8	7.84	0.02	7.66	8.31			82.2	11.5			**0.98**
HDM	11-10	12	7.83	0.11	7.73	7.99			89.7	3.0			**0.90**
HDM	03-11	12	8.36	0.26	7.94	8.72			131.7	19.2			**0.81**
HDM	05-11	12	7.73	0.16	7.52	7.96			76.5	12.9			**0.82**
HDM	07-11	7	7.72	0.14	7.57	7.92			75.6	5.9			**0.96**
HDM	11-11	7	7.92	0.13	7.78	8.05	7.87	0.18	88.4	5.5	92.8	23.7	**0.85**
NF	07-10	11	8.24	0.17	7.99	8.45			123.2	43.7			**0.85**
NF	08-10	10	8.08	0.01	7.83	8.37			94.6	32.8			0.28
NF	11-10	8	7.97	0.02	7.75	8.31			81.7	9.8			**0.98**
NF	03-11	12	8.06	0.23	7.77	8.57			98.0	8.2			0.04
NF	05-11	12	8.00	0.51	7.66	8.93			99.9	67.5			0.71
NF	07-11	13	7.95	0.21	7.72	8.35			88.9	44.1			0.50
NF	11-11	7	8.24	0.00	8.21	8.30	8.05	0.26	90.0	9.0	97.5	39.9	-0.21
DSK	07-10	10	7.97	0.02	7.78	8.45			83.3	34.4			0.59
DSK	09-10	12	7.85	0.16	7.65	8.08			67.9	15.5			**0.74**
DSK	03-11	12	7.66	0.15	7.51	7.91			113.7	33.7			**0.73**
DSK	07-11	8	7.94	0.19	7.80	8.35			98.9	40.0			**0.90**
DSK	11-11	8	7.97	0.12	7.72	8.07	7.84	0.18	86.1	6.1	89.8	32.3	**0.61**

concentrations increased from September to November 2010 (Figure 6.3). In 2011 the pattern was reversed with lowest concentrations in November and highest in March 2011.

At NF a clear increase from 4788 µmol kg^{-1} to 14175 µmol kg^{-1} (Figure 6.3) was observed from March 2011 to November 2011. In 2010 no such pattern was visible. At DSK a trend of increasing maximum seepage DIC concentrations could only be observed in 2011 (Figure 6.3).

Tidal variation

The tidal variation variations of concentrations and partial pressures during each sampling day were considerable (Figure 6.3). Including all samples, DIC concentrations ranged from 1898 – 5276 µmol kg^{-1} at the freshwater site. At NF and DSK a higher variability was observed spanning from 1480 to 14273 µmol kg^{-1} and 2742 – 12236 µmol kg^{-1}, respectively.
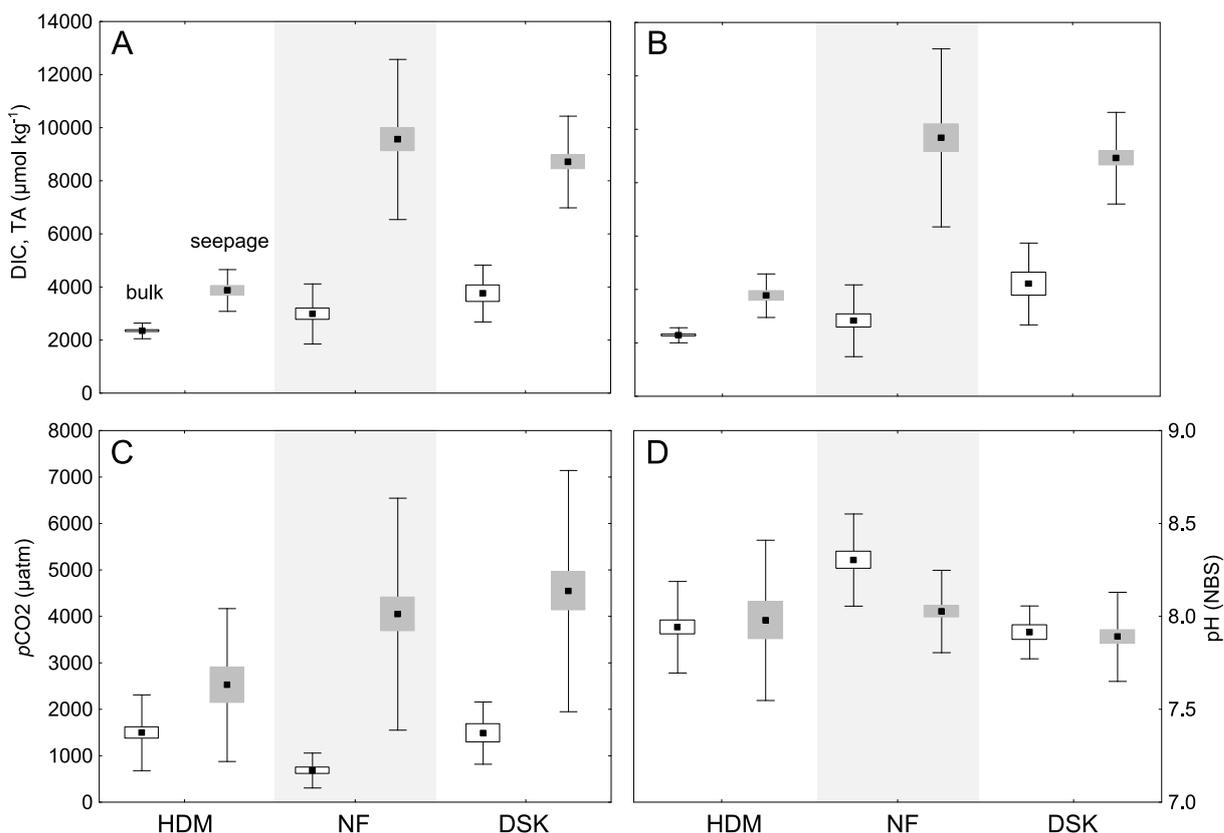

Figure 6.2 Comparison of seepage and bulk pH, pCO$_2$, DIC and TA concentrations at the three sampling locations. A) DIC, B) TA, C) pCO$_2$, D) pH. Black squares are the means, boxes represent the standard error of the mean (white bulk water samples, grey seepage water samples), and whiskers the standard deviation of the mean.

Values of pCO_2 were under-saturated with respect to atmospheric pCO_2 of 390 µatm (March 2011 at HDM and NF, and May 2011 at NF) in 9 out of 172 samples. The remaining 163 samples had pCO_2 well above 390 µatm. In the seepage water the mean super-saturation was 10.5 times the atmospheric value (range 2.6-17.9), the bulk water samples also were supersaturated but on a lower level (3.3-fold, range 0.4-7.8). At HDM the variability as well as the absolute range of pCO_2 was the lowest of all sampling locations (Figure 6.3). The pCO_2 maxima reached only 5434 µatm, whereas values of 10232 µatm and 10191 µatm were reached at NF and DSK, respectively (Figure 6.3).

Diurnal variation during the seepage phase

During the sampling of 2011-03-14 it was possible to observe diurnal changes in the seepage water stream (Figure 6.4) because the tidal creek was not flooded due to a very low high tide. DO saturation increased more than 2-fold from the first sampling time point until 14:30h. After that point the DO saturation dropped to their starting value,

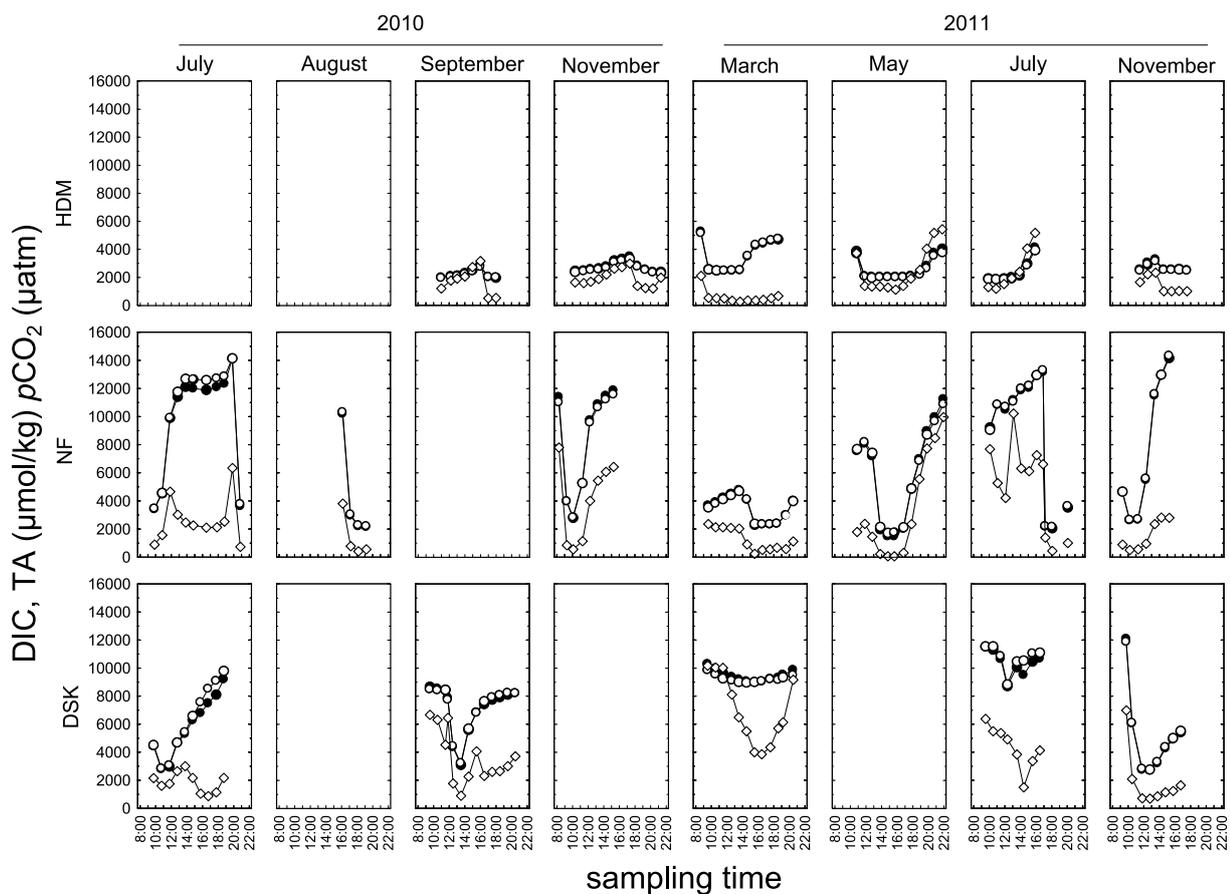Figure 6.3: Tidal variation of DIC, TA and pCO2 of all samplings. Open diamonds = pCO_2, open circles = DIC, filled circles = TA. During the March 2011 sampling only seepage water was sampled at DSK because no flooding of the tidal creek occurred.
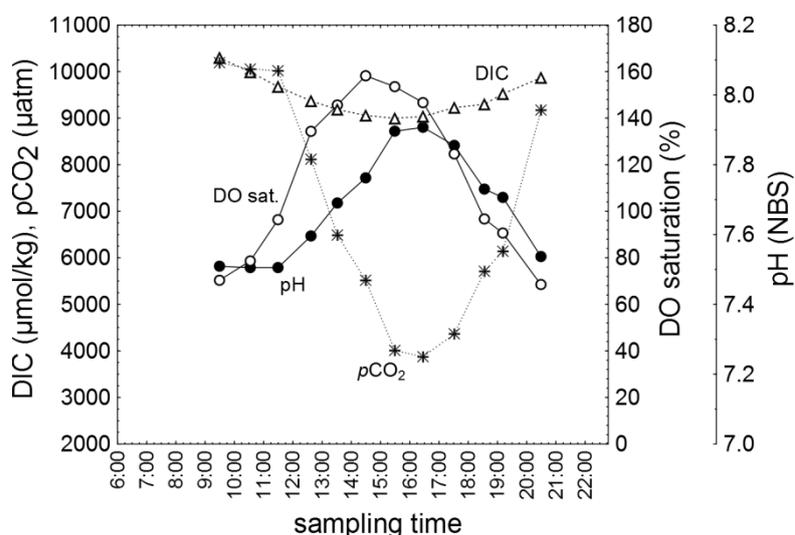
Figure 6.4: Diurnal pattern of DIC, pH, pCO_2 and DO saturation during a 12h sampling campaign in March 2011 at DSK.

creating a nearly bell shaped pattern. The DIC concentration also showed a symmetrical pattern of decrease and increase during the sampling day, reaching their minimum at 15:30h. Within the first seven hours of sampling the concentrations dropped by 1303 µmol kg^{-1}, or about 11% of the starting value.

The pH change followed the change of pCO_2. Both parameters started to change after 11:30h. The pH increased from 7.50 to 7.90 at 16:30h and returned to its starting values at the end of the sampling. The pCO_2 decreased from 10000 µatm to 3870 µatm and nearly reached its starting values at the last sampling point.

6.5.2 Carbonate speciation

In the observed pH range there was little difference of the carbonate species distribution between the three sampling sites. The DIC of the seepage water consisted mainly of HCO_3^- which represented 95.1 ± 1.1%, 96.1 ± 0.6%, and 94.4 ± 1.9% at HDM, NF, and DSK, respectively, causing nearly identical DIC and TA concentrations in the samples (Figure 6.3). The fraction of CO_2 was highest at HDM with 4.4 ± 1.6%. At NF and DSK only 1.9 ± 0.8% and 1.9 ± 1.0% were present as CO_2, respectively. The carbonate ion percentage was highest at DSK and represented 3.7 ± 2.7% of the DIC. At NF the percentage was slightly lower with 1.9 ± 1.2%. The lowest CO_3^{2-} concentration was calculated for HDM, where it only was 0.4 ± 0.4%. These numbers were occasionally exceeded when primary production shifted the carbonate system to more basic conditions. This happened during the sampling at NF in May 2011 and at DSK in both July 2010 and 2011 when the fraction of CO_3^{2-} was then 0.4 – 14.4 % of the DIC and the CO_2 only 0.2 – 0.5%.
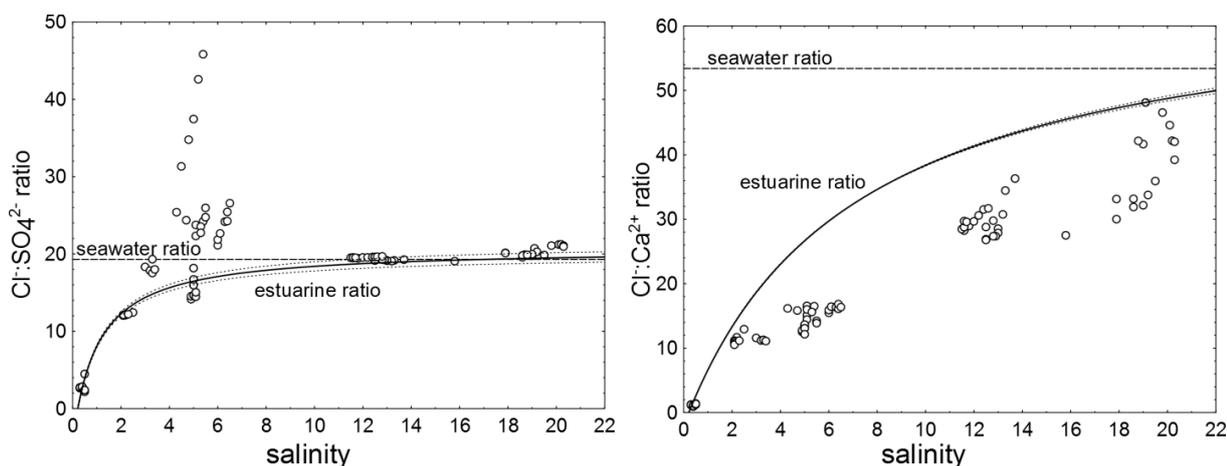
Figure 6.5: Cl^-:SO_4^{2-} and Cl^-:Ca^{2+} ratios in the seepage water samples as a function of salinity. For comparison the modeled estuarine Cl^-:SO_4^{2-} and Cl^-:Ca^{2+} ratios (solid line) as well as the constant seawater ratios are shown (dashed line). The dotted lines indicate the 95% confidence band of the non-linear regressions.

6.5.3 Sources of DIC and TA

The comparison of seepage water sample Cl^-:Ca^{2+} and Cl^-:SO_4^{2-} ratios with the estuarine ratios showed deviations from the estuarine mixing line (Figure 6.5). Because Cl^- concentrations in the seepage samples behaved conservatively (Appendix 4), the deviation from the estuarine ratios indicates addition of Ca^{2+} or removal of SO_4^{2-}, respectively.

While SO_4^{2-} removal was obvious in seepage samples from NF (salinity 3-6.5), the samples from DSK and HDM had Cl^-:SO_4^{2-} ratios that were not clearly distinguishable from the variability induced by measurement errors. The NF samples that showed a clear deviation from the conservative mixing line in July and August, where temperatures were high. All Cl^-:Ca^{2+} ratios of the NF and DSK samples deviated clearly from the estuarine ratios, while four samples from HDM lay above the mixing line

The net contribution of $CaCO_3$ dissolution and SO_4^{2-} reduction to DIC and TA concentrations is summarised in Table 6.2. The SO_4^{2-} depletion at NF accounted for about $20 \pm 13\%$ of the DIC measured in the seepage water, which is similar to the relative contribution of $CaCO_3$ dissolution at NF and DSK. The values do not change substantially, if the negative values were removed. The per cent contribution of $CaCO_3$ dissolution to DIC at NF and DSK was 100% higher than at HDM. When removing the negative percentages from the HDM data, the contribution to DIC nearly doubled. $CaCO_3$

79

dissolution accounted for 23.3-46.7% of the TA. Removing negative values from the HDM samples shifted the contribution to 42.6-57.7%.

6.5.1 DIC export

The individual DIC export fluxes from the three sampling sites, including bulk and seepage phase, ranged from 0.06 ± 0.03 to 0.24 ± 0.07 mol m^{-2} d^{-1} (Figure 6.6). With exception of the November 2010 sampling and despite the much larger water volume that was exported during ebb tide (Figure 6.7), the export fluxes were the lowest at HDM. The DIC export in during the seepage phase contributed between 24%-89% of the total DIC export of a given sampling date (Appendix 7). Extrapolation of the average DIC export per sampling station to the total area of the three different salinity zones of the estuary yielded a total export flux of 11.3 Mmol d^{-1} (range 4.8 – 17.7 Mmol d^{-1}).

The export calculations of the bulk phase contribution were most influenced by the water volume, derived from the DEM (Figure 6.7 A). Variation in the estuarine DIC concentrations had little effect on the DIC export (Figure 6.7 B), with exceptions for the sampling day in November 2010 and July 2011 at HDM, due to a higher variability of the estuarine DIC concentrations in the HDM interval.

Table 6.2: Summary of relative contributions of SO_4^{2-} reduction and $CaCO_3$ dissolution to the DIC and TA concentrations in the seepage water samples.

| Location | N | %DIC SO_4^{2-} reduction (%) | | | | %TA SO_4^{2-} reduction | | | |
		mean	stdev	min	max	mean	stdev	min	max
NF	31	20.7	13.7	-10.4	48.9	20.4	13.1	-10.3	46.4
NF*	23.0	23.9	12.6	1.3	48.9	23.5	11.9	1.4	46.4

| Location | N | %DIC $CaCO_3$ dissolution (%) | | | | %TA $CaCO_3$ dissolution (%) | | | |
		mean	stdev	min	max	mean	stdev	min	max
HDM	14	11.6	28.9	-35.0	43.6	23.3	57.7	-70.0	87.2
HDM*		28.9	6.8	23.9	43.6	57.7	13.5	47.8	87.2
NF	30	23.3	8.8	13.4	40.9	46.7	17.5	26.9	81.8
DSK	37	21.3	7.3	0.0	30.7	42.6	14.6	0.1	61.4

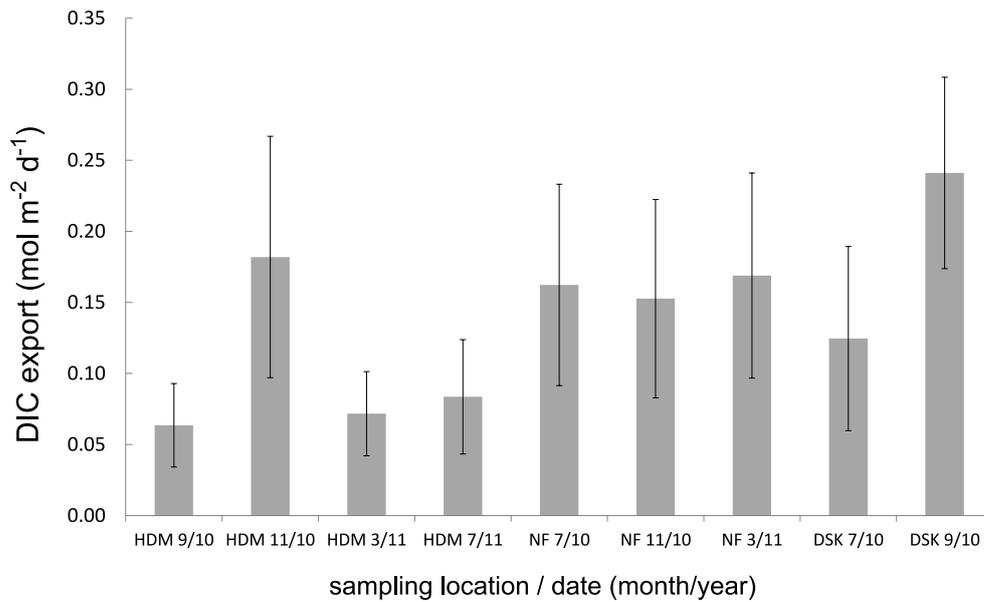*: negative values excluded for the calculations

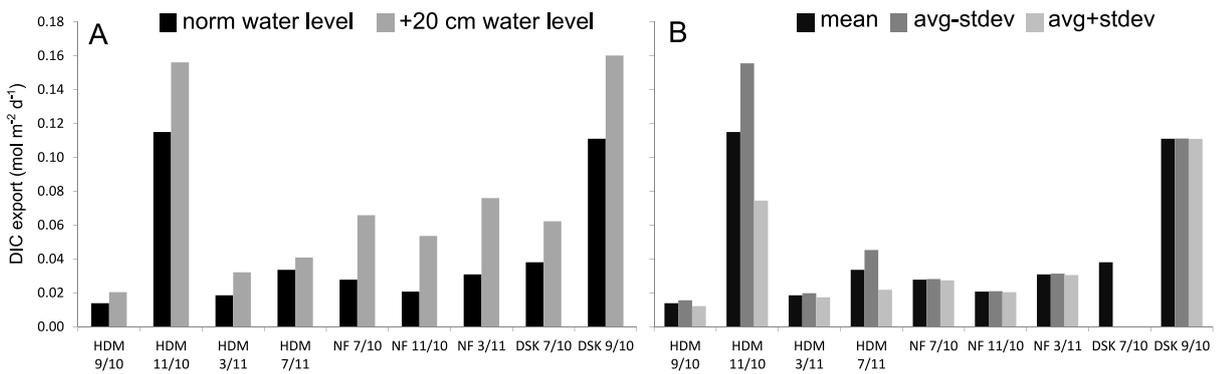Figure 6.6: Average DIC export +/- standard deviation for all sampling sites.

Figure 6.7: Influence of (A) water volume and (B) estuarine DIC concentrations and on the DIC export flux calculations.

6.6 Discussion

6.6.1 Calcium carbonate dissolution as alkalinity source in tidal marsh sediments

The Ca^{2+} excess calculations clearly show that the dominant TA source at all three sampling stations is $CaCO_3$ dissolution, which is a new finding, considering tidal marsh related literature. The first studies that addressed the carbonate system in tidal marshes and their adjacent estuaries were all conducted at the east coast of the US, either in the Georgia salt marsh complexes (Cai et al. 1999, Cai et al. 2000, Wang & Cai 2004) or the Chesapeake Bay area, more specific in the Sweet Hall freshwater marsh of the Pamunkey River, Virginia (Neubauer & Anderson 2003). In several studies about estuarine DIC and TA dynamics it was hypothesised that sulphate reduction is the main source of TA (Cai & Wang 1998, Raymond et al. 2000). For example, Raymond et al. (2000) could show that the accumulation of sulphide in the sediment of a representative site directly adjacent to the York River estuary was sufficient to account for the net export of alkalinity. Several other studies showed that sulphate reduction in concert with pyrite burial is an important process in those marsh systems (Howarth 1979, Howarth & Teal 1979, Luther III et al. 1982, Howarth & Giblin 1983). Only on study showed data that confirmed that $CaCO_3$ dissolution took place in a surficial groundwater aquifer located in a tidal marsh system in South Carolina (Cai et al. 2003b). This process, however, was only of major importance in groundwater of low salinity. The north European marshes and the eastern US marshes can thus be characterised as the $CaCO_3$ type and the SO_4^{2-} type, respectively, with respect on the main source of TA. The tidal marshes of the Elbe estuary belong to the $CaCO_3$ type.

6.6.2 Differences between tidal marshes of the US east coast and northern Germany

Several studies conducted in tidal marshes of Maryland, Virginia, Massachusetts, Rhode Island and Georgia showed mean soil pH values that were in general lower than those typically observed in tidal marshes of the Elbe estuary (see Table 6.3). The pH difference is probably related to the above mentioned differences in soil types. The peat in the US marsh soils is a possible source for organic acids which might lower the soil

pH. Additionally, re-oxidation of pyrite releases protons, which could also cause a steep pH drop. Although this events are rather infrequent, they can decrease the soil pH by 1 unit within 24 hours (Seybold et al. 2002).

Table 6.3: Comparison of different soil properties from tidal marshes of the east coast of the US and the Elbe estuary, Germany. Salinity refers to the values in the adjacent water bodies (estuary, coastal zone).

Location	salinity	pH				C_{org} content	depth (cm)	vegetation	source
		mean	stdev	min	max				
Chesapeake Bay, Maryland	n.d.	6.4	0.7	4.0	7.0	15% (0.1-47.3%)	0-150	n.d.	Darmody & Foss (1979)
Ware Creek Marsh, Maryland	4	6.1	0.1	n.d.	n.d.	n.d.	n.d.	S.c.	Mendelssohn et al. (1976)
Carter Creek Marsh, Maryland	10	6.1	0.1	n.d.	n.d.	n.d.	n.d.	S.a., D.s., S.p.	Mendelssohn et al. (1976)
Wachapreague Marshes, Virginia	30	6.7	0.1	n.d.	n.d.	n.d.	n.d.	S.a, S.v.	Mendelssohn et al. (1976)
Carter Creek Marsh, Maryland	4-16	6.4	0.1	n.d.	n.d.	n.d.	0	S.a.	Wolaver et al. (1986)
	4-16	6.1	0.3	n.d.	n.d.	n.d.	10		Wolaver et al. (1986)
	4-16	5.8	0.2	n.d.	n.d.	n.d.	0	mixed zone	Wolaver et al. (1986)
	4-16	6.5	0.1	n.d.	n.d.	n.d.	10		Wolaver et al. (1986)
	4-16	5.9	0.6	n.d.	n.d.	n.d.	0	S.p., D.s.	Wolaver et al. (1986)
	4-16	5.8	0.4	n.d.	n.d.	n.d.	10		Wolaver et al. (1986)
North Sunken Meadow, Massachussetts	25-30	6.3	0.1	6.2	6.7		45	S.a., S.p., D.s.	Portnoy & Giblin (1997)
Kennon Marsh, Virginia	0	7.3	0.3	6.4	7.8	90-100 g/kg	20	Z.a., B.l.	Seybold et al. (2002)
	0	6.5	0.3	6.1	7.3	50-80 g/kg	50		Seybold et al. (2002)
Chace Cove Marsh, Massachussetts	n.d.	4.7	1	n.d.	n.d.	60.0 ± 10.2 %	0	S.p.	Twohig & Stolt (2011)
	n.d.	7	0.5	n.d.	n.d.	80.0 ± 11.6 %	50		Twohig & Stolt (2011)
Colonel Green Marsh, Massachussetts	n.d.	6.5	1.1	n.d.	n.d.	47.4 ± 7.8 %	0	S.p.	Twohig & Stolt (2011)
	n.d.	7.4	0.7	n.d.	n.d.	53.6 ± 9.4 %	50		Twohig & Stolt (2011)
Elbe estuary, Germany	0-5	7.1	0.3	6.5	8.5	< 5%	0-150	P.a., mixed grasses	Andresen (1996)

B.l. = Bidens laevis, D.s.= Distichlis spicata, P.a. = Phragmites australis, S.a. = S. alterniflora, S.c. = Spartina cynosuroides, S.p. = Spartina patens, S.v. = Salicornia virginica, Z.a. = Zizania aquatic.. n.d. = no data

The difference of the soil porewater pH could link the carbon cycle to the silica cycle in an interesting way. Tidal marshes are well known for their high silica content, because of the production of phytoliths by marsh vegetation (Struyf & Conley 2009). These phytoliths consist of amorphous silica which dissolves 100-100,000 times faster than clay minerals, primary mafic silicates and feldspars (Fraysse et al. 2009). Applying the function for phytoliths dissolution (Fraysse et al. 2009, equation 9) for the pH of 6.3 and 7.1, representative for the top 150 cm of soil of the US and Elbe marshes (see Table 6.3), respectively, yield a 0.40-1.03% difference in dissolution rates. This difference, albeit very small, could potentially alter the long term burial efficiency for phytoliths. It is possible that the pH in the first centimetre of the marsh soil is higher than the average values used in the calculation, due to the presence of higher amounts of $CaCO_3$, which would increase the difference in dissolution rates even more. This would partly explain the fast dissolution of phytoliths in reed litter observed in a tidal freshwater marsh in the Scheldt estuary, Belgium (Struyf et al. 2007), an estuary which lies also in the influence of the Wadden Sea and thus receives $CaCO_3$ rich sediments, which is mirrored in the high amounts of $CaCO_3$ in the sediments of intertidal freshwater areas (Hellings et al. 2000).

6.6.3 $CaCO_3$ sources and transport in the Elbe estuary

The $CaCO_3$ buffer of the Elbe marsh soils is sustained by the delivery of $CaCO_3$ rich sediments to the marsh surface. The deposition of these sediments in the tidal marshes of the Elbe estuary is driven by external processes, which create the prerequisites for the $CaCO_3$ dissolution based TA generation. The first process is the production of $CaCO_3$ rich sediments in the coastal zone of the Elbe estuary, the second process is the transport of these sediments into the estuary.

The origin of the $CaCO_3$ rich sediments is the Wadden Sea, an extensive intertidal zone in the south-eastern part of the North Sea, which includes the area of the outer Elbe estuary. There large amounts of $CaCO_3$ are produced by molluscs, with long term averages of the living standing stock shell weight of 16 g m^{-2} for the bivalve *Macoma baltica* (Beukema 1980) and 104 g m^{-2} for the bivalve *Cerastoderma edule* (Beukema 1982). These molluscs are heavily predated by birds, crabs, and fishes, which results in the fragmentation of the carbonate shells (Cadée 1994) to a size-range from <0.1 to 8mm. The biologically mediated fragmentation of the shells facilitates the displacement of

CaCO$_3$ particles by tidal currents, which otherwise were too weak to transport the whole shells (Flemming et al. 1992). As a result, the calcite content in the 2-63 μm fraction of sediments in the outer Elbe estuary can be as high as 17 %-wt. (Schwedhelm et al. 1988).

Due to the funnel shape of the estuary and the deepening of the shipping channel, the flood current has higher velocities than the ebb current and is of longer duration. This means that sediment, which is suspended during flood tide, travels a longer distance than during ebb tide, resulting in a net upstream movement. This process is known as tidal pumping. As a result, sediment from the Wadden Sea is distributed throughout the whole estuary. At HDM (Elbe km 657) between 30% and 60% are of marine origin, increasing to 80-90% at DSK (Elbe km 713.5) (Schwedhelm et al. 1988). The calcite content in the 2-63 μm fraction of the suspended matter (SPM) lies between 3 and 14 %-wt. Independent measurements of PIC concentrations in bulk suspended matter samples collected during 16 cruises on the Elbe estuary between 2009 and 2011 showed values between 1-9 %-wt. (T. Amann, in prep.). The PIC content of the suspended matter is higher than in the tidal marsh soils. In the upper 40 cm PIC concentrations were always lower than 1% (0.75 ± 0.13% – 0.92 ± 0.18%; K. Hansen, pers. comm.), indicating loss of PIC, which is in line with the observed Ca^{2+} excess.

The CaCO$_3$ rich suspended matter of the Elbe estuary reaches the tidal marsh areas during flood tides. The sedimentation on the marsh surface is heterogenic process and driven by extreme events, because the sedimentation rate is an exponential function of the inundation time of the marsh surface (Temmerman et al. 2003). This means, that of storm surges, which have water levels, that can be greater than 1 m above the marsh surface, contribute above-average to the sediment deposition. For example, during one major flooding at DSK in 2009, 36% of all sediments recorded for a study period of 23 month were deposited (Müller et al. in press).

6.6.4   Carbonate system of the seepage water

Spatial patterns

The absolute DIC and TA concentrations are much higher than previously reported for seepage water. They lie in a concentration range that is found in marsh soil porewater (Neubauer & Anderson 2003, Keller et al. 2009) or marine sediment profiles (e.g. Beck et

al. 2008) in several centimetre to decametre depth. Taking the porewater data from Neubauer and Anderson (2003, table 1) as an example, the influence hydrology and soil permeability can have on seepage and porewater concentrations is explained. The dataset shows that the DIC concentrations increase with distance from the creek bank. This observation is in line with the knowledge about seepage water hydrology in marsh soils. Gardner (2005b) showed that the seepage discharge of a tidal creek is mostly derived from sediments within several metres of the creek bank. Additionally, infiltration into the marsh soil only takes place if the water level surpasses the height of the creek bank, because flooding reduces the hydraulic pressure gradient between the porewater near the creek bank and the one farer away (Fischer 1994, Gardner 2005b). The infiltration occurs with maximum efficiency when the water level does exceed the height of the creek bank (Harvey et al. 1987, Fischer 1994, Xin et al. 2011). The Sweet Hall marsh is typically flooded to a depth of 20-40 cm at high tide, as opposed to the sampling locations in the Elbe estuary. During the study period they were flooded to a depth of 10 cm 12.7% (HDM), 7.2% (NF) and 4.5% (DSK) of the time. The frequent inundation of the Sweet Hall marsh allows infiltration of estuarine water with lower DIC concentrations, which could explain the DIC concentration gradient perpendicular to the creek bank. It could also explain the concentration difference with respect to HDM, because HDM is less frequently flooded as the Sweet Hall marsh sampling site.

The differences in flooding frequency together with different soil permeabilities, could also explain the concentration differences observed along the salinity gradient (Figure 6.2). Data from an environmental impact study (UVU 1997), which analysed soil parameters in the tidal marshes of the Elbe estuary, showed that the average saturated water conductivity was higher at HDM (10-40 cm d^{-1}) than at NF or DSK (1-10 cm d^{-1}, respectively). A flooding event would thus lead to a higher infiltration volume per time at HDM, diluting the porewater stronger than at NF or DSK. Dissolved silica concentrations (Chapter 3), measured in samples taken together with samples for DIC and TA, displayed the same spatial pattern. This finding corroborates the hypothesis that the difference in soil permeability is the determining factor for the DIC and TA concentration distribution

Another process that can decrease the concentration of dissolved matter is dilution due to precipitation. At the sampling sites dilution can occur through precipitation and tidal

inundation. Monthly mean precipitation during the sampling period was slightly higher at NF and DSK (about 40 mm per month; German Weather Service, DWD). Despite higher rainfall at NF and DSK, lowest concentrations were observed at HDM, ruling total precipitation amount out as a main driving factor for the observed concentration differences.

The differences in pCO$_2$ values between HDM and NF as well as DSK (Figure 6.2) are result of the higher DIC concentrations at the latter sites. Although the relative amount of CO$_2$ was higher at HDM (4.4%) than at NF and DSK (1.9%) the absolute was not, because of the lower DIC concentration. Because temperature and salinity differed not very much between the sites the CO$_2$ concentration affected the pCO$_2$ calculation most.

Tidal variation

The different concentrations in the bulk and the seepage phase were commonly observed by other researchers as well. Neubauer and Anderson (2003) reported DIC concentrations during low tide which were 1.8 to 5.3-fold higher than the high tide concentrations, which is in the range of the observed concentration differences in this study. Wang and Cai (2004) measured a 10% difference between low tide and high tide water. The much lower concentration difference can be attributed to the bigger size of the tidal creek in the study, which reduces the ratio of marsh to estuarine water in the creek and thus the influence of the marsh seepage water on the DIC signal in the creek, as shown by Tzortziou et al. (2011). The high tide concentrations were in general higher than the estuarine DIC concentrations, due to the mixing with DIC enriched water during the flood phase. All three sampling stations are bordered with extensive tidal flats. The flooding water thus exchanges with the tidal flat porewater and is enriched in DIC and TA before it reaches the tidal creek.

As benthic microalgae were present in all three sampling creeks throughout the year (A. Weiss, pers. observation) it is most likely that their activity was responsible for the observed correlation between pH and DO saturation in the tidal creeks. The sampling campaign at DSK in March 2011 clearly showed the influence of primary production in the physico-chemical parameters of the seepage water, which give further confidence in the interpretation of cause of the high pH and DO saturation values (see below).

Seasonal variation and the concept of the marsh CO$_2$ pump

Seasonal increase of DIC concentrations in a tidal marsh system was only reported by one study. Wang and Cai (2004) observed an increase of DIC concentrations from spring to fall in the Duplin River, a marsh dominated tidal creek system in Georgia, USA. They proposed a "marsh CO$_2$ pump" concept to explain the observed seasonal variation of DIC concentrations and export. During spring and summer the marsh pumps in large amounts of atmospheric CO$_2$ because of high rates of primary production, while the export is relatively small. This corresponds to an accumulation stage. In fall, primary production decreases while respiration increases and therefore less CO$_2$ from the atmosphere is pumped into the marsh and more inorganic and organic carbon is pumped out. This situation corresponds to a releasing stage. In winter, both primary production and respiration in the marsh are at their annual low.

While it can be assumed that the seasonal temperature differences have an influence on the soil respiration processes, the DIC and TA concentrations of the Elbe marshes do not reflect it in a way as shown by Wang and Cai (2004) for the Duplin River. The reason for this is most likely the difference in size between the two creek systems. The Duplin River is a 12.5 km long marsh-dominated nonriverine tidal river. It has a very long water residence time, compared to small tidal creeks of the Elbe marshes that are filled and drained every tidal cycle. The larger residence time turns the water mass in the Duplin river into a buffer that integrates the DIC signal from marsh export as well as from processes in the water column. It is therefore more comparable to estuaries than to small scale tidal marsh creeks. In small scale tidal creeks the tidal influence, i.e. complete water exchange during one tidal cycle, does not allow for an accumulation of DIC as in the case of the Duplin River. Additionally, small scale systems are also influenced by the tidal action with regard to their dissolved matter concentrations of the seepage water as described in the previous section. These two factors make the detection of a seasonal signal in the seepage water of the Elbe marshes impossible. The data from Neubauer and Anderson (2003), who sampled a creek system comparable in size, also showed no seasonal signal of DIC concentrations in the low tide seepage water and even in soil porewater taken near the creek bank. Furthermore, the DIC concentrations of two consecutive tides in November differed by more than a factor of two. It therefore can be concluded, that on the scale of a single small sized tidal creek the "marsh CO$_2$ pump"

concept might not be applied and may be limited to larger scales, such as the marsh-dominated nonriverine tidal rivers of the salt marsh system of Georgia, USA.

Diurnal variation: the influence of benthic primary production on the carbonate system in the seepage water

The sampling in March 2011 at DSK clearly showed the influence of primary production on the carbonate system in the seepage water of tidal creek (Figure 6.4). The creek banks were inhabited by benthic algae which formed dense mats (A. Weiss, pers. Obs.). The influence of benthic microalgae on the carbonate system of the seepage water is mediated through their potentially high primary production rates (Macintyre et al. 1996), which can increase the DO saturation as well as the pH on the sediment surface (Revsbech et al. 1988). The pH increase is a result of CO_2 uptake by these organisms. Together with the physical water-air CO_2 flux, the primary production leads to a decrease of the DIC concentrations, as observed during the sampling (Figure 6.4). It can be assumed that the reduction of the DIC concentrations by benthic algae will be higher in summer month, because primary production rates are positively correlated with temperature and solar radiation (Cadée & Hegeman 1974). However, only during 3 out of 18 samplings (DSK 2010-07, DSK 2011-03, NF 2011-07, Figure 6.5) the pCO_2 pattern showed signs of primary production during the seepage phase, indicating that the tidal influence can override the biological signal.

Another intriguing hypothesis can be derived from the pH variation in the seepage water, which is induced by benthic primary production. As observed in March 2011 at DSK (Figure 6.4) benthic primary production can increase the pH by at least 0.5 units or even 1.5 units when considering the micro environment of the microbial mat (Revsbech et al. 1983). The shift of the pH from its initial values of about 7.1 in the soil to 8.6 in the seepage water could increase the dissolution rates of biogenic silica by 10-38%. Benthic diatoms could therefore increase their supply of DSi, by enhancing the dissolution of amorphous silica, including the frustules of dead diatoms. This process illustrates nicely the role tidal creeks play in routing and shaping the flow of matter from the tidal marsh system to the estuary.

6.6.5 DIC export

The daily DIC export rates of 0.06 ± 0.03 to 0.24 ± 0.07 mol m^{-2} d^{-1} (Figure 6.6) lie in the same range of previously reported fluxes. Neubauer and Anderson (2003) reported values of 0.033 ± 00.15 to 0.082 ± 0.049 mol C m^{-2} d^{-1} for a freshwater tidal marsh. Another study reported marsh-water column fluxes of 0.054-0.126 mol m^{-2} d^{-1} for the Sapelo Island marsh, Georgia (Cai et al. 1999).

Compared to the mean annual DIC export from the Elbe watershed, which is 63.5 Gmol yr^{-1} (Amann et al. in prep), the flux from the tidal marsh areas in the estuary accounts for 2.8 to 10.2%. Normalized to area, the marsh flux is 194 to 621-fold higher than the DIC export from the Elbe watershed. Because of the high specific fluxes from the marsh areas, they contribute significantly to the estuarine excess DIC. Regarding the excess DIC (i.e. DIC in excess of that expected from conservative mixing between seawater and freshwater and equilibrium with the atmosphere) produced in the inner Elbe estuary, which is 23.3 Gmol yr^{-1} (T. Amann, in prep.), the tidal marsh export could account for 7.5 – 27.8%. This number is smaller than the one calculated by Neubauer and Anderson (2003) for the Pamunkey River and the York River, which is 47 ± 23%. In a global perspective the mean annual DIC flux of 51.9 Mmol km^{-2} yr^{-1} from the tidal marsh areas of the Elbe estuary is 312 time higher than the global average of 0.166 Mmol km^{-2} yr^{-1} reported for rivers (Hartmann et al. 2009) and still 7.8 times higher than the DIC flux from highly active weathering regions, like volcanic areas (6.6 Mmol km^{-2} yr^{-1}, Dessert et al. (2003)).

It is interesting that, despite the differences in the methodology applied to calculate the export rates and the differences of the tidal marsh ecosystems, similar results were obtained. Because of the current lack of comparable studies considering different tidal marsh environments, it is not possible to determine, whether the similarity of the export rates is mere coincidence or a feature of these ecosystems. The complexity of these systems, regarding the influence of hydrology on all biogeochemical processes that can affect the DIC export, makes it impossible to more than speculate about the reasons for different in export fluxes at different study sites. Detailed knowledge of the hydrology and the soil biogeochemistry of different sampling sites is the prerequisite for a meaningful comparison. Therefore, future studies should assess the parameters of the

sampling site in detail and combine their results with theoretical work (e. g. Gardner 2005b), to advance the development of general model that can be used for the calculation of export fluxes from tidal marshes.

6.6.6 Uncertainty assessment

Because the same methodology as in chapter 3 was used, the uncertainty discussion is strongly based on it. To derive the correct water volume from the DEM the model has to represent the creeks and drainage ditches at the sampling watersheds. The comparison with aerial photos confirmed that the large creeks and ditches were reproduced correctly by the DEM (Figure 2.3) However, the extent of smaller drainage ditches were not reproduced accurately. The reason for this underestimation of the creek length is the interference of vegetation with the LIDAR technique. If the vegetation covers the channel, the incoming laser impulses cannot reach the channel bottom, which leads to false values in the DEM. The elevation bias was shown to be highest in tidal creeks where the real elevation is overestimated (Chassereau et al. 2011). That means that the actual creek bed elevation is lower than represented in the DEM. Overestimation of the DEM elevation leads to an underestimation in the volume of the creek channel network. Because of the volume term in Eq. 6.2, the DIC export would also be underestimated. These errors alone lead to an underestimation of the export rates during the bulk phase. The other error source is related to the export rates calculated for the seepage phase. They are based on only two crude measurements of seepage discharge in July 2011 and literature data from other marsh areas in the Elbe estuary. We argue that these values are a rather conservative estimation of the seepage discharge, because all values are from July, when the marsh soil was very dry. Additionally, the measurements at NF and DSK were not made after a total marsh flooding, when seepage discharge was normally higher, due to the marsh soils "sponge effect" (see Müller et al. (in press).

6.7 Conclusion

In this study the spatio-temporal variability of the carbonate system of three tidal marshes in the Elbe estuary, Germany, was assessed. Most of the observed variability could be explained by differences in site specific properties such as soil permeability, vegetation cover and flooding frequency. Short term control on the carbonate system

was influenced by benthic primary production, especially during the seepage phase and has the potential to decrease DIC export fluxes. Furthermore it was shown that the main source for TA was $CaCO_3$ dissolution. If compared to previous studies from the US, where sulphate reduction was thought to be the main TA generating process, this finding adds new information to the variability of factors influencing the carbonate system in tidal marshes. The presence of the $CaCO_3$ buffer in is linked to regional processes in the Wadden Sea, e.g. $CaCO_3$ formation by molluscs and other organisms, and fragmentation of shells by their predators and may also be found in other parts of the world, where a Wadden Sea like ecosystem are present, e.g. Yellow Sea. The seasonal marsh CO_2 pump, a concept developed for marsh dominated estuaries along the continental margin of the South Atlantic Bight, cannot be applied for the settings of the Wadden sea marshes, specifically for marshes with smaller tidal creeks. These findings stress the importance and the need for regional studies of tidal marshes around the Wadden Sea, because assumptions based on knowledge gained in US tidal marshes do not apply in those systems.

7 Synthesis

7.1 Silica in tidal marshes: spatial-temporal patterns and lateral fluxes

Part one of the thesis studied the spatio-temporal patterns of DSi concentrations in tidal creeks and the distribution of BSi in the marsh soil along a salinity gradient in the Elbe estuary, Germany. It could be shown that the general tidal patterns, i.e. high DSi concentrations in the seepage water and low concentrations in the bulk water, were present at all three sampling sites. Seasonally, DSi concentrations increased from spring to autumn at the brackish and saline site. At the freshwater site the variation was lower, which was attributed to different saturated water conductivities of the soils. Compared to other studies, DSi concentrations were among the highest reported in peer-reviewed literature (Müller et al. in press, table 2). Mean annual seepage DSi concentrations increased along the salinity gradient from 270 µmol L^{-1} to 380 µmol L^{-1}. BSi concentration of the soil showed the opposite trend decreasing from 15.8 to 4.8 mg g^{-1}, which was explained with the catalytic effect of higher salinities on the dissolution rates of BSi. The DSi export from the total estuarine marsh area in July was significant and could account for 52-70% of the monthly Elbe river load, which was in line with a previous finding (Struyf et al. 2006a) in the eutrophied Scheldt estuary. Additionally, the importance of diurnal benthic DSi uptake by diatoms on the seepage DSi concentrations was shown. Concentrations were lower around noon than at sunrise or sunset. This observation implicates that DSi concentrations during the nightly seepage phase are higher than during daytime. Estimations of DSi Export which are solely based on daytime observations therefore might be underestimated. Future studies should include nightly sampling to assess difference in DSi export during day and night time. A comparison with DSi mobilisation fluxes from highly active weathering regions, i.e. pyroclastic flows and fresh volcanic rocks (Beusen et al. 2009, Hartmann et al. 2010), showed similar DSi export rates (~1,4 Mmol Si km^2 yr^{-1}) stressing the importance of tidal marsh areas in the coastal silica cycle, despite their limited size.

In the second part the relevance of DSi export from tidal salt marsh areas for regional land ocean DSi fluxes was assessed using the North Sea Basin as an example. Because of the importance of tidal marsh DSi fluxes in estuarine systems (local scale) it was hypothesised, that salt marshes could also be significant sources of DSi in the North Sea silicon budget (regional scale). However, it could be shown that mean annual DSi fluxes from the tidal salt marsh areas around the North Sea accounted for only 0.7% of the annual riverine inputs. During summer, when riverine DSi concentrations are low, the contribution did still not exceed 2.4%. Nonetheless, for smaller regions with favourable geographic conditions of low river inputs and large marsh areas, like the English Channel, salt marsh DSi exports accounted for up to 15% of the riverine DSi flux in summer. The importance of salt marsh DSi flux might be further enhanced in regions, where the benthic-pelagic coupling is reduced due to deeper water depth. There, the surficial supply of DSi into the coastal water would provide DSi which is instantly available, because its supply is independent from mixing processes. Concluding, for the North Sea as a whole, salt marsh DSi fluxes are insignificant for the total DSi budget and do not need to be included in models of DSi fluxes for the regional sea scale (e.g. Meybeck et al. 2007) to global scale (e.g. Tréguer & De La Rocha 2013). Because of the importance of salt marsh DSi fluxes at local scale, however, studies resolving individual coastal segments ("COSCATS" (Meybeck et al. 2006, Beusen et al. 2009, Garnier et al. 2010), should include salt marshes DSi fluxes to improve the estimation of land-ocean DSi fluxes.

7.2 Isotopes of dissolved silicon in the Elbe estuary and its tidal marshes

7.2.1 Tidal marshes

The third part of this thesis analysed spatial and temporal patterns of δ^{30}Si in tidal marshes along an estuarine salinity gradient as well as along the main axis of the estuary, from the freshwater reaches to intermediate salinities. At the tidal marsh areas three tidal patterns of δ^{30}Si were observed. Little variation between bulk and seepage phase δ^{30}Si values (range 1.71 ± 0.08‰ to 1.87 ± 0.13‰) at the freshwater site was explained by previous tidal flooding of the area which led to high percentages of estuarine fraction in the seepage water. At the brackish site seepage δ^{30}Si values were higher than bulk values (~0.8‰, reaching up to 3.26 ± 0.10‰), reflecting the discrimination against heavy

isotopes during plant uptake of DSi. At the saline site the patter was reversed. Additionally, absolute δ^{30}Si values of the seepage water were ~1.8‰ lower than at the brackish site. It was hypothesised that differences in respiration rates of the dominant plant species were responsible. Seasonal variation of δ^{30}Si at the brackish site was similar during May, July, and October. The δ^{30}Si values measured in the seepage water of the brackish site surpass the highest published values for soil solutions (Opfergelt & Delmelle 2012), showing once more that silica is intensely recycled in tidal marsh ecosystems.

7.2.2 Elbe estuary

The data from the estuary showed that alterations of δ^{30}Si occurred mainly in its freshwater part, a new finding for estuarine δ^{30}Si cycling. The distribution of δ^{30}Si during the October cruise could be explained by two processes. The first one was diatom production increasing δ^{30}Si values and decreasing DSi concentrations. The second process was conservative mixing. In December DSi concentrations increased along the estuarine axis, possible due to inputs from tributaries and marshes. The δ^{30}Si signature showed a local drop of 0.6‰ in the harbour area of the city of Hamburg. Due to the poor data coverage it was not possible to pinpoint the exact process which led to the observed patterns. It was hypothesised that a combined effect of mixing with tributary water and fractionation due to adsorption/desorption on suspended matter was responsible. Yet, to answer the remaining open question, what processes were responsible for the alteration of the δ^{30}Si signal in the tidal freshwater reach of the Elbe estuary, future sampling campaigns must be carried out, including all possible DSi sources, such as tributaries, groundwater and the sewage treatment plant discharge. Additionally, the role of the harbour basins in altering DSi and δ^{30}Si signals should be analysed to quantify the influence of anthropogenic disturbance on the distribution of δ^{30}Si in the estuary.

The study showed that the estuarine transition can lead to relevant alterations in the riverine δ^{30}Si signal. Despite the importance of estuarine Si transformations (Laruelle et al. 2009) for land ocean silica fluxes, up to date only rivers and lakes are included in the representation of the isotopic silica cycle (Basile-Doelsch 2006, Opfergelt & Delmelle 2012). So far, only two publications include δ^{30}Si values from estuaries (Ding et al. 2004, Hughes et al. 2012). The here presented data clearly showed that estuaries have the potential to influence the riverine δ^{30}Si signal before it reaches the ocean. The

consideration of estuarine $\delta^{30}Si$ alterations should therefore be included into representations of the silica cycle, because of their possible influence on the whole ocean $\delta^{30}Si$ signature. Future studies should take up the effort of this study to improve the poor data coverage of estuarine systems with respect to $\delta^{30}Si$ values to help to close this knowledge gap in the land ocean silica cycle. This would help not only to improve the understanding of the present day silica cycle, with respect to anthropogenic disturbances, but would also help to reconstruct the marine silica cycle of palaeo-oceans. Because of the link between the marine silica cycle and the global climate, this knowledge might help to reconstruct palaeo-climates and might also improve our understanding of the future climate in a changing world.

7.3 Carbonate system: spatial-temporal patterns and lateral fluxes

The last part of the thesis dealt with the carbonate system of tidal marsh creeks in and the export of DIC to the Elbe estuary. The DIC export rates were comparable to rates measured in other systems. The flux from the tidal marsh areas accounted for 2.8-10.2% of the mean annual DIC export from the Elbe watershed and for 7.5-27.8% of the excess DIC in the estuary (i.e. DIC in excess of that expected from conservative mixing between seawater and freshwater and equilibrium with the atmosphere), which was in line with a previous finding (Neubauer & Anderson 2003). It was shown that the tidal marshes of the Elbe estuary are sources for DIC and TA. The main TA source was calcium carbonate dissolution. The presence of the $CaCO_3$ buffer was linked to regional processes in the Wadden Sea, like $CaCO_3$ formation, subsequent fragmentation and the import to the marsh areas by storm tides. Compared to previous studies from the US (Cai et al. 1999, Raymond et al. 2000, Neubauer & Anderson 2003, Wang & Cai 2004), where sulphate reduction is thought to be the main TA generating process, this finding adds new information to the variability of factors influencing the carbonate system in tidal marshes. It was hypothesised that the presence of the $CaCO_3$ buffer in the Elbe marshes could link the inorganic carbon cycle with the silicon cycle. A comparison of soil pH data from US marshes with data from the Elbe marshes showed, that US marsh soils are more acidic. Higher pH values increase the solubility of BSi (Loucaides et al. 2008, Fraysse et al. 2009), which could led to decreased long term storage of BSi in the Elbe marshes compared to US marsh system.

7.4 Future work

In times of anthropogenic disturbance of the land ocean silica fluxes (Laruelle et al. 2009), the presence of tidal marshes in coastal ecosystems could mitigate the negative effects. The riverine DSi flux is decreased mostly by damming (Humborg et al. 1997, Ittekkot et al. 2000), which traps BSi in the artificial lake environments, i.e. dams. This Si, as opposed to nitrogen and phosphorous, is not resupplied by anthropogenic activities downstream of the dams (Ittekkot et al. 2000), which leads to an increase in N:Si and P:Si nutrient ratios, with unfavourable effects for the aquatic ecosystems (Garnier et al. 2010). Because tidal marsh areas drastically declined in the last centuries due to land reclamation, dyke construction, and the conversion of tidal marsh areas to farmland (Mitsch & Gosselink 1993, Reise 2005), the effectiveness of the natural Si buffer also declined, increasing the anthropogenic pressure on coastal ecosystems. Tidal marshes not only mitigate silicon limitation but are also important areas with respect to flood prevention. In light of rising sea-levels and increased tidal amplitudes in estuaries due to deepening of the shipping channel (Rolinski & Eichweber 2000, Meire et al. 2005), the renaturation of tidal marsh areas came into focus of ecosystem managers (e.g. Sigmaplan 2012). Because artificial tidal marsh system can differ from natural systems with regard to their biogeochemical cycling of nutrients (c.f. Anisfeld 2012), the controlling factors for the silica cycling and the controlling factors of DSi export from artificial tidal marsh areas should be addressed in future studies. This scientific background knowledge would enable the impact assessment of nutrient cycling in coastal ecosystems where tidal marsh areas will be created.

The isotopic silica cycle in the land ocean transition zone is a new field of research with only episodic data reports (Ding et al. 2004, Hughes et al. 2012; this study). This knowledge is needed to improve the global budget for the Si cycle and to constrain the size and isotopic input of the ridge flank hydrothermal flux of Si (and Si isotopes) into the ocean. Future studies of estuarine silica cycling should therefore inculde δ^{30}Si measurements to help to close the knoweldge gap regarding alterations of the riverine δ^{30}Si signal during estuarine transition. Despite the relative good knowledge about the main processes that drive silica cycling in tidal marshes (Jacobs et al. 2008, Struyf & Conley 2009, Schoelynck et al. 2013) and despite their importance for the coastal Si cylce,

the isotopic cycling has not been assessed. Future work should be focused on the transformation processes, i.e. plant uptake, BSi dissolution, and absorption, which drive the isotopic fractionation to establish a baseline for δ^{30}Si values in tidal wetlands. If the isotopic tidal marsh endmembers, i.e. plants, soil, porewater, are better characterised it may be possible to use it as a tool to quantify the contribution of marsh derived DSi to coastal DSi budgets.

The here presented results show that the tidal marshes of the Elbe estuary export DIC and TA to the coastal zone, which confirms the findings from US studies (Cai et al. 1999, Cai et al. 2000, Neubauer & Anderson 2003). However, the presence of a "marsh CO_2 pump" (Wang & Cai 2004) could not be confirmed. Due to the difference of DIC and TA generating processes in the Elbe marshes and the marshes in the US, comparative studies should be carried out to assess if the presence or absence of a carbonate buffer affects the cycling of other elements, too. This knowledge would help to create a typology of tidal marsh areas in the coastal zone that could be implemented in recent coastal typologies, i.e (Meybeck et al. 2006), which are used for land ocean matter flux studies. Furthermore, in contrast to the US, where it was shown that the tidal marsh dominated continental margin has a significant influence on the carbonate system of the US Southern Bight (Cai et al. 2003a, Jiang et al. 2013), no such assessment has been made for the North Sea or other regional seas. As in the case of DSI fluxes, DIC fluxes in regions with large tidal marsh areas, i.e. English Channel, could be of significant importance for the coastal carbon budget. Because of rising atmospheric CO_2 concentrations, due to anthropogenic emissions, the assessment of sinks and sources in the coastal zone was a major undertaking in the past years (Borges 2005, Chen & Borges 2009, Laruelle et al. 2010), to improve the marine carbon budget. These studies however did not include tidal marsh areas as a separate compartment. Studies which would assess the regional DIC fluxes could help to decide whether or not coastal tidal marsh systems should be included as an individual part of the coastal carbon cycle.

In summary, the study of tidal marsh systems with respect to the silica and carbonate system and fluxes from a biogeochemical point of view has only begun recently. Future studies should aim to integrate the new findings about tidal marsh silica cycling in existing concepts of tidal marsh ecology, which were developed since the 1960s, to

deepen the understanding of these exceptional ecosystems in relation to nutrient cycling in the coastal zone.

References

Abril G, Etcheber H, Delille B, Frankignoulle M, Borges A (2003) Carbonate dissolution in the turbid and eutrophic Loire estuary. Marine Ecology Progress Series 259:129-138. DOI 10.3354/meps259129

Abril G, Nogueira M, Etcheber H, Cabeçadas G, Lemaire E, Brogueira MJ (2002) Behaviour of Organic Carbon in Nine Contrasting European Estuaries. Estuarine, Coastal and Shelf Science 54:241-262. DOI 10.1006/ecss.2001.0844

Abril G, Riou SA, Etcheber H, Frankignoulle M, de Wit R, Middelburg JJ (2000) Transient, Tidal Time-scale, Nitrogen Transformations in an Estuarine Turbidity Maximum—Fluid Mud System (The Gironde, South-west France). Estuarine, Coastal and Shelf Science 50:703-715. DOI 10.1006/ecss.1999.0598

Adams MS, Ballin U, Gaumert T, Hale BW, Kausch H, Kruse R (2002) Monitoring selected indicators of ecological change in the Elbe River since the fall of the Iron Curtain. Environmental Conservation 28:333-344. DOI 10.1017/s0376892901000364

Allen JRL (2000) Morphodynamics of Holocene salt marshes: a review sketch from the Atlantic and Southern North Sea coasts of Europe. Quaternary Science Reviews 19:1155-1231. DOI 10.1016/S0277-3791(99)00034-7

Amann T, Weiss A, Hartmann J (2012) Carbon dynamics in the freshwater part of the Elbe estuary, Germany: Implications of improving water quality. Estuarine, Coastal and Shelf Science 107:112-121. DOI 10.1016/j.ecss.2012.05.012

Anderson DM, Glibert PM, Burkholder JM (2002) Harmful algal blooms and eutrophication: Nutrient sources, composition, and consequences. Estuaries 25:704-726. DOI 10.1007/Bf02804901

Anderson GF (1986) Silica, diatoms and a freshwater productivity maximum in Atlantic Coastal Plain estuaries, Chesapeake Bay. Estuarine, Coastal and Shelf Science 22:183-197. DOI 10.1016/0272-7714(86)90112-5

Anisfeld S (2012) Biogeochemical Responses to Tidal Restoration. In: Roman C, Burdick D (eds) Tidal Marsh Restoration. Island Press/Center for Resource Economics

ARGE (2000) Stoffkonzentrationen in mittels Hubschrauber entnommenen Elbewasserproben (1979–1998). Arbeitsgemeinschaft zur Reinhaltung der Elbe

Arndt S, Regnier P, Vanderborght J-P (2009) Seasonally-resolved nutrient export fluxes and filtering capacities in a macrotidal estuary. Journal of Marine Systems 78:42-58. DOI 10.1016/j.jmarsys.2009.02.008

Bartoli F, Wilding LP (1980) Dissolution of Biogenic Opal as a function of its Physical and Chemical Properties. Soil Science Society of America Journal 44:873-878. DOI 10.2136/sssaj1980.03615995004400040043x

Bartoli M, Nizzoli D, Viaroli P (2003) Microphytobenthos activity and fluxes at the sediment-water interface: interactions and spatial variability. Aquatic Ecology 37:341-349. DOI 10.1023/B:AECO.0000007040.43077.5f

Basile-Doelsch I (2006) Si stable isotopes in the Earth's surface: A review. Journal of Geochemical Exploration 88:252-256. DOI 10.1016/j.gexplo.2005.08.050

Bauer A (2010) Einfluss der Beweidung auf den Siliciumgehalt von Pflanzen der Salzmarschen. Bachelor unpublished Bachelor Thesis, Universität Hamburg, Hamburg

Beck M, Dellwig O, Liebezeit G, Schnetger B, Brumsack H-J (2008) Spatial and seasonal variations of sulphate, dissolved organic carbon, and nutrients in deep pore waters of intertidal flat sediments. Estuarine, Coastal and Shelf Science 79:307-316. DOI 10.1016/j.ecss.2008.04.007

Bergemann M, Blöcker G, Harms H, Kerner M, Meyer-Nehls R, Petersen W, Schroeder F (1996) Der Sauerstoffhaushalt der Tideelbe. Die Küste 58:200-261. DOI not available

Bergemann M, Gaumert T (2010) Elbebericht 2008. FGG Elbe, Hamburg

Beukema JJ (1980) Calcimass and carbonate production by mollusks on the tidal flats in the Dutch Wadden Sea: I. The tellinid bivalve *Macoma balthica*. Netherlands Journal of Sea Research 14:323-338. DOI 10.1016/0077-7579(80)90006-x

Beukema JJ (1982) Calcimass and carbonate production by molluscs on the tidal flats in the Dutch Wadden Sea: II the edible cockle, cerastoderma edule. Netherlands Journal of Sea Research 15:391-405. DOI 10.1016/0077-7579(82)90066-7

Beusen AHW, Bouwman AF, Dürr HH, Dekkers ALM, Hartmann J (2009) Global patterns of dissolved silica export to the coastal zone: Results from a spatially explicit global model. Global Biogeochemical Cycles 23:1-13. DOI 10.1029/2008gb003281

Bianchi TS (2007) Biogeochemistry of estuaries. Oxford University Press, New York

Bidle KD (1999) Accelerated dissolution of diatom silica by marine bacterial assemblages. Nature 397:508-512. DOI 10.1038/17351

Bidle KD, Azam F (2001) Bacterial control of silicon regeneration from diatom detritus: Significance of bacterial ectohydrolases and species identity. Limnology and Oceanography 46:1606-1623. DOI 10.4319/lo.2001.46.7.1606

Borey RB, Harcombe PA, Fischer FM (1983) Water and organic carbon fluxes from an irregularly flooded brackish marsh on the upper Texas coast, USA. Estuarine,

Coastal and Shelf ScienceCoastal and Shelf Science 16:379-402. DOI 10.1016/0272-7714(83)90101-4

Borges AV (2005) Do we have enough pieces of the jigsaw to integrate CO_2 fluxes in the coastal ocean? Estuaries 28:3-27. DOI 10.1007/bf02732750

Brush GS, Davis FW (1984) Stratigraphic evidence of human disturbance in an estuary. Quaternary Research 22:91-108. DOI 10.1016/0033-5894(84)90009-7

Brzezinski MA (1992) Cell-cycle effects on the kinetics of silicic acid uptake and resource competition among diatoms. Journal of Plankton Research 14:1511-1539. DOI 10.1093/plankt/14.11.1511

BSH (2010) Gezeitenkalender. Bundesamt für Seeschifffahrt und Hydrographie

Cadée GC (1994) Eider, shelduck, and other predators, the main producers of shell fragments in the Wadden Sea: Paleoecological implications. Paleontology 37:181-202. DOI not available

Cadée GC, Hegeman J (1974) Primary production of the benthic microflora living on tidal flats in the dutch wadden sea Netherlands Journal of Sea Research 8:260-291. DOI 10.1016/0077-7579(74)90020-9

Cadée GC, Laane RWPM (1983) Behavior of POC, DOC and flourescence in the freshwater tidal compartment of the river Ems. In: Degens ET, Kempe S, Soliman H (eds) Transport of Carbon and Minerals in Major World Rivers, Book 55. Geologisch-Paläontologisches Institut Universität Hamburg

Cai W-J, Wang AZ, Wang Y (2003a) The role of marsh-dominated heterotrophic continental margins in transport of CO_2 between the atmosphere, the land-sea interface and the ocean. Geophysical Research Letters 30:1-4. DOI 10.1029/2003gl017633

Cai W-J, Wiebe WJ, Wang Y, Sheldon JE (2000) Intertidal Marsh as a Source of Dissolved Inorganic Carbon and a Sink of Nitrate in the Satilla River-Estuarine Complex in the Southeastern U.S. Limnology and Oceanography 45:1743-1752. DOI 10.4319/lo.2000.45.8.1743

Cai WJ, Pomeroy LR, Moran MA, Wang Y (1999) Oxygen and Carbon Dioxide Mass Balance for the Estuarine-Intertidal Marsh Complex of Five Rivers in the Southeastern US. Limnology and Oceanography 44:639-649. DOI not available

Cai WJ, Wang Y (1998) The chemistry, fluxes, and sources of carbon dioxide in the estuarine waters of the Satilla and Altamaha Rivers, Georgia. Limnology and Oceanography 43:657-668. DOI 10.2307/2839075

Cai WJ, Wang Y, Hodson RE (1998) Acid-base properties of dissolved organic matter in the estuarine waters of Georgia, USA. Geochimica et Cosmochimica Acta 62:473-483. DOI 10.1016/S0016-7037(97)00363-3

Cai WJ, Wang YC, Krest J, Moore WS (2003b) The geochemistry of dissolved inorganic carbon in a surficial groundwater aquifer in North Inlet, South Carolina, and the carbon fluxes to the coastal ocean. Geochimica et Cosmochimica Acta 67:631-639. DOI 10.1016/s0016-7037(02)01167-5

Capone DG, Kiene RP (1988) Comparison of Microbial Dynamics in Marine and Freshwater Sediments: Contrasts in Anaerobic Carbon Catabolism. Limnology and Oceanography 33:725-749. DOI 10.2307/2837220

Carbonnel V, Lionard M, Muylaert K, Chou L (2009) Dynamics of dissolved and biogenic silica in the freshwater reaches of a macrotidal estuary (The Scheldt, Belgium). Biogeochemistry 96:49-72. DOI 10.1007/s10533-009-9344-6

Cardinal D, Alleman LY, de Jong J, Ziegler K, Andre L (2003) Isotopic composition of silicon measured by multicollector plasma source mass spectrometry in dry plasma mode. Journal of Analytical Atomic Spectrometry 18:213-218. DOI 10.1039/b210109b

Cary L, Alexandre A, Meunier J-D, Boeglin J-L, Braun J-J (2005) Contribution of phytoliths to the suspended load of biogenic silica in the Nyong basin rivers (Cameroon). Biogeochemistry 74:101-114. DOI 10.1007/s10533-004-2945-1

Chalmers AG, Wiegert RG, Wolf PL (1985) Carbon balance in a salt marsh: Interactions of diffusive export, tidal deposition and rainfall-caused erosion. Estuarine, Coastal and Shelf Science 21:757-771. DOI 10.1016/0272-7714(85)90071-x

Chassereau JE, Bell JM, Torres R (2011) A comparison of GPS and lidar salt marsh DEMs. Earth Surface Processes and Landforms 36:1770-1775. DOI 10.1002/esp.2199

Chen C-TA, Borges AV (2009) Reconciling opposing views on carbon cycling in the coastal ocean: Continental shelves as sinks and near-shore ecosystems as sources of atmospheric CO_2. Deep Sea Research Part II: Topical Studies in Oceanography 56:578-590. DOI 10.1016/j.dsr2.2009.01.001

Claquin P, Martin-Jézéquel V, Kromkamp J, Veldhuis MJW, Kraay GW (2002) Uncoupling of silicon compared with carbon and nitrogen metabolism and the role of the cell cycle in continuous cultures of *Thalassiosira pseudonana* (Bacillariophyceae) under light, nitrogen, and phosphorous control. Journal of Phycology 38:922-930. DOI 10.1046/j.1529-8817.2002.t01-1-01220.x/full

Conley DJ (1997) Riverine contribution of biogenic silica to the oceanic silica budget. Limnology and Oceanography 42:774-777. DOI 10.4319/lo.1997.42.4.0774

Cunha MA, Almeida MA, Alcantara F (2000) Patterns of ectoenzymatic and heterotrophic bacterial activities along a salinity gradient in a shallow tidal estuary. Marine Ecology Progress Series 204:1-12. DOI 10.3354/meps204001

Daly Ma, Mathieson aC (1981) Nutrient fluxes within a small north temperate salt marsh. Marine Biology 61:337-344. DOI 10.1007/bf00401573

Dankers N, Binsbergen M, Zegers K, Laane R, van der Loeff R (1984) Transportation of water, particulate and dissolved organic and inorganic matter between a salt marsh and the Ems-Dollard estuary, The Netherlands. Estuarine, Coastal and Shelf Science 19:143-165. DOI 10.1007/BF02256686

de Bakker N, Hemminga M, van Soelen J (1999) The relationship between silicon availability, and growth and silicon concentration of the salt marsh halophyte Spartina anglica. Plant and Soil 215:19-27. DOI 10.1023/A:1004751902074

De La Rocha CL, Bescont P, Croguennoc A, Ponzevera E (2011) The silicon isotopic composition of surface waters in the Atlantic and Indian sectors of the Southern Ocean. Geochimica et Cosmochimica Acta 75:5283-5295. DOI 10.1016/j.gca.2011.06.028

De La Rocha CL, Brzezinski Ma, Deniro MJ (1996) Purification, recovery, and laser-driven fluorination of silicon from dissolved and particulate silica for the measurement of natural stable isotope abundances. Analytical chemistry 68:3746-3750. DOI 10.1021/ac960326j

De La Rocha CL, Brzezinski MA, DeNiro MJ (1997) Fractionation of silicon isotopes by marine diatoms during biogenic silica formation. Geochimica et Cosmochimica Acta 61:5051-5056. DOI 10.1016/s0016-7037(97)00300-1

Delstanche S, Opfergelt S, Cardinal D, Elsass F, André L, Delvaux B (2009) Silicon isotopic fractionation during adsorption of aqueous monosilicic acid onto iron oxide. Geochimica et Cosmochimica Acta 73:923-934. DOI 10.1016/j.gca.2008.11.014

Demarest MS, Brzezinski MA, Beucher CP (2009) Fractionation of silicon isotopes during biogenic silica dissolution. Geochimica et Cosmochimica Acta 73:5572-5583. DOI 10.1016/j.gca.2009.06.019

DeMaster DJ (1981) The supply and accumulation of silica in the marine environment. Geochimica et Cosmochimica Acta 45:1715-1732. DOI 10.1016/0016-7037(81)90006-5

Derry La, Kurtz AC, Ziegler K, Chadwick OA (2005) Biological control of terrestrial silica cycling and export fluxes to watersheds. Nature 433:728-731. DOI 10.1038/nature03299

Dessert C, Dupré B, Gaillardet J, François LM, Allègre CJ (2003) Basalt weathering laws and the impact of basalt weathering on the global carbon cycle. Chemical Geology 202:257-273. DOI 10.1016/j.chemgeo.2002.10.001

Deutsche Kommission zur Reinhaltung des Rheins (DK Rhein) (2008) Zahlentafeln der chemisch-physikalischen Untersuchungen 2006. DK Rhein, Worms

Dickson AG, Sabine CL, Christian JR (eds) (2007) Guide to best practices for ocean CO_2 measurements, Vol 3

Ding T, Wan D, Wang C, Zhang F (2004) Silicon isotope compositions of dissolved silicon and suspended matter in the Yangtze River, China. Geochimica et Cosmochimica Acta 68:205-216. DOI 10.1016/s0016-7037(03)00264-3

Ding TP, Ma GR, Shui MX, Wan DF, Li RH (2005) Silicon isotope study on rice plants from the Zhejiang province, China. Chemical Geology 218:41-50. DOI 10.1016/j.chemgeo.2005.01.018

Ding TP, Tian SH, Sun L, Wu LH, Zhou JX, Chen ZY (2008a) Silicon isotope fractionation between rice plants and nutrient solution and its significance to the study of the silicon cycle. Geochimica et Cosmochimica Acta 72:5600-5615. DOI 10.1016/j.gca.2008.09.006

Ding TP, Zhou JX, Wan DF, Chen ZY, Wang CY, Zhang F (2008b) Silicon isotope fractionation in bamboo and its significance to the biogeochemical cycle of silicon. Geochimica et Cosmochimica Acta 72:1381-1395. DOI 10.1016/j.gca.2008.01.008

Dürr HH, Meybeck M, Hartmann J, Laruelle GG, Roubeix V (2011) Global spatial distribution of natural riverine silica inputs to the coastal zone. Biogeosciences 8:597-620. DOI 10.5194/bg-8-597-2011

Duve J (1999) Bilanzierung des Stoffaustausches zwischen Elbe und Deichvorland am Beispiel zweier tidebeeinflusster Untersuchungsgebiete. PhD PhD Thesis, Universtität Hamburg, Hamburg

Eckelmann W, Sponagel H, Grottenthaler W, Hartmann K-J (2006) Bodenkundliche Kartieranleitung. 5. verbesserte und erweiterte Auflage. Schweizerbart'sche Verlagsbuchhandlung, Stuttgart

Eisma D, Bernard P, Boon JJ, Van Grieken R, Kalf J, Mook WG (1985) Loss of particulate organic matter in Estuaries as exemplified by the Ems and Gironde Estuaries. In: Degens ET, Kempe S (eds) Transport of Carbon and Minerals in Major World Rivers, Book 58. Geologisch-Palaeontologisches Institut, Universitaet Hamburg

Engström E, Rodushkin I, Baxter DC, Ohlander B (2006) Chromatographic purification for the determination of dissolved silicon isotopic compositions in natural waters by high-resolution multicollector inductively coupled plasma mass spectrometry. Analytical chemistry 78:250-257. DOI 10.1021/ac051246v

Falkowski PG, Barber RT, Smetacek V (1998) Biogeochemical Controls and Feedbacks on Ocean Primary Production. Science 281:200-207. DOI 10.1126/science.281.5374.200

FGG Elbe (2012) Datenbank der Flussgebietsgemeinschaft Elbe. In: Elbe F (ed)

Fischer SM (1994) Untersuchungen zum Wasserhaushalt Tidebeeinflusster Vorlandmarschen im Ästuar der Elbe. PhD pHd, Universität Hamburg, Hamburger Bodenkundliche Arbeiten

Flemming BW, Schubert H, Hertweck G, Müller K (1992) Bioclastic tidal-channel lag deposits: a genetic model. Senckenbergiana Maritima 22:109-129. DOI not available

Flick RE, Murray JF, Ewing LC (1999) Trends in U.S. Tidal Datum Statistics and Tide Range: A Data Report Atlas. SIO Reference Series No 99-20. Scripps Institution of Oceanography, La Jolla, CA

Forja JM, Ortega T, Ponce R, La Paz M, Rubio JA, Gomez-Parra A (2003) Tidal transport of inorganic carbon and nutrients in a coastal salt marsh (Bay of Cadiz, SW Spain). Ciencias Marinas 29:469-481. DOI not available

Frankignoulle M, Abril G, Borges a, Bourge I, Canon C, Delille B, Libert E, Theate J (1998) Carbon dioxide emission from european estuaries. Science 282:434-436. DOI 10.1126/science.282.5388.434

Fraysse F, Pokrovsky OS, Schott J, Meunier J-D (2009) Surface chemistry and reactivity of plant phytoliths in aqueous solutions. Chemical Geology 258:197-206. DOI 10.1016/j.chemgeo.2008.10.003

Fry B, Wainright SC (1991) Diatom sources of ^{13}C-rich carbon in marine food webs. Marine Ecology Progress Series 79:149-157. DOI 10.3354/meps076149

Gardner LR (2005a) A modeling study of the dynamics of pore water seepage from intertidal marsh sediments. Estuarine, Coastal and Shelf Science 62:691-698. DOI 10.1016/j.ecss.2004.10.005

Gardner LR (2005b) Role of geomorphic and hydraulic parameters in governing pore water seepage from salt marsh sediments. Water Resources Research 41: W07010. DOI 10.1029/2004wr003671

Garnier J, Beusen A, Thieu V, Billen G, Bouwman L (2010) N:P:Si nutrient export ratios and ecological consequences in coastal seas evaluated by the ICEP approach. Global Biogeochemical Cycles 24 DOI 10.1029/2009gb003583

Garrels RM, Mackenzie FT (1971) Evolution of sedimentary rocks. Norton, New York,

Gattuso JP, Frankignoulle M, Wollast R (1998) Carbon and Carbonate Metabolism in Coastal Aquatic Ecosystems. Annual Review of Ecology and Systematics 29:405-434. DOI 10.1146/annurev.ecolsys.29.1.405

Gehlen M, Malschaert H, van Raaphortst W (1995) Spatial and temporal variability of benthic silica fluxes in the southeastern North Sea. Continental Shelf Research 15:1675-1696. DOI 10.1016/0278-4343(95)00012-P

Gerard F, Francois M, Ranger J (2002) Processes controlling silica concentration in leaching and capillary soil solutions of an acidic brown forest soil (Rhone, France). Geoderma 107:197-226. DOI 10.1016/S0016-7061(01)00149-5

Goosen NK, Kromkamp J, Peene J, van Rijswijk P, van Breugel P (1999) Bacterial and phytoplankton production in the maximum turbidity zone of three European estuaries: the Elbe, Westerschelde and Gironde. Journal of Marine Systems 22:151-171. DOI 10.1016/s0924-7963(99)00038-x

Grunwald M, Dellwig O, Kohlmeier C, Kowalski N, Beck M, Badewien TH, Kotzur S, Liebezeit G, Brumsack H-J (2010) Nutrient dynamics in a back barrier tidal basin of the Southern North Sea: Time-series, model simulations, and budget estimates. Journal of Sea Research 64:199-212. DOI 10.1016/j.seares.2010.02.008

Hackney CT, Cahoon LB, Preziosi C, Norris A (2000) Silicon is the link between tidal marshes and estuarine fisheries: A new paradigm. Springer, Dordrecht

Hallegraeff GM (1993) A Review of Harmful Algal Blooms and Their Apparent Global Increase. Phycologia 32:79-99. DOI 10.2216/i0031-8884-32-2-79.1

Hansen HP, Koroleff F (1983) Determination of nutrients. In: Grasshoff K, Ehrhardt M, Kremling K (eds) Methods of Seawater Analysis. Verlag Chemie, Weinheim

Hartmann J, Jansen N, Dürr H, Harashima A, Okubo K, Kempe S (2010) Predicting riverine dissolved silica fluxes to coastal zones from a hyperactive region and analysis of their first-order controls. International Journal of Earth Sciences 99:207-230. DOI 10.1007/s00531-008-0381-5

Hartmann J, Jansen N, Dürr HH, Kempe S, Köhler P (2009) Global CO_2-consumption by chemical weathering: What is the contribution of highly active weathering regions? Global and Planetary Change 69:185-194. DOI 10.1016/j.gloplacha.2009.07.007

Hartmann J, Levy JK, Kempe S (2011) Increasing dissolved silica trends in the Rhine River: an effect of recovery from high P loads? Limnology 12:63-73. DOI 10.1007/s10201-010-0322-4

Harvey JW, Germann PF, Odum WE (1987) Geomorphological control of subsurface hydrology in the creekbank zone of tidal marshes. Estuarine, Coastal and Shelf Science 25:677-691. DOI 10.1016/0272-7714(87)90015-1

Hecky RE, Kilham P (1988) Nutrient Limitation of Phytoplankton in Freshwater and Marine Environments: A Review of Recent Evidence on the Effects of Enrichment. Limnology and Oceanography 33:796-822. DOI 10.4319/lo.1988.33.4_part_2.0796

Hellings L, van den Driessche K, Baeyens W, Dehairs F (2000) Origin and fate of dissolved inorganic carbon in interstitial waters of two freshwater intertidal areas: A case study of the Scheldt Estuary, Belgium. Biogeochemistry 51:141-160. DOI 10.1023/A:1006472213070

Herbst M, Kappen L (1999) The ratio of transpiration versus evaporation in a reed belt as influenced by weather conditions. Aquatic Botany 63:113-125. DOI 10.1016/S0304-3770(98)00112-0

Herman PMJ, Heip CHR (1999) Biogeochemistry of the MAximum TURbidity Zone of Estuaries (MATURE): some conclusions. Journal of Marine Systems 22:89-104. DOI 10.1016/S0924-7963(99)00034-2

Hiemstra T, Barnett MO, van Riemsdijk WH (2007) Interaction of silicic acid with goethite. J Colloid Interf Sci 310:8-17. DOI 10.1016/j.jcis.2007.01.065

Howarth RW (1979) Pyrite: Its Rapid Formation in a Salt Marsh and Its Importance in Ecosystem Metabolism. Science 203:49-51. DOI 10.1126/science.203.4375.49

Howarth RW, Giblin A (1983) Sulfate Reduction in the Salt Marshes at Sapelo Island, Georgia. Limnology and Oceanography 28:70-82. DOI 10.4319/lo.1983.28.1.0070

Howarth RW, Teal JM (1979) Sulfate reduction in a New England salt marsh. Limnology and Oceanography 24:999-1013. DOI 10.4319/lo.1979.24.6.0999

Hughes HJ, Bouillon S, Andre L, Cardinal D (2012) The effects of weathering variability and anthropogenic pressures upon silicon cycling in an intertropical watershed (Tana River, Kenya). Chemical Geology 308:18-25. DOI 10.1016/j.chemgeo.2012.03.016

Humborg C, Ittekkot V, Cociasu A, von Bodungen B (1997) Effect of Danube River dam on Black Sea biogeochemistry and ecosystem structure. Nature 386:385-388. DOI 10.1038/386385a0

IKSE (2005) Die Elbe und ihr Einzugsgebiet - Ein geographisch-hydrologischer und wasserwirtschaftlicher Überblick. In: Elbe IKzSd (ed). Internationale Kommission zum Schutz der Elbe, Magdeburg, Germany

Imberger J, Berman T, Christian RR, Sherr EB, Whitney DE, Pomeroy LR, Wiegert RG, Wiebe WJ (1983) The Influence of Water Motion on the Distribution and Transport of Materials in a Salt Marsh Estuary. Limnology and Oceanography 28:201-214. DOI 10.4319/lo.1983.28.2.0201

Ittekkot V, Humborg C, Schäfer P (2000) Hydrological Alterations and Marine Biogeochemistry: A Silicate Issue? BioScience 50:776-782. DOI 10.1641/0006-3568(2000)050[0776:haamba]2.0.co;2

Jacobs S, Struyf E, Maris T, Meire P (2008) Spatiotemporal aspects of silica buffering in restored tidal marshes. Estuarine, Coastal and Shelf Science 80:42-52. DOI 10.1016/j.ecss.2008.07.003

Jansen N, Hartmann J, Lauerwald R, Dürr HH, Kempe S, Loos S, Middelkoop H (2010) Dissolved Silica mobilization in the conterminous USA. Chemical Geology 270:90-109. DOI 10.1016/j.chemgeo.2009.11.008

Jiang L-Q, Cai W-J, Wang Y (2008) A comparative study of carbon dioxide degassing in river- and marine-dominated estuaries. Limnology and Oceanography 53:2603-2615. DOI 10.4319/lo.2008.53.6.2603

Jiang LQ, Cai WJ, Wang Y, Bauer JE (2013) Influence of terrestrial inputs on continental shelf carbon dioxide. Biogeosciences 10:839-849. DOI 10.5194/bg-10-839-2013

Jones DL, Kochian LV (1996) Aluminium-organic acid interactions in acid soils. Plant and Soil 182:221-228. DOI 10.1007/BF00029053

Jones LHP, Handreck KA (1963) Effects of Iron and Aluminium Oxides on Silica in Solution in Soils. Nature 198:852-853. DOI 10.1038/198852a0

Kamatani A (1982) Dissolution rates of silica from diatoms decomposing at various temperatures. Marine Biology 68:91-96. DOI 10.1007/bf00393146

Kaufman PB, Dayanandan P, Y. T, Bigelow WC, Jones JD, R. I (1981) Silica in shoots of higher plants. In: Simpson TL, Volcani BE (eds) Silicon and siliceous structures in biological systems. Springer-Verlag, New York

Keller JK, Sutton-Grier AE, Bullock AL, Megonigal JP (2012) Anaerobic Metabolism in Tidal Freshwater Wetlands: I. Plant Removal Effects on Iron Reduction and Methanogenesis. Estuaries and Coasts DOI 10.1007/s12237-012-9527-6

Keller JK, Wolf AA, Weisenhorn PB, Drake BG, Megonigal JP (2009) Elevated CO_2 affects porewater chemistry in a brackish marsh. Biogeochemistry 96:101-117. DOI 10.1007/s10533-009-9347-3

Kempe S (1979) Carbon in the rock cycle. In: Bolin B, Degens ET, Kempe S, Ketner P (eds) The Global Carbon Cycle. J. Wiley & Sons, Chichester, New York, Brisbane, Toronto

Kempe S (1982) Valdivia Cruise, October 1981: Carbonate Equilibria in the Estuaries of Elbe, Weser, Ems and in the Southern German Bight. In: Degens ET (ed) Transport of Carbon and Minerals in Major World Rivers (Volume 1, SCOPE/UNEP special issue 52), Book 52. Mitt. Geol. Palaeont. Inst. Univ. Hamburg

Kempe S (1992) Die Elbe, der geologische BIick. Die Elbe - Ein Lebenslauf. Deutsches Historisches Museum und Nicolai, Berlin

Kempe S, Pettine M, Cauwet G (1991) Biogeochemistry of Europe rivers. In: Degens ET, Kempe S, Richey JE (eds) Biogeochemistry of Major World Rivers. John Wiley, Chichester, New York, Brisbane, Toronto, Singapore

Kerner M (1997) Utilization of phytoplankton in seston aggregates from the Elbe estuary, Germany, during early degradation processes. Marine Ecology Progress Series 158:87-102. DOI not available

Krinitz J (2000) Stoffkonzentrationen in mittels Hubschrauber entnommenen Elbewasserproben (1979 bis 1998): allgemeine Gewässergüte, biologische

Kenngrößen, Schwermetalle und Arsen, organische Schadstoffe. Arbeitsgemeinschaft für die Reinhaltung der Elbe, Potsdam

La Paz M, Gómez-Parra A, Forja J (2008) Tidal-to-seasonal variability in the parameters of the carbonate system in a shallow tidal creek influenced by anthropogenic inputs, Rio San Pedro (SW Iberian Peninsula). Continental Shelf Research 28:1394-1404. DOI 10.1016/j.csr.2008.04.002

Lanning F, Eleuterius L (1983) Silica and ash in tissues of some coastal plants. Annals of Botany 51:835-850. DOI not available

Laruelle GG, Dürr HH, Slomp CP, Borges AV (2010) Evaluation of sinks and sources of CO_2 in the global coastal ocean using a spatially-explicit typology of estuaries and continental shelves. Geophysical Research Letters 37:1-6. DOI 10.1029/2010gl043691

Laruelle GG, Roubeix V, Sferratore a, Brodherr B, Ciuffa D, Conley DJ, Dürr HH, Garnier J, Lancelot C, Le Thi Phuong Q, Meunier JD, Meybeck M, Michalopoulos P, Moriceau B, Ní Longphuirt S, Loucaides S, Papush L, Presti M, Ragueneau O, Regnier P, Saccone L, Slomp CP, Spiteri C, van Cappellen P (2009) Anthropogenic perturbations of the silicon cycle at the global scale: Key role of the land-ocean transition. Global Biogeochemical Cycles 23:1-17. DOI 10.1029/2008gb003267

Lauerwald R, Hartmann J, Moosdorf N, Kempe S, Raymond PA (2013) What controls the spatial patterns of the riverine carbonate system? — A case study for North America. Chemical Geology 337–338:114-127. DOI 10.1016/j.chemgeo.2012.11.011

Leynaert A, Longphuirt SN, An S, Lim J-H, Claquin P, Grall J, Kwon BO, Koh CH (2011) Tidal variability in benthic silicic acid fluxes and microphytobenthos uptake in intertidal sediment. Estuarine, Coastal and Shelf Science 95:59-66. DOI 10.1016/j.ecss.2011.08.005

Loucaides S, van Cappellen P, Behrends T (2008) Dissolution of biogenic silica from land to ocean: Role of salinity and pH. Limnology and Oceanography 53:1614-1621. DOI 10.4319/lo.2008.53.4.1614

Lundberg A (1996) Environmental change and nature management in Norway. Norsk Geografisk Tidsskrift - Norwegian Journal of Geography 50:143-156. DOI 10.1080/00291959608622036

Luther III GW, Giblin A, Howarth RW, Ryans RA (1982) Pyrite and oxidized iron mineral phases formed from pyrite oxidation in salt marsh and estuarine sediments. Geochimica et Cosmochimica Acta 46:2665-2669. DOI 10.1016/0016-7037(82)90385-4

Macintyre HL, Geider RJ, Miller DC (1996) Microphytobenthos: The Ecological Role of the "Secret Garden" of Unvegetated, Shallow-Water Marine Habitats. I Distribution, Abundance and Primary Production. Estuaries 19:186-201. DOI 10.2307/1352224

Manning BA, Goldberg S (1996) Modeling arsenate competitive adsorption on kaolinite, montmorillonite and illite. Clay Clay Miner 44:609-623. DOI 10.1346/Ccmn.1996.0440504

Meire P, Ysebaert T, Damme S, Bergh E, Maris T, Struyf E (2005) The Scheldt estuary: a description of a changing ecosystem. Hydrobiologia 540:1-11. DOI 10.1007/s10750-005-0896-8

Meybeck M, Durr HH, Roussennac S, Ludwig W (2007) Regional seas and their interception of riverine fluxes to oceans. Marine Chemistry 106:301-325. DOI 10.1016/j.marchem.2007.01.002

Meybeck M, Dürr HH, Vorosmarty CJ (2006) Global coastal segmentation and its river catchment contributors: A new look at land-ocean linkage. Global Biogeochemical Cycles 20:GB1S90. DOI 10.1029/2005GB002540

Michalopoulos P, Aller RC (2004) Early diagenesis of biogenic silica in the Amazon delta: alteration, authigenic clay formation, and storage. Geochimica et Cosmochimica Acta 68:1061-1085. DOI 10.1016/j.gca.2003.07.018

Middelburg JJ, Herman PMJ (2007) Organic matter processing in tidal estuaries. Marine Chemistry 106:127-147. DOI 10.1016/j.marchem.2006.02.007

Milligan AJ, Varela DE, Brzezinski MA, Morel FMM (2004) Dynamics of silicon metabolism and silicon isotopic discrimination in a marine diatom as a function of pCO$_2$. Limnology and Oceanography 49:322-329. DOI 10.4319/lo.2004.49.2.0322

Mitsch WJ, Gosselink JG (1993) Wetlands. Wiley & Sons, New York

Moosdorf N, Hartmann J, Lauerwald R (2011) Changes in dissolved silica mobilization into river systems draining North America until the period 2081-2100. Journal of Geochemical Exploration 110:31-39. DOI 10.1016/j.gexplo.2010.09.001

Morse JW, Arvidson RS, Lüttge A (2007) Calcium carbonate formation and dissolution. Chemical reviews 107:342-381. DOI 10.1021/cr050358j

Mucha AP, Almeida CMR, Bordalo Aa, Vasconcelos MTSD (2010) LMWOA (low molecular weight organic acid) exudation by salt marsh plants: Natural variation and response to Cu contamination. Estuarine, Coastal and Shelf Science 88 DOI 10.1016/j.ecss.2010.03.008

Müller F, Struyf E, Hartmann J, Weiss A, Jensen K (in press) Impact of grazing management on silica export dynamics of Wadden Sea saltmarshes. Estuarine, Coastal and Shelf Science DOI 10.1016/j.ecss.2013.03.010

Nelson DM, Tréguer P, Brzezinski Ma, Leynaert a, Quéguiner B (1995) Production and dissolution of biogenic silica in the ocean: Revised global estimates, comparison with regional data and relationship to biogenic sedimentation. Global Biogeochemical Cycle 9:359-372. DOI not available

Neubauer SC, Anderson IC (2003) Transport of Dissolved Inorganic Carbon from a Tidal Freshwater Marsh to the York River Estuary. Limnology and Oceanography 48:299-307. DOI 10.4319/lo.2003.48.1.0299

Neubauer SC, Givler K, Valentine SK, Megonigal JP (2005) Seasonal patterns and plant-mediated controls of subsurface wetland biogeochemistry. Ecology 86:3334-3344. DOI 10.1890/04-1951

Ní Longphuirt S, Ragueneau O, Chauvaud L, Martin S, Jean F, Thouzeau G, Leynaert A (2009) Diurnal heterogeneity in silicic acid fluxes in shallow coastal sites: Causes and implications. Estuarine, Coastal and Shelf Science 82:495-502. DOI 10.1016/j.ecss.2009.02.014

Norris AR, Hackney CT (1999) Silica Content of a Mesohaline Tidal Marsh in North Carolina. Estuarine, Coastal and Shelf Science 49:597-605. DOI 10.1006/ecss.1999.0506

Odum EP (2000) Tidal marshes as outwelling/pulsing systems. In: Weinstein MP, Kreeger DA (eds) Concepts and Controversies in Tidal Marsh Ecology

Officer C, Ryther J (1980) The Possible Importance of Silicon in Marine Eutrophication. Marine Ecology Progress Series 3:83-91. DOI 10.3354/meps003083

Opfergelt S, Cardinal D, Henriet C, Draye X, André L, Delvaux B (2006) Silicon Isotopic Fractionation by Banana (Musa spp.) Grown in a Continuous Nutrient Flow Device. Plant and Soil 285:333-345. DOI 10.1007/s11104-006-9019-1

Opfergelt S, Delmelle P (2012) Silicon isotopes and continental weathering processes: Assessing controls on Si transfer to the ocean. Comptes Rendus Geoscience 344:723-738. DOI 10.1016/j.crte.2012.09.006

Opfergelt S, Delvaux B, André L, Cardinal D (2008) Plant silicon isotopic signature might reflect soil weathering degree. Biogeochemistry 91:163-175. DOI 10.1007/s10533-008-9278-4

Paasche E (1980) Silicon. In: Morris I (ed) The Physiological ecology of phytoplankton / edited by I Morris. Blackwell Scientific, Oxford :

Peterson BJ, Howarth RW (1987) Sulfur, Carbon, and Nitrogen Isotopes Used to Trace Organic Matter Flow in the Salt-Marsh Estuaries of Sapelo Island, Georgia. Limnology and Oceanography 32:1195-1213. DOI 10.4319/lo.1987.32.6.1195

Pierrot D, Lewis E, Wallace D (2006) MS Excel Program Developed for CO_2 System Calculations. Carbon Dioxide Information Analysis Center, Oak Ridge National Laboratory, U.S. Department of Energy, Oak Ridge, Tennessee, ORNL/CDIAC-105a

Poulin P, Pelletier É, Koutitonski VG, Neumeier U (2009) Seasonal nutrient fluxes variability of northern salt marshes: examples from the lower St. Lawrence Estuary. Wetlands Ecology and Management 17:655-673. DOI 10.1007/s11273-009-9141-y

Proctor R, Holt JT, Allen JI, Blackford J (2003) Nutrient fluxes and budgets for the North West European Shelf from a three-dimensional model. Science of the Total Environment 314–316:769-785. DOI 10.1016/S0048-9697(03)00083-4

Querné J, Ragueneau O, Poupart N (2011) In situ biogenic silica variations in the invasive salt marsh plant, Spartina alterniflora: A possible link with environmental stress. Plant and Soil 352:157-171. DOI 10.1007/s11104-011-0986-5

Raven JA (2003) Cycling silicon - the role of Accumulation in Plants. New Phytologist 158:419-421. DOI 10.1046/j.1469-8137.2003.00778.x

Raymond PA, Ab B (1997) Carbon Dioxide Concentration and Atmospheric Flux in the Hudson River. Estuaries 20:381-390. DOI 10.2307/1352351

Raymond PA, Bauer JE, Cole JJ (2000) Atmospheric CO_2 evasion, dissolved inorganic carbon production, and net heterotrophy in the York River estuary. Limnology and Oceanography 45:1707-1717. DOI 10.4319/lo.2000.45.8.1707

Reise K (2005) Coast of change: habitat loss and transformations in the Wadden Sea. Helgoland Marine Research 59:9-21. DOI 10.1007/s10152-004-0202-6

Revsbech NP, Jorgensen BB, Blackburn TH, Cohen Y (1983) Microelectrode Studies of the Photosynthesis and O_2, H_2S, and pH Profiles of a Microbial Mat. Limnology and Oceanography 28:1062-1074. DOI 10.2307/2836269

Revsbech NP, Nielsen J, Hansen PK (1988) Benthic Primary Production and Oxygen Profiles. In: Blackburn H, Sorenson J (eds) Nitrogen Cycling in Coastal Marine Environments, Book Part 2. John Wiley & Sons, Chichester, New York, Brisbane, Toronto, Singapore

Rickert D, Schlüter M, Wallmann K (2002) Dissolution kinetics of biogenic silica from the water column to the sediments. Geochimica et Cosmochimica Acta 66:439-455. DOI 10.1016/S0016-7037(01)00757-8

Rolinski S, Eichweber G (2000) Deformations of the tidal wave in the elbe estuary and their effect on suspended particulate matter dynamics. Physics and Chemistry of the Earth, Part B: Hydrology, Oceans and Atmosphere 25:355-358. DOI 10.1016/S1464-1909(00)00025-3

Roubeix V, Becquevort S, Lancelot C (2008a) Influence of bacteria and salinity on diatom biogenic silica dissolution in estuarine systems. Biogeochemistry 88:47-62. DOI 10.1007/s10533-008-9193-8

Roubeix V, Rousseau V, Lancelot C (2008b) Diatom succession and silicon removal from freshwater in estuarine mixing zones: From experiment to modelling. Estuarine, Coastal and Shelf Science 78:14-26. DOI 10.1016/j.ecss.2007.11.007

Schelske CL, Stoermer EF (1971) Eutrophication, silica depletion, and predicted changes in algal quality in Lake Michigan. Science 173:423-424. DOI 10.1126/science.173.3995.423

Schoelynck J, Bal K, Backx H, Okruszko T, Meire P, Struyf E (2010) Silica uptake in aquatic and wetland macrophytes: a strategic choice between silica, lignin and cellulose? New Phytologist 186:385-391. DOI 10.1111/j.1469-8137.2009.03176.x

Schoelynck J, Müller F, Vandevenne F, Bal K, Barão L, Smis A, Opdekamp W, Meire P, Struyf E (2013) Silicon–vegetation interaction in multiple ecosystems: a review. Journal of Vegetation Science DOI 10.1111/jvs.12055

Schwedhelm E, Salomons W, Schoer J, Knauth H-D (1988) Provenance of the sediments and the suspended matter of the Elbe estuary. GKSS-Forschungszentrum Geesthacht GmbH

Scudlark JR, Church TM (1989) The Sedimentary Flux of Nutrients at a Delaware Salt-Marsh Site - A Geochemical Perspective. Biogeochemistry 7:55-75. DOI 10.1007/BF00000897

Seybold CA, Mersie W, Huang J, McNamee C (2002) Soil redox, pH, tempertaure, and water-table patterns of a freshwater tidal wetland. Wetlands 22:149-158. DOI 10.1672/0277-5212(2002)022[0149:srptaw]2.0.co;2

Sherr EB (1982) Carbon isotope composition of organic seston and sediments in a Georgia salt marsh estuary in ecosystems. Geochimica et Cosmochimica Acta 46:1227-1232. DOI 10.1016/0016-7037(82)90007-2

Sicko-Goad LM, Schelske CL, Stoermer EF (1984) Estimation of Intracellular Carbon and Silica Content of Diatoms from Natural Assemblages Using Morphometric Techniques. Limnology and Oceanography 29:1170-1178. DOI 10.4319/lo.1984.29.6.1170

Sigmaplan (2012) Sigmaplan meet the Schledt. Accessed 25.4.2013. http://www.sigmaplan.be/en/

Sigmon DE, Cahoon LB (1997) Comparative effects of benthic microalgae and phytoplankton on dissolved silica fluxes. Aquatic Microbial Ecology 13:275-284. DOI 10.3354/ame013275

Smayda TJ (1990) Novel and nuisance phytoplankton blooms in the sea: evidence for a global epidemic. In: Granéli E, Sundström B, Edler L, Anderson DM (eds) Toxic marine phytoplankton: proceedings of the Fourth International Conference on Toxic Marine Phytoplankton held June 26-30 in Lund, Sweden. Elsevier, New York

Smith VT, Hollibaugh JT (1993) Coastal Metabolism and the Oceanic Organic Carbon Balance. Reviews of Geophysics 31:75-89. DOI 10.1029/92RG02584

Strickland JD, Parsons TR (1972) A Practical Handbook of Seawater Analysis. Fisheries Research Board of Canada, Otawa, ON, Canada

Struyf E, Conley DJ (2009) Silica: an essential nutrient in wetland biogeochemistry. Frontiers in Ecology and the Environment 7:88-94. DOI 10.1890/070126

Struyf E, Conley DJ (2011) Emerging understanding of the ecosystem silica filter. Biogeochemistry 107:9-18. DOI 10.1007/s10533-011-9590-2

Struyf E, dausse A, Van Damme S, Gribsholt B, Boschker HTS, Middelburg JJ, Meire P (2006a) Tidal marshes and biogenic silica recycling at the land-sea interface. Limnology and Oceanography 51:838-846. DOI 10.4319/lo.2006.51.2.0838

Struyf E, Temmerman S, Meire P (2006b) Dynamics of biogenic Si in freshwater tidal marshes: Si regeneration and retention in marsh sediments (Scheldt estuary). Biogeochemistry 82:41-53. DOI 10.1007/s10533-006-9051-5

Struyf E, van Damme S, Gribsholt B, Bal K, Beauchard O, Middelburg JJ, Meire P (2007) Phragmites australis and silica cycling in tidal wetlands. Aquatic Botany 87:134-140. DOI 10.1016/j.aquabot.2007.05.002

Struyf E, van Damme S, Gribsholt B, Meire P (2005a) Freshwater marshes as dissolved silica recyclers in an estuarine environment (Schelde estuary, Belgium). Hydrobiologia 540:69-77. DOI 10.1007/s10750-004-7104-0

Struyf E, van Damme S, Gribsholt B, Middelburg J, Meire P (2005b) Biogenic silica in tidal freshwater marsh sediments and vegetation (Schelde estuary, Belgium). Marine Ecology Progress Series 303:51-60. DOI 10.3354/meps303051

Sullivan MJ, Monceriff CA (1990) Edaphic algae are an important component of salt marsh food-webs: evidence from multiple stable isotope analyses. Marine Ecology Progress Series 62:149-159. DOI 10.3354/meps062149

Sutton-Grier AE, Keller JK, Koch R, Gilmour C, Megonigal JP (2011) Electron donors and acceptors influence anaerobic soil organic matter mineralization in tidal marshes. Soil Biology and Biochemistry 43:1576-1583. DOI 10.1016/j.soilbio.2011.04.008

Temmerman S, Govers G, Wartel S, Meire P (2003) Spatial and temporal factors controlling short-term sedimentation in a salt and freshwater tidal marsh, Scheldt estuary, Belgium, SW Netherlands. Earth Surface Processes and Landforms 28:739-755. DOI 10.1002/esp.495

Tréguer P, Nelson DM, van Bennekom aJ, Demaster DJ, Leynaert a, Quéguiner B (1995) The silica balance in the world ocean: a reestimate. Science 268:375-379. DOI 10.1126/science.268.5209.375

Tréguer PJ, De La Rocha CL (2013) The World Ocean Silica Cycle. Annu Rev Mar Sci 5:477-501. DOI 10.1146/annurev-marine-121211-172346

Tzortziou M, Neale PJ, Megonigal JP, Pow CL, Butterworth M (2011) Spatial gradients in dissolved carbon due to tidal marsh outwelling into a Chesapeake Bay estuary. Marine Ecology Progress Series 426:41-56. DOI 10.3354/meps09017

Tzortziou M, Osburn CL, Neale PJ (2007) Photobleaching of dissolved organic material from a tidal marsh-estuarine system of the Chesapeake Bay. Photochemistry and photobiology 83:782-792. DOI 10.1111/j.1751-1097.2007.00142.x

UNESCO (2013) The Wadden Sea. Accessed 4-22-2013. http://whc.unesco.org/en/list/1314

UVU (1997) Umweltverträglichkeitsuntersuchung Zur Anpassung der Fahrrinne der Unter- und Aussenelbe an die Containerschiffahrt. Wasser- und Schifffahrtsamt Hamburg

Vieillard AM, Fulweiler RW, Hughes ZJ, Carey JC (2011) The ebb and flood of Silica: Quantifying dissolved and biogenic silica fluxes from a temperate salt marsh. Estuarine, Coastal and Shelf Science 95:415-423. DOI 10.1016/j.ecss.2011.10.012

Wang AZ, Cai W-J (2004) Carbon dioxide degassing and inorganic carbon export from a marsh-dominated estuary (the Duplin River): A marsh CO_2 pump. Limnology and Oceanography 49:341-354. DOI 10.4319/lo.2004.49.2.0341

Weiss JV, Emerson D, Megonigal JP (2004) Geochemical control of microbial Fe(III) reduction potential in wetlands: comparison of the rhizosphere to non-rhizosphere soil. FEMS Microbiol Ecol 48:89-100. DOI 10.1016/j.femsec.2003.12.014

Wheat CG, McManus J (2005) The potential role of ridge-flank hydrothermal systems on oceanic germanium and silicon balances. Geochimica et Cosmochimica Acta 69:2021-2029. DOI 10.1016/j.gca.2004.05.046

Winter PED, Schlacher TA, Baird D (1996) Carbon flux between an estuary and the ocean: a case for outwelling. Hydrobiologia 337:123-132. DOI 10.1007/BF00028513

Wolfstein K, Kies L (1995) A case study on the oxygen budget in the freshwater part of the Elbe estuary. 3. Variations in phytoplankton pigments in the Elbe before and during the oxygen minima in 1992 and 1993. Archiv für Hydrobiologie (Supplement) 110:39-54. DOI not available

Xin P, Yuan L-R, Li L, Barry Da (2011) Tidally driven multiscale pore water flow in a creek-marsh system. Water Resources Research 47:1-19. DOI 10.1029/2010wr010110

Yamada SS, D'elia CF (1984) Silicic-Acid Regeneration from Estuarine Sediment Cores. Marine Ecology-Progress Series 18:113-118. DOI 10.3354/meps018113

Zeebe RE, Caldeira K (2008) Close mass balance of long-term carbon fluxes from ice-core CO_2 and ocean chemistry records. Nature Geoscience 1:312-315. DOI 10.1038/ngeo185

Ziegler K, Chadwick OA, Brzezinski MA, Kelly EF (2005) Natural variations of $\delta^{30}Si$ ratios during progressive basalt weathering, Hawaiian Islands. Geochimica et Cosmochimica Acta 69:4597-4610. DOI 10.1016/j.gca.2005.05.008
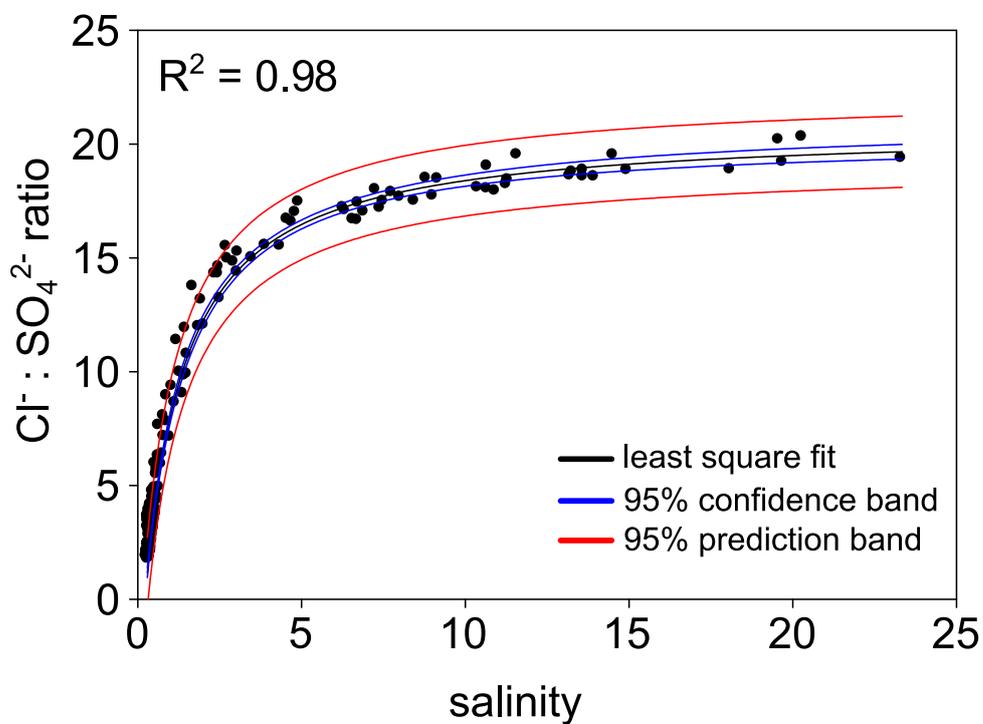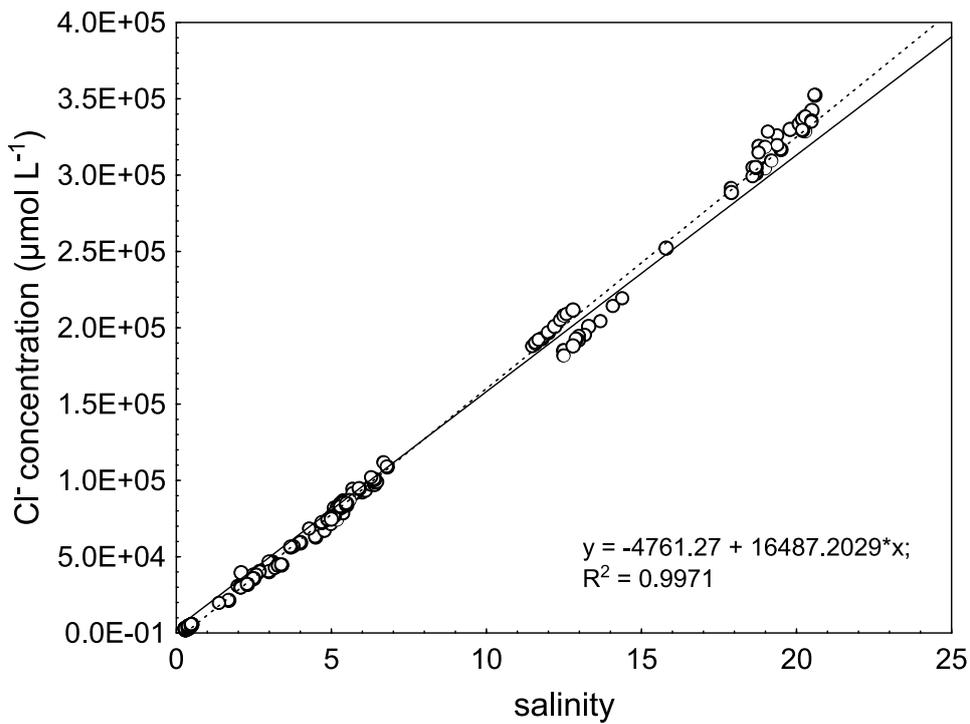
Appendix
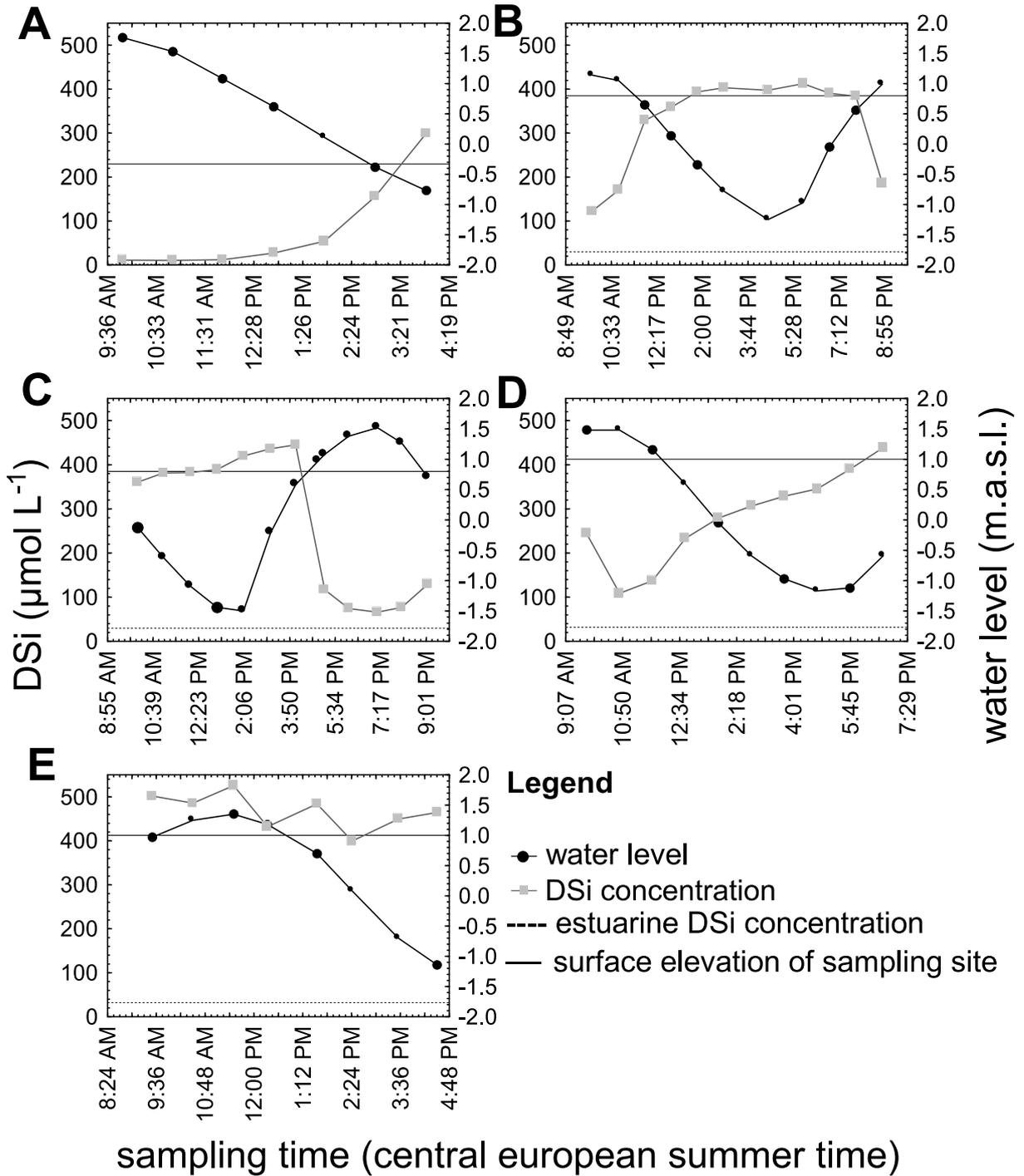
Appendix 1: Overview of tidal cycles from July samplings which were used for the DSi export calculations. Time is given in central European summer time (CEST = UTC+2). A) freshwater site, July 2010. B) brackish site, July 2010. C) brackish site, July 2011. D) saline site, July 2010. E) saline site, July 2011.
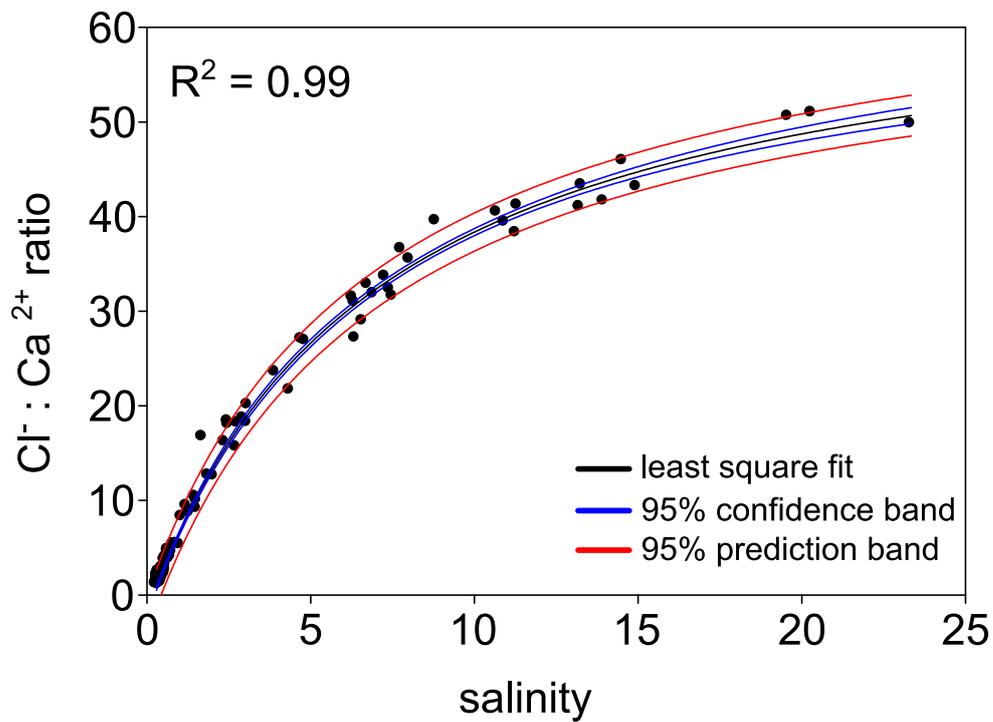
Appendix 2: Cl⁻:Ca²⁺ ratios in the Elbe estuary as a function of salinity. The non-linear fit (black line), the respective 95% confidence bands (blue lines) and the 95% prediction bands (red lines) are shown. The non-linear fit followed the equation y = a+b*x/(c+x).

Appendix 3: Cl⁻:SO₄²⁻ ratios in the Elbe estuary as a function of salinity. The non-linear fit (black line), the respective 95% confidence bands (blue lines) and the 95% prediction bands (red lines) are shown. The non-linear fit followed the equation y = a+b*x/(c+x).

Appendix 4: Seepage water chloride concentrations as a function of salinity. The linear least square regression line (dotted) and the conservative mixing line (solid) are shown for comparison. Note that the deviation of the data points from the mixing line is within the measurement error. The function shows the result of the linear least square regression.
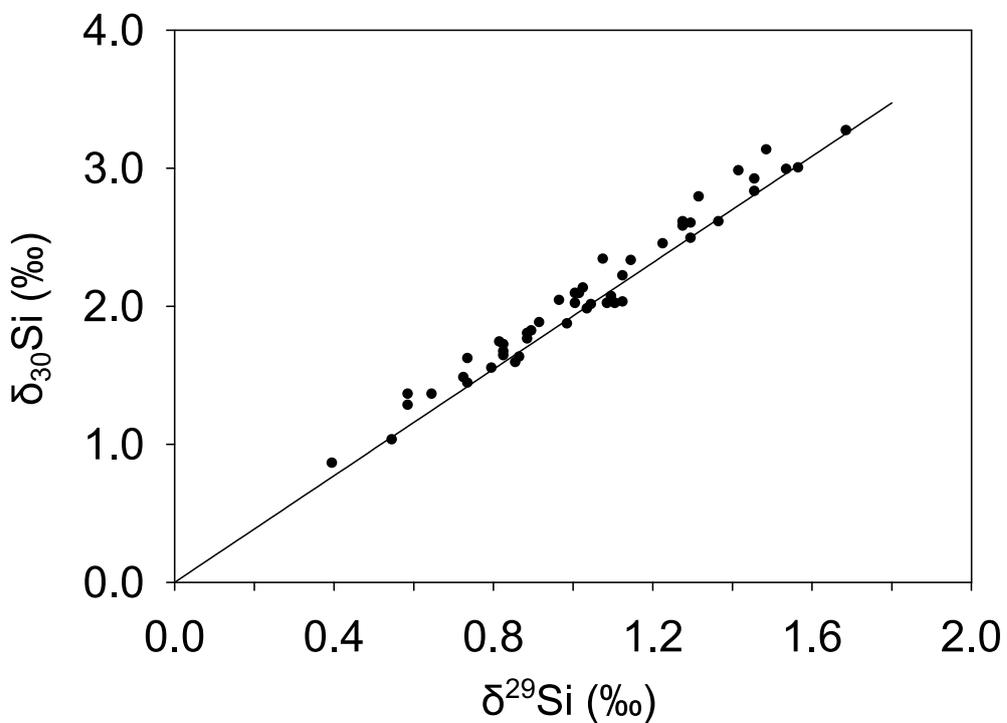
Appendix 5: Mass fractionation line of $\delta^{29}Si$ versus $\delta^{30}Si$ for the here presented samples. The slid line is the theoretical mass fractionation line of $\delta^{30}Si = 1.93 * \delta^{29}Si$.

Appendix 6: Estuarine DIC concentrations used for the calculation of marsh DIC enrichment. The average concentration was calculated from all available samples in a certain spatial interval. The interval for HDM was Elbe km 630-670, for NF it was Elbe km 670-710 and for DSK Elbe km 710-724 was used.

sampling location	date	DIC$_{river}$ (µmol kg^{-1})		
		average	avg-stdev	avg+stdev
HDM	2010-09	1994	1981	2007
HDM	12010-11	2252	2148	2356
HDM	02011-03	2281	2251	2312
HDM	2011-07	1811	1754	1868
NF	2010-07	2144	2092	2196
NF	2010-11	2459	2432	2486
NF	2011-03	2313	2303	2323
DSK	2010-07	1963	1959	1967
DSK	2010-09	2106	n.d.	n.d.

n.d. = only 1 sample available

Appendix 7: Upper and lower limit of seepage and total DIC export and the percentage contribution of the seepage export to the total export.

location	date	seepage DIC export (mol m^{-2} d^{-1})		total export (mol m^{-2} d^{-1})		% of total export (%)	
		lower limit	upper limit	lower limit	upper limit	lower limit	upper limit
HDM	2010-09	0.02	0.07	0.04	0.09	66	82
HDM	12010-11	0.02	0.07	0.10	0.23	24	31
HDM	02011-03	0.02	0.07	0.04	0.09	57	78
HDM	2011-07	0.02	0.07	0.05	0.11	52	61
NF	2010-07	0.06	0.17	0.09	0.20	68	86
NF	2010-11	0.06	0.17	0.08	0.19	74	89
NF	2011-03	0.06	0.17	0.09	0.20	65	85
DSK	2010-07	0.05	0.16	0.09	0.20	58	81
DSK	2010-09	0.05	0.16	0.16	0.27	32	59

Weiss, A., Amann, T., Hartmann, J. (2013) Silica Dynamics of Tidal Marshes in the Inner Elbe Estuary, Germany.	**Research Idea:** A. Weiss, J. Hartmann **Analysis:** A. Weiss **Results:** A. Weiss **Discussion:** A. Weiss, T. Amann, J. Hartmann
Amann, T., **Weiss, A**., Hartmann, J. (2012) Carbon dynamics in the freshwater part of the Elbe estuary, Germany: Implications of improving water quality	**Research Idea:** J. Hartmann, T. Amann **Analysis:** T. Amann, A. Weiss **Results:** T. Amann, A. Weiss **Discussion:** T. Amann, A. Weiss, J. Hartmann
Müller, F., Struyf, E., Hartmann, J., **Weiss, A**., Jensen, K. (in press) Impact of grazing management on silica export dynamics of Wadden Sea saltmarshes.	**Research Idea:** F. Müller, K. Jensen **Analysis:** F. Müller **Results:** F. Müller **Discussion:** F. Müller, E. Struyf, K. Jensen, J. Hartmann, A. Weiss
Moosdorf, N., **Weiss, A**., Müller, F., Lauerwald, R., Worrall, F., Hartmann, J. (submitted) The role of salt marshes in the silica budget of the North Sea.	**Research Idea:** N. Moosdorf **Analysis:** N. Moosdorf, R. Lauerwald, F. Worrall **Results:** N. Moosdorf, A. Weiss **Discussion:** N. Moosdorf, A. Weiss, F. Müller, J. Hartmann
Weiss, A., Böttcher, M. Amann, T., Jensen, K., Hartmann, J. (in prep.) Sources and export of DIC and TA from tidal creeks along a salinity gradient in the Elbe estuary, Germany	**Research Idea:** A. Weiss, J. Hartmann **Analysis:** A. Weiss, M. Böttcher **Results:** A. Weiss **Discussion:** A. Weiss, M. Böttcher, J. Hartmann, T. Amann
Weiss, A., De La Rocha, C., Amann, T., Hartmann, J. (in prep.) Silicon isotopes in the Elbe estuary, Germany.	**Research Idea:** A. Weiss, J. Hartmann, C. De La Rocha **Analysis:** A. Weiss, De La Rocha **Results:** A. Weiss, De La Rocha **Discussion:** A. Weiss, De La Rocha, J. Hartmann
Amann, T., **Weiss, A**., Hartmann, J. (in prep.) Inorganic carbon cycling and CO_2 fluxes in the inner Elbe estuary, Germany.	**Research Idea:** T. Amann, J. Hartmann **Analysis:** T. Amann **Results:** T. Amann **Discussion:** T. Amann, J. Hartmann, A. Weiss
Amann, T., **Weiss, A**., Hartmann, J. (in prep.) A silica budget of the inner Elbe estuary, Germany	**Research Idea:** T. Amann, J. Hartmann **Analysis:** T. Amann **Results:** T. Amann **Discussion:** T. Amann, J. Hartmann, A. Weiss

Danksagung

Viele Personen haben mich während der letzten drei ein halb Jahre in meinem Unterfangen, eine Doktorarbeit zu schreiben, unterstützt. Diesen gebührt ein aufrichtiges Dankeschön meinerseits.

Zuallererst möchte ich Jens Hartmann, dafür danken, dass er mir – trotz gewagtem Bewerbungsfoto – die Möglichkeit gegeben hat, mit dem Stipendium der ESTRADE Graduiertenschule diese Doktorarbeit in seiner Arbeitsgruppe anzufertigen. Auch für die zahlreichen Diskussionen aus der geologischen Sichtweise, die mir immer wieder Denkanstöße gegeben haben, sei ihm herzlichst Gedankt.

Thorben, Tom, Nils, Ronny und Frauke gebührt ebenfalls ein großer Dank, da sie mit Rat und Tat zum Gelingen dieser Arbeit beigetragen haben. Besonders möchte ich Thorben für seinen selbstlosen Einsatz während zahlreicher Probennahmen danken. Ohne ihn ware es nicht möglich gewesen die Daten zu erheben.

An dieser Stelle möchte ich Christina de la Rocha herzlich danken, die es mir mit ihrem persönlichen Einsatz ermöglicht hat, in ihrer Arbeitsgruppe in Brest zu arbeiten. Die Zeit in Frankreich war sowohl persönlich als auch fachlich eine tolle Bereicherung.

Ein weiteres Dankeschön geht an alle Mitglieder der ESTRADE Graduiertenschule und deren Betreuer, die mir auf "Retreats" und einer "Winter School" die Gelegenheit gegeben haben, auch mal über den eigenen Tellerrand zu schauen. An dieser Stelle seien auch den Koordinatoren von ESTRADE gedankt, ohne die dieser rege Austausch auf den "Retreats" nicht stattgefunden hätte.

Ein ganz großes Dankeschön geht an meine Familie, ohne deren finanzielle und moralische Unterstützung ich nicht dort angekommen wäre, wo ich heute bin.

Meine ganz besondere Dankbarkeit gebührt Berivan, die immer an mich geglaubt und mir in kritischen Zeiten den Rücken frei gehalten hat. Ohne Sie, wäre die Arbeit wohl immer noch nicht fertig.